Catalonia Institute for Energy Research

Departament d'Enginyeria Elèctrica

UNIVERSITAT POLITÈCNICA DE CATALUNYA

CITCEA • Centre d'Innovació Tecnològica en Convertidors Estàtics i Accionaments

UNIVERSITAT POLITÈCNICA DE CATALUNYA

Jesús M. Quintero — Assessment of Color Quality and Energy Efficiency: New Insights for Modern Lighting

Assessment of Color Quality and Energy Efficiency: New Insights for Modern Lighting

Part I. Color quality in general lighting applications

Part II. Mesopic photometry and street lighting

Jesús M. Quintero

Doctoral Dissertation

Barcelona, December 2014

Universitat Politècnica de Catalunya

Departament d'Enginyeria Elèctrica

CITCEA - Centre d'Innovació Tecnològica en Convertidors Estàtics i Accionaments

Dissertation presented in partial fulfilment of the requirements for the degree of Doctor of Engineering

Assessment of Color Quality and Energy Efficiency: New Insights for Modern Lighting

Part I. Color quality in general lighting applications
Part II. Mesopic photometry and street lighting

Author: **Jesús M. Quintero**

Main Advisor: **Dr. Josep Carreras**
Co-advisor: **Prof. Dr. Antoni Sudrià-Andreu**

Barcelona, December 2014

Universitat Politècnica de Catalunya
Departament d'Enginyeria Elèctrica
Centre d'Innovació Tecnològica en Convertidors Estàtics i Accionament
Av. Diagonal, 647. Pl. 2
08028 Barcelona

Imprès a Barcelona per CPDA, S.L.
Primera impressió, 2014

ISBN:

ACTA DE QUALIFICACIÓ DE LA TESI DOCTORAL

Reunit el tribunal integrat pels sota signants per jutjar la tesi doctoral:

Títol de la tesi: .....

Autor de la tesi: .....

Acorda atorgar la qualificació de:

- ☐ No apte
- ☐ Aprovat
- ☐ Notable
- ☐ Excel·lent
- ☐ Excel·lent Cum Laude

Barcelona, ……. de/d'…..……. de .....….

El President

.....
(nom i cognoms)

El Secretari

.....
(nom i cognoms)

El vocal

.....
(nom i cognoms)

El vocal

.....
(nom i cognoms)

El vocal

.....
(nom i cognoms)

To my Mother and Father

Mercedes and *Jesús María*

Acknowledgments

I would like to thank the people who supported me during my doctoral research. First, I would like to thank the final supervisor of this thesis, Dr. Josep Carreras, who guided me and was very patient throughout all of my doctoral research. He opened the door to scientific research for me, and by his example, insightful questions and comments, I have learned to appreciate scientific research and physics.

I am also very grateful to my thesis assessor, Dr. Antoni Sudrià-Andreu for sharing with me his knowledge about power electronics at UPC-CITCEA at the beginning of the doctoral program, for helping me with his comments and advice during the whole doctoral program, and especially for recommending me for a doctoral fellowship at the IREC.

I am also deeply indebted to Antoni Martinez, who gave me the opportunity to be part of the start-up of the Lighting Group at the Catalonia Institute for Energy Research-IREC. It was an honour to work with him directly when IREC had no more than ten members.

Furthermore, I would like to thank Professor Charles E. Hunt, for taking the time and having the patience to read, edit and give me his advice on all of my publications, as well as for being my advisor at the beginning of this process. Undoubtedly, a key part of my training as a researcher was received in the light and lighting laboratory of Kaho Sint-Lieven in Ghent. I have only good memories of my stay there. I owe all this to Professor Peter Hanselaer who made me part of his research group. He listened, supported and guided me in my research. My warmest expressions of gratitude to Stefan Forment, who not only was my mentor but my friend. I am deeply grateful for his guidance. I am also immensely grateful for the warm welcome offered by Jonas, Sven, Wim, Arno and specialy Wouter Ryckaert. Thank you Wim for being an excellent co-worker at IREC, as well.

There is a long list of co-workers at IREC; to everyone who was part of the lighting group and power electronics department, I also want to say thank you. I want to express my warmest appreciation to my colleagues and friends Fernando, Pacho, Jhon-Jairo, Leo, Jairo, Germán, Paula, Lizeth and Yury. They were always there to give the right advice and support my choices.

It would be unfair not to mention my colleague Rodrigo, who invited me to come to Barcelona to begin this adventure, for offering me a chair beside him and for showing me the city and the academic life at UPC.

Last but not least, I cannot express how grateful I am to my family: Mom, Dad, Nelly, Oscar, Angela and especially to Wilson for his unconditional support and invaluable help. I would also like to thank my niece María Paula and nephews Alexis, Farid and Julian for being the tenderness of my life.

Jesús M. Quintero

Bogotá, 2014

The research presented in this dissertation was entirely funded by the European Regional Development Funds (ERDF, "FEDER Programa Competitivitat de Catalunya 2007-2013") and conducted at the Lighting Group of the Catalonia Institute for Energy Research-IREC in Barcelona, Spain.

Abstract

In colorimetry and color vision science, the shape and width of the light source's spectrum has a fundamental importance. The emergence of different types of light-emitting diodes-LEDs in general lighting, has generated a wide range of spectra available in this area due to diversity of colors, the width of their spectrum and the possibility of controling their intensity through power electronic circuits. Until the emergence of such light sources in general lighting, the availability of different spectra-type lamps were limited to standard light sources such as traditional incandescent, vapour of mercury and sodium at low and high pressure, as well as metal halides. In terms of spectra, these standard and well known lamps, have a very poor flexibility for changing or controling their spectra.

This new wide range of possibilities in the spectra of light sources has brought new challenges to the way we currently make prediction and measurements of the color rendering of light sources. Currently, there is only one index approved by the International Committee on Illumination (CIE): The CRI or Color Rendering Index. It is well known that this indicator fails with light sources having narrow spectra as those generated by LEDs, and besides, it only represents one of the variables involved in what can be called "color quality"of white light sources. For this feature there is not yet a standardized definition nor a precise way to measure it accurately and effectively, in order to indicate the benefits or limitations that may occur in the perception that people have about the colors of any element illuminated with any white lighr source. This issue can be very important in the design of general lighting or for specific lighting applications. The fact that the "Color quality"is also linked to the subjective perception of color and color preference that people have, makes the process of qualifying and quantifying this feature complex.

On the other hand, it is well known that there is a trade-off between the color quality and luminous efficacy of radiation for white light sources due to the conformation of its spectrum. This feature requires that the selection process of a light source for a specific lighting design, must choose between having a good color quality or a high efficacy. This creates a direct dependence on the lighting application and light source's parameters such as color quality and luminous efficacy. In other words, there are lighting applications where color quality is very important regardless of the low luminous efficacy, e.g. museums, retail, pre-press rooms, etc. There are also applications where

color quality can be forgone in order to achieve high luminous efficiency, e.g. public street lighting, parking lots, low traffic corridors, tunnels, etc.

This dissertation are divided in two parts: The first one deals with both aspects mentioned above, i.e color quality and luminous efficacy of light sources. The second one deals with technical and color quality aspects of the mesophic photometry applied in street or outdoor lighting.

The first part begins by proposing a method to generate a new color rendering index, consisting of a three-dimensional visual index, which was named 3D-CRM. In order to illustrate the use of this method and index, three examples of lighting application were performed: Artwork, meat and fruit. The results show the goodness of the visual index 3D-CRM, that is also accompanied by a numeric index that indicates how the light source tested fits with the gamut of colors required by the specific lighting application.

Complementing the preceding proposal, a statistical analysis was performed in order to define the parameters that make up the color quality of light sources. This statistical study was based on a collection of more than 100 real and ideal spectra of light sources. As a result, it was found that there is another variable that can complement the CRI index to indicate the color quality. This is the proposed index O_c (Optimal Color), which is based on the calculation of volumes generated with the spectrum of test source and several ideal spectra of reflectance to get optimal colors (high saturated colors) at different luminance levels.

This fisrt part of the dissertation ends by proposing an index to generate a classification of light sources according to the requirements of the lighting application and the parameters such as correlated color temperature (CCT), luminous efficacy of radiation (LER) and color quality (CQ). It was demonstrated that the new proposed index called ECQ (Efficacy and Color Quality), is able to generate a useful ranking when assessing a collection of spectra, by giving a desired CCT and the weight that efficacy and color quality have in the lighting application studied. By using some examples of different lighting applications (i.e. different weights for color quality and efficacy) it was demonstrated how versatile and useful the ECQ index is.

In the second part of this dissertation, a comparison of laboratory measurements between two different types of goniophotometers is made. The first one is a standard and photometer-based one, that uses the far-field for measurement. The second one has a more recent technology, uses a CCD camera and photometer as sensors, as well as the near field for measurement. This comparison is needed in order to validate the measurements from the near-field goniophotometer, since up to moment, for this type of

measurement and type of sensor (CCD camera), there are no laboratories with international traceability that can verify or calibrate this measurement system. The comparison exercise shows that there is a very good fit between both measures, therefore results of the near-field goniophotometer are validated. It is also shown that the near-field goniophotometer generates a high-resolution matrix of intensities (LID) due to the fact that interval angle of measurement is much more smaller than far-field goniophotometer. In recent measures performed at the Light and liegting laboratory of K.U. Leuven in Ghent, it was found that near field goniophotometer has a reduced luminous intensity dynamic range, for this reason exists an error measuring low luminous intensities in a luminarie with a sharp LID such as PAR30 Spot light bulb.

After that, some aspects of the "Recommended System for Mesopic Photometry Based on Visual Performance, CIE191:2010"are analysed. Regarding the correction values to convert photopic to mesopic luminance, a comparison between correction values given by the table in the CIE 191:2010 and the values provided by the implementation of the algorithm was performed. It was found that errors made when using approximate values from the table, are less than 0.2%.

Finally it is presented a proposal of a new metrics called Energy Consumption Index (Q_{sa}) intended to assessing possible energy savings on street lighting systems. In this chapter, by using the Energy Consumption Index a evaluation of three different hypothetical scenarios for a typical city is performed to demonstrate how flexible and intuitive this index is. these scenarios assess different characteristics of the light system such as light sources types, dimming systems and also the use of photopic and mesopic photometry. This index do not take into account the economic and finalcial issues. It was found that by using mesopic photometry the energy saving were not significative, less than 8.2% savings were found, on the contrary by using dimming systems on each fixture the saving found were close to 70%.

Contents

List of Figures

List of Tables

List of Tables

Nomenclature

Subscripts

O_c Optimal Colors Index

Q_a General Color Quality Scale

Q_g CQS-Gamut Area Scale

R_a General Color Rendering Index

R_i Special Color Rendering Index

V_{ch} Optimal Colors Solid Volume

Acronyms

CCT Correlated Color Temperature

CIE International Commission on Illumination

CIECAM02 CIE 2002 Color Appearance Model

CIELAB CIE 1976 $L^*a^*b^*$ Color Space

CIELUV CIE 1976 $L^*u^*v^*$ Color Space

CITCEA Centre d'Innovaciò Tecnològica en Convertidors Estàtics i Accionaments

CQ Color Quality

CQS Color Quality Scale

CRI Color Rendering Index

CRM Color Rendering Map

ECQ Efficacy and Color Quality Index

GAI Gamut Area Index

Nomenclature

IREC Catalonia Institute for Energy Research

LED Light-Emitting Diode

MCRI Memory Color Rendering Index

NCS Natural Color System

OSA Optical Society of America

UPC Universitat Politècnica de Catalunya

USC Uniform Color Space

Part I

Color Quality in general lighting applications

Chapter 1

The color rendering map: A graphical metric for assessment of illumination

The method of evaluating color rendering using a visual, graphical metric is presented. A two-dimensional Color Rendering Map (CRM) of a light source's color-rendering capabilities is explained and demonstrated. Extension of this technique to three-dimensional CRMs of objects under illumination is explained, including the method of introducing numerical indices in order to evaluate standards for specific applications in lighting. Three diverse applications, having a range from subtle to significant color variation, are shown with their respective CRMs. These three applications are also used to demonstrate how three differing light sources produce different maps. The results show a flexible, simple method to obtain a clear, visual determination of color rendering performance from differing sources used in differing illumination applications. The use of numeric indices in these applications shows how specific standards can be imposed in assessing the applicability of a light source.

1.1 Introduction

The CIE Color Rendering Index (CRI), first proposed in 1964, and later updated in 1974 [CIE13.3, 1995], is the most common metric currently in use for assessment of artificial light sources in their ability to render visible colors. The Special CRI or R_i, as individual color difference index of 14 color test samples, and the General CRI, or R_a as the index averaging the color difference of the first eight of the R_i color-test samples (all taken from the Munsell Book of Color), involve an obsolete chromatic adaptation and use a color space which is not uniform. It has been shown that these metrics incorrectly estimate the color rendering capabilities of light sources, notably white Light-Emitting Diodes (LED) [CIE177, 2007] . There is general consensus that the General CIE-CRI (R_a), and Special CRI (R_i), need

a re-evaluation [Ohno, 2004].

In recent years, there have been several proposals for improving the CIE-CRI, or for establishing a different metric which evaluates a light source's color-rendering capabilities. All of these proposals can be categorized as either objective or subjective-based measures. The majority are objective-based, using a reference illuminant for comparison and intended for improving the CIE-CRI. The subjective measure proposals focus on color preference or memory colors. The following proposals are among the most recent and relevant.

The Gamut Area Index (GAI) [Rea and Freyssinier-Nova, 2008] is an objective measure calculated as a percentage of the area of the polygon defined by the chromaticities in CIE-1964 coordinates of the eight CIE color test samples as specified in [CIE13.3, 1995] when illuminated by a test light source, compared to the same polygon area when illuminated by a reference, equal energy white spectrum. The GAI is complementary to the CIE-CRI, and the test source is deemed both "natural" and "vivid" when both the CRI and GAI have values exceeding 80.

The Color Quality Scale (CQS) [Davis and Ohno, 2010] is a method which mixes color fidelity and people's preference for chroma enhancement, by using more saturated test-color samples. The CQS does not penalize (nor reward) for increased chroma, includes improvements for chromatic adaptation, and uses a more homogeneous color space in evaluating color differences.

The Memory Color Rendering Index (MCRI) [Smet et al., 2010] MCRI evaluates a more subjective aspect of color rendition by calculating the degree of similarity between a set of familiar objects illuminated by the test source and their memory colors.

The proposed CRI-CAM02UCS [Luo, 2011] improves upon the CIE-CRI because it uses the CAM02-UCS that is not only a color appearance model but also a uniform color space, replacing the obsolete Von-Kries chromatic adaptation and the less uniform CIE 1964 ($U^*V^*W^*$) space.

Among the proposals for a better, or different metric of color rendering, some focus on the test-sample set of colors (or color-order system), others use a uniform color space, others redefine the existing CIE-CRI in order to give better qualification to specific light sources, and, finally, some focus on subjective issues. Because these approaches are general metrics, none of them take into account the specific color rendering requirements constrained by particular applications. We present here, and demonstrate, a new approach, called the Color Rendering Map (CRM), which is used for evaluating and assessing light sources. The CRM is flexible with the choice

of color-order system, can work in a uniform (or non-uniform) color space, is light-source technology neutral, and can be either used as a general evaluation metric, or adapted to assess a source's value to any specific illumination application (such as artwork, food, public places, portraiture, etc.). Therefore, the CRM incorporates the useful qualities of several of other evaluation techniques which have been developed. The method produces a visual, graphical result (a "map") over the chosen color space, providing more descriptive information than is possible using exclusively one or two metrics. From these representations, single number, application-dependent indices can easily be extracted when so required. Van der Burgt has also noted the need for more informative color-rendering evaluation methods [van der Burgt and van Kemenade, 2010]. However, his description is based on specifying color-shift directions plotted on the CIELab space. The CRM method is more generic in the sense that gives absolute values of rendering indices along a color space, and color rendering shifts can be easily obtained by calculating gradient plots of our data. It also has the potential to readily allow the user to evaluate a source (or compare multiple sources) specific to a particular application.

In this work, we first describe and demonstrate the use of a 2-D CRM in the process of giving a general evaluation of any light source. We then show the method to obtain a 3-D CRM of a light source to a specific application, based on the illuminated test-samples reflectance values. These 3-D representations provide immediate, intuitive information concerning the color-rendering capability that any light source has when used for that specific application. Several example applications are given to demonstrate that a lamp's color rendering can vary, according to each application. These results demonstrate an alternative to a single-number color-rendering metric.

1.2 The general Color Rendering Map of a source

We first demonstrate mapping the color rendering of a light source without any consideration of a specific application. This results in a two-dimensional CRM. Figure 1.1, depicts the process whereby a 2D-CRM is generated. Following the method defined in [CIE13.3, 1995], established for calculation of the Special CIE-CRI (where $R_i = 100 - 4.6 \cdot \Delta E_i$ to each one of the 14 test color samples), the evaluation of all 1269 R_i values from the Munsell Book of Color is performed using the Lamp under Test, resulting in the data which is plotted in a map (the CRM), with a range encompassing all values of the data points. This results in a two-dimensional CRM. A mathematical

transform has been used to avoid negative values for R_i, not altering those R_i values higher than 20. Although it is known that Munsell samples are highly correlated because are made of a limited number of pigments, Munsell set of reflectance samples is used because it is well known for the non-expert, and has a large-area gamut of colors to describe a wide range of applications, which will be useful for the 3D-CRM later on.

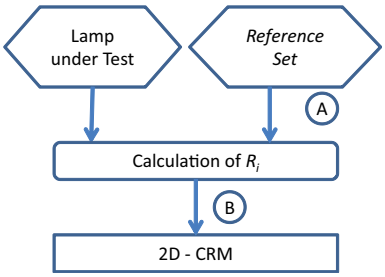

Figure 1.1: Flow chart depicting how to create 2D-CRM. (A) Using the 1269 Munsell Colors, the R_i values are evaluated by comparison with a *Reference Set*. (B) The R_i values are plotted over the CIE x-y plane.

As an example of this, consider the three spectra shown in Figs. 1.2(a)–1.2(c). These correspond to (a) a tri-junction R-G-B LED lamp, (b) a trichromatic fluorescent lamp, and (c) a Plankian source, band-passing the 450-650nm region of the visible spectrum. Figure 1.2 also lists the spectral luminous efficacy of radiation (LER) for each source, which are approximately equivalent. Although the spectra in Fig. 1.2 are obviously different, and render colors based on their own spectral content throughout the visible region, the CIE calculations give virtually identical R_a=85 and CCTs (∼3000K) for all three. This is a clear indication that these numbers by themselves provide insufficient information. The resultant danger of relying on one or two-metric evaluations is the potential to obtain a light source with spectral content mismatched to its intended application. In CIE Publication 13.3, the appearance of fifteen color samples (Special CRI or R_i for $1 \leq i \leq 14$) illuminated by the light source being tested, is compared to the appearance of the same samples illuminated by a reference illuminant. The eight first differences are averaged, resulting in the General CRI (R_a) value, $R_a = \frac{1}{8}\sum_{i=1}^{8} R_i$. Any deficiency results in a R_a less than 100, but there is no indication in which part of the source's spectral content the deficiency lies.

To generate the 2-D CRM, the source being tested is evaluated by following exactly the same procedure as described in CIE 13.3, but substituting

the 14 Munsell reflectance patterns by our *Reference (color) Set* of the entire 1269 Munsell set. The final map is obtained by plotting the entire set of R_i values over the x-y color coordinates plane, as shown in Fig. 1.2d. This calculation is quickly performed from the measured spectrum of the source being tested, on the computer, using a packaged engineering environment such as Matlab. The individual R_i numbers, in this example, are graphed using colors (deep blue = 0 up to deep red = 100), resulting in the CRM figures seen next to their respective spectra, in Figs. 1.2(a)–1.2(c). The result is an intuitive, visual description of the three different sources, immediately demonstrating where are the respective strengths and deficiencies in their ability to render color, despite the fact that their R_a and CCT are identical.

It should be noted that, for purposes of demonstration, we have used the Munsell set as our reference, the CIE x-y coordinates, and color depiction of the R_i numbers within the *Reference Set*. Proposing other test samples with superior colorimetric properties or avoiding metameric correlation among test samples lies out of the scope of this work. In the following section, we present a new methodology to assess light quality of sources for a particular application.

In the demonstration examples through this paper, uniform color spaces like CIELAB and CIECAM02 are used to measure color distances, but in most cases the xyY color space is used only for graphical representation of the CRM.

1.3 The 3-D CRM and its application

The map technique described in Section 2 only gives a color-rendering description of a light source without considering the application. However, there are specific cases where color quality is of highest importance, and where the careful selection of a suitable spectral content is critical. In such specific situations, general indices are not a valid option.

We present in this section a methodology for assessment of the color quality of light sources under a particular application. As inputs, this method requires not only the spectrum of the light source, but also the chromaticity coordinates of all the illuminated elements (i.e. image pixels obtained with a luminance/color camera) under a reference illuminant (in our case, a D65 simulator). We use a Class B, (which is in the limit of being Class A since the measured Metameric Index is MI_{vis}=0.268 (under CIE-L*a*b*) and MI_{vis}=0.328 (under CIE-L*u*v*)), which has enough resemblance to the

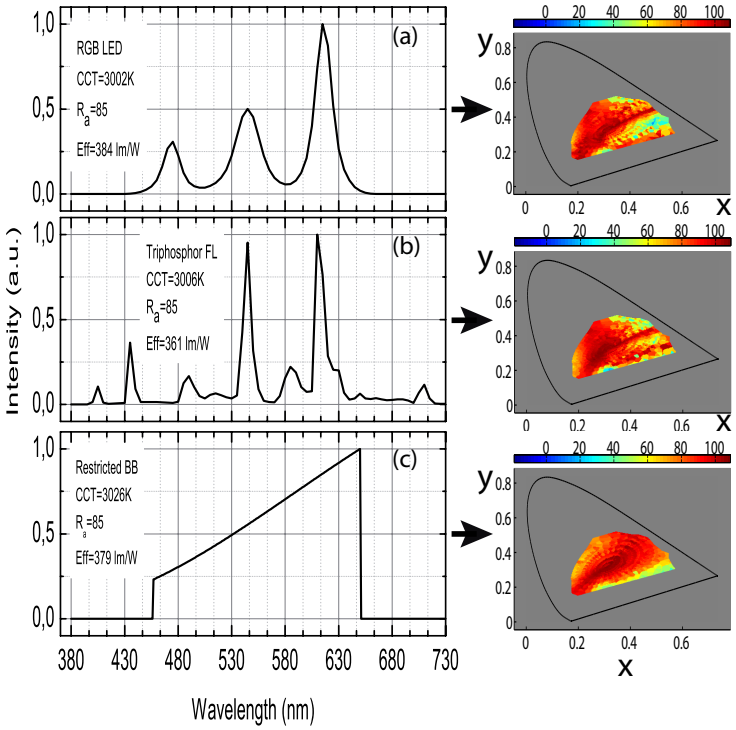

Figure 1.2: Three differing CCT=3000K spectra, (a) white R-G-B LED, (b) trichromatic fluorescent, and (c) filtered Plankian, all having the same CRI (R_a) values and approximately identical LER values. The Color Rendering Maps (CRMs) are depicted next to their respective spectra.

D65 CIE standard illuminant for our purposes, since the minimum distance between consecutive samples of the Munsell set is ΔE_{Lab}=4.86.

For a particular application (i.e. artwork, food, retail, etc.) we use a 3D representation of the color coordinates obtained with the luminance camera. This is performed by using different color spaces, such as CIE 1931 xyY [Malacara, 2002], the CIE 1976 L*a*b* (CIELAB) [Ohta and Robertson, 2005], and the CIECAM02 [Fairchild, 2005], each of these having increasing complexity and computational power demands.

In order to evaluate how a light source renders the whole set of colors present in a particular application, the process followed is to first choose an ordered set of colors based on a color order system, resulting in what we call a *Reference Set*. The color coordinates of the object of interest in

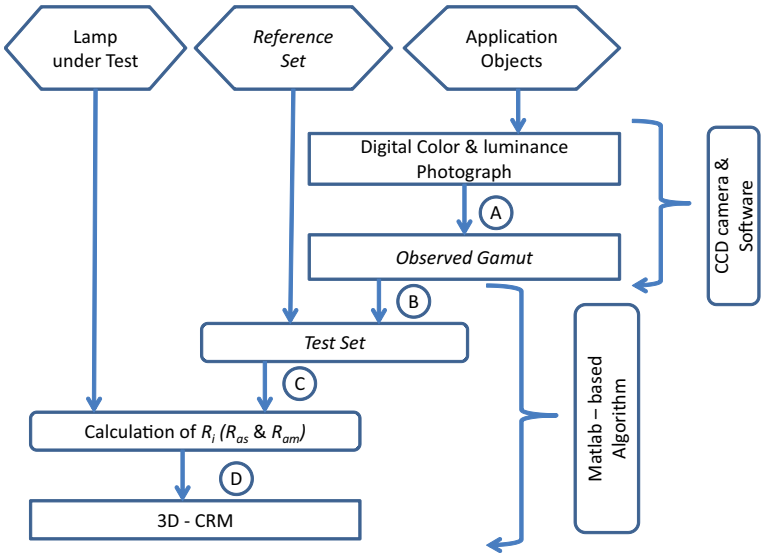

Figure 1.3: Flow chart for the evaluation of the 3-D CRM. (A) A calibrated digital photograph measures all luminance and color coordinates of the application object, giving the *Observed Gamut*. (B) The *Test Set* is obtained by finding the closest Euclidian distance between each pixel in the Measured Set to the Colors of the *Reference Set*. (C) As before, the R_i values for the complete *Test Set* (as well as the R_{as} and R_{am} indices) are computed. (D) Finally, the 3-D CRM is plotted using the R_i values of the Test Sample.

the application are then measured with the luminance camera (which incorporates filters emulating the 2° observer matching functions, $\hat{x}$, $\hat{y}$ and $\hat{z}$ as illuminated by our D65 simulator, the resulting set of color coordinates being what is called the *Observed Gamut*. Again, although filters incorporated in these cameras are not perfect matches to the CIE matching functions, the x-y error is less than $\Delta E \leq 2 \cdot 10^{-3}$ under A CIE standard illuminant. Finally, a sub-set of the *Reference Set* is selected by finding minimum distances between the *Observed Gamut* and the *Reference Set*, resulting in the *Test Set*. This *Test Set* is then mapped in the 3-D color space chosen, creating the CRM. The flow chart in Fig. 1.3 depicts this process. There is also available an online animation depicting the whole CRM build-up process, see Fig. 1.3.

The *Reference Set* requires a group of test colors of a sufficiently wide

range of hue, chroma and lightness, such that this set contains all the colors present in all the objects associated with application of interest. For purposes of the examples which follow, we use a reflectance database of the 1269 color samples corresponding to the Munsell color system, as was used in Section 2. This *Reference Set* is 90% of the color samples of the Munsell Book of Color (used for color assessment in industrial applications [X-Rite®, 2012]), and although it demonstrates some metameric weaknesses, it suffices to demonstrate the CRM in the cases we tested. Other authors have demonstrated good color appearance modeling using 1000 reference colors [Luo, 2011], and reasonable improvement (as compared with R_a) with as few as 17 reference colors [Smet and Whitehead, 2011].

Test objects which have a very limited gamut, or require illumination at very-low CCT values may fall not be properly mapped using the Musell set. In such cases, a *Reference Set* drawn from a different color ordering system, such as the NCS or OSA Uniform Color Scale (depending on the objects and illumination conditions) will likely be needed to generate an accurate CRM.

Using a digital luminance camera, we obtain a picture of the test objects illuminated by our D65 simulator. It is necessary to calibrate the color and luminance of the camera using a standard illuminant, and include (during the test) a test card of a range of the reference colors to verify the accuracy. Editing the area(s) of interest of the picture, removing any test cards or surfaces of the experimental viewing booth from consideration in the data, the set of pixels that represent the chromaticity of the test objects are obtained (*Observed Gamut*). Subsets of these areas of interest can also be examined, which may give rise to a slightly different *Observed Gamut*, depending on the diversity of colors in the test objects of the application. While this variability might be seen as a weakness of the method, it actually emphasizes the high level of customization that it is able to provide, assessing color rendering aimed at each special case. In those applications where the diversity of colors is extremely broad, the benefits of our CRM are not so clearly seen, and other metrics that only depend on the spectrum of the light source but not on the input gamut might make more sense.

The *Observed Gamut* is compared to the *Reference Set*, resulting in a sub-set (of the *Reference Set*) which is the *Test Set* that represents the color gamut of the objects. This comparison is performed between each single pixel of the *Observed Gamut* to all samples of the *Reference Set* and assigning to the *Test Set* the nearest color within a uniform color space (such as CIELAB or CIECAM02). Colors in the *Observed Gamut* can occur multiple times, which is noted using a multiplicity factor, m_i, with a integer value $m_i \geq 1$, for each element in the *Test Set*. The *Test Set*, along with

the respective m_i values, allows us to create the 3-D Color Rendering Map and two associated numerical indices as seen in Eqs. (1) and (2). These indices are used for color-rendering evaluation of the test light source; but are specific to the application being studied, and are not intended as a replacement or substitute for the CIE-R_a, but as a complement for those applications for which color must be accurately controlled. It is evident that the value of multiplicity is highly dependent both on the diversity of color in the test objects, as well as to the size of the area of interest chosen from which to draw the *Observed Gamut*. The user of the CRM chooses, according to his requirements, the value of R_{as} and/or R_{am} which can be considered acceptable for the application being studied.

Once the *Test Set* is defined, and using the spectrum of the Lamp under Test (see stage C in Fig. 1.3), the average of all R_i values, as defined in [CIE13.3, 1995], of this set is the index R_{as}. Considering that some samples have greater weight, if their $m_i \gg 1$ (a likely situation in most applications) in the gamut, the color rendering is also calculated as a weighted index, R_{am}. The sum of all pixels in the *Observed Gamut*, given their respective m_i values is evaluated as:

$$R_{as} = \frac{1}{s} \sum_{i=1}^{s} R_i \tag{1.1}$$

$$R_{am} = \frac{1}{u} \sum_{i=1}^{s} m_i \cdot R_i \tag{1.2}$$

$$u = \sum_{i=1}^{s} m_i \tag{1.3}$$

Where:

s: Number of elements in the *Test Set*.

u: Number of elements (pixels) of the *Observed Gamut*.

m_i: Multiplicity of the i-th element in the *Test Set*.

It is important to note that the index values vary for a single light source, since the *Test Set* changes with differing applications. Therefore, R_{am} and R_{as} cannot serve to replace general CRI, R_a, but are application specific. Because an end user selects the "area of interest" to assess, even within a particular application, a given light source can produce differing indices if the user places attention on differing areas of interest. However, in general, the index value will become of lesser utility for smaller areas. Furthermore,

we have not included issues of metamerism in these indices, and in some applications those conditions need to be addressed.

Considering that human vision has adapted to natural daylight, an artificial light source is perceived as "natural" if it emulates a Planckian radiator [Hertog et al., 2014]. By this standard, color quality can be objectively measured by considering parameters such as the Correlated Color Temperature (CCT) and the deviation of the chromaticity coordinates from the black body locus (Δ_{uv}) in addition to its R_a value. However, color quality assessment in general lighting sources has some subjective components such as color preference, memory colors and other issues varying with individuals [Pérez-Carpinell et al., 1998]. The selection of areas of interest is already a subjective process reflected by the *Observed Gamut*; however, this is unique to each application, and defined by the user. Furthermore, although objective measurements can find the chromaticity of a source based on the spectral power distribution, the phenomena of metamerism, where two sources with the same chromatic coordinates (but different spectral content) generate different color perception of some objects [Schanda, 2011], would have to be evaluated using a metamerism index for a more complete assessment of the color quality. Such subjective measures can be included in mapping an *Observed Gamut* by using methods which have been proposed by others who have described these phenomena, and how to evaluate them; but this is beyond the scope of this work which focuses on using the CRM for visual mapping of color rendering. Also, efficacy of a light source, which is of paramount importance, often has a significant, measureable tradeoff with color quality [Hertog et al., 2014], and a user's threshold efficiency constraints can be incorporated into a CRM by plotting only the final data values which meet or exceed whatever value is chosen. The standards of how natural, efficient, metameric, or other qualities, as they would be incorporated in a CRM, are not addressed in the following application examples, and are reserved for future work.

1.4 Application examples

The tools used to complete the measurement, shown in Fig. 1.4, include a viewing booth, both for calibration and for illumination of the objects by the chosen test sources, a CCD camera (calibrated for color and luminance), both color and gray checker cards, and software for data management and graphical representation. With these tools we are able to obtain an *Observed Gamut* for each application, and compute the *Test Set*, as well as portray

the CRM.

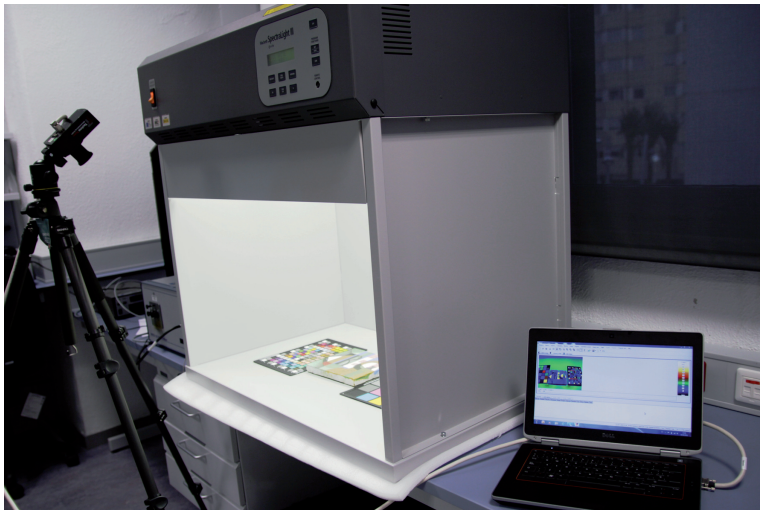

Figure 1.4: Experimental viewing booth, for generating *Test Sets*, with a simulator of the standard illuminant CIE-D65, calibrated CCD camera and a computer for editing and selecting the areas of interest. Also seen in the booth are color-checker patches. All measurements are performed with room lights dark.

To assure the color and luminance calibration of the camera/software, in the test setup of Fig. 1.4, a color-checker card is placed in the same scene of the objects under test in the viewing booth. Test measurements are performed with ambient room lights dark. Each photograph is edited, by selecting the areas of interest, and then grouping these areas, exporting the data with CIE-1931 xyY identifiers.

Demonstrating the 1269 Munsell samples of our chosen *Reference Set* in 3-D is seen in Fig. 1.5, in (the non-uniform) CIE-1931 xyY color space (a) as well as uniform CIELAB (b) and CIECAM02 (c) color space. Figures 1.5(a)– 1.5(c) show, in each case, two differing angles of view of the color coordinates of the *Reference Set*. These data, which include the luminance values, represent the 3-D analogue of the 2-D *Reference Set* shown in Fig. 1.2(d).

Three diverse, practical lighting applications here demonstrate the CRM, seen in Figs. 1.6(a)– 1.6(c) using our D65 simulator. The first case, lighting of meat in displays, seen in Fig. 1.6(a), examines a lighting application where the illuminated object has somewhat subtle color variations. The

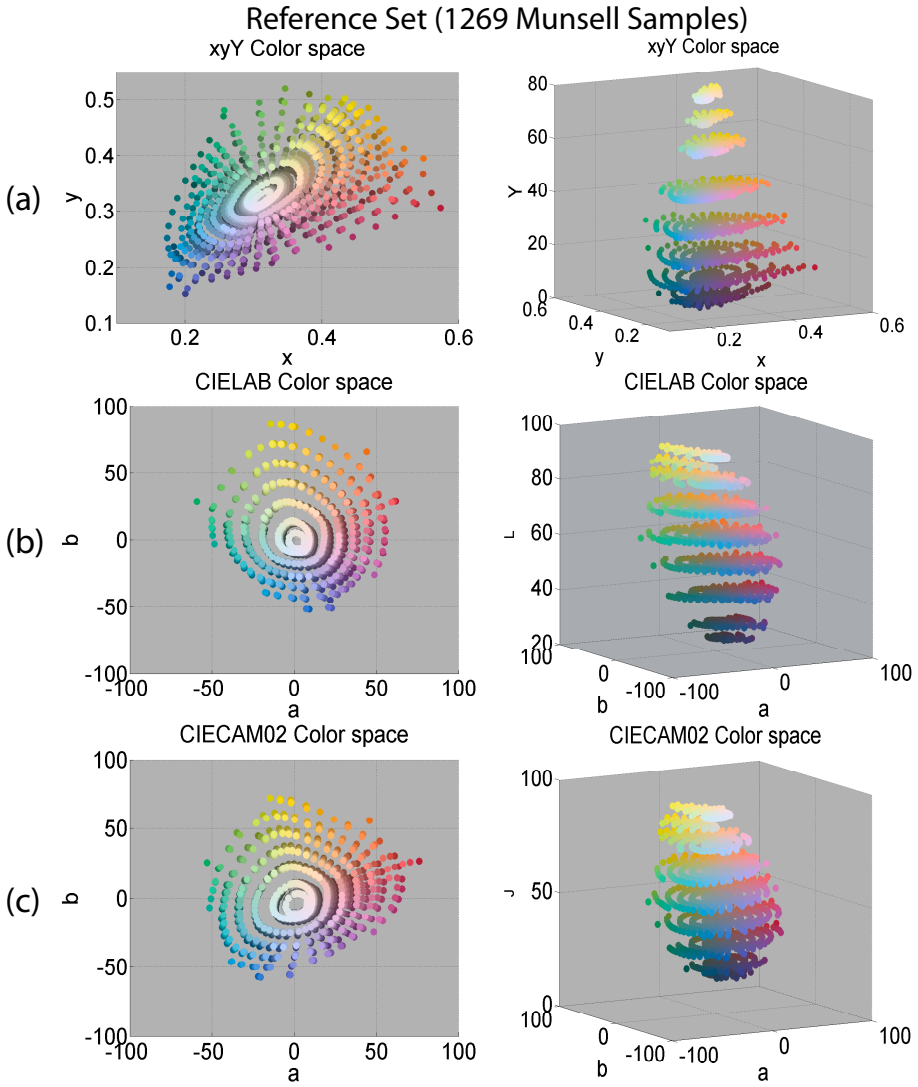

Figure 1.5: 3-D color space depiction of the 1269 color *Reference Set*, analogous to 2-D representation of Figure 1.2d, as used in the application examples. These are seen in two views: Azimuth = 0°, Elevation = 90° (left column) and Azimuth = -30°, Elevation = 10° (right column). The equivalent *Reference Set* is demonstrated in three versions of color space: (a) CIE-1931 xyY, (b) CIE-1976 CIE L*a*b*, and (c) CIECAM02.

second, a collection of various fruits, Fig. 1.6(b), looks at a broader range of colors. Finally, Fig. 1.6(c), lighting of artwork, covers a most-diverse usage of colorfulness, saturation and lightness. For these three applications, we follow the method described in Section 3, determining the *Test Set* and evaluating R_{as} and R_{am} indices with differing light sources. Finally, we show the CRMs for each case. Table 1.1 shows some figures for *Observed Gamut* (pixels) and *Test Set* (selected Munsell samples) obtained for the three applications in Fig. 1.6.

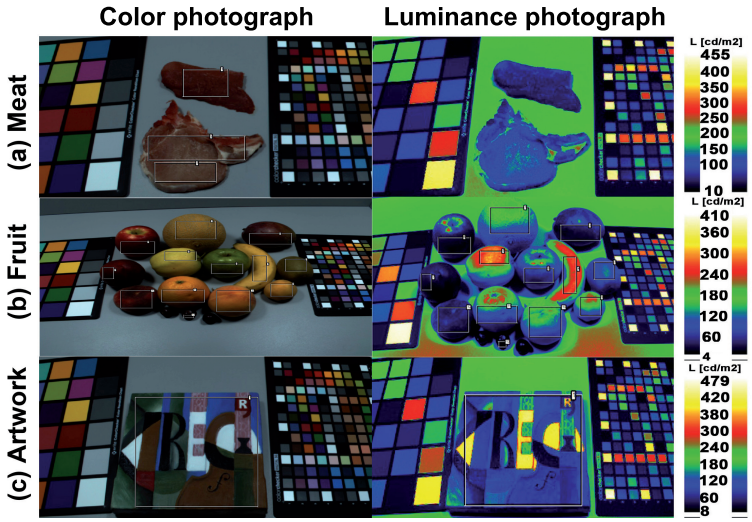

Figure 1.6: Color photograph (left column), taken under a D65 CIE standard illuminant simulator, of meat samples (a), assorted fruit (b) and artwork (c), along with corresponding luminance photographs of each scene (right column). The rectangles delineate the areas of interest to be analyzed. The color-checker cards are used to verify the calibration of the camera.

Table 1.1 highlights that the color differences (in our case, using the Munsell color samples) between *Test Sets* obtained using CIELAB and CIECAM02 for these three chosen applications is negligible.

The size of any *Observed Gamut* may comprise several mega-pixels, varying on how many, and how large, the selected areas of interest are. Therefore, an algorithm that extracts the volume surface of the *Observed Gamut*, is used to optimize data management for the CRM to be represented in a 3-D graphics.

The resulting *Test Set* (solely for the meat application), is shown in Figs.

Table 1.1: Comparative Results of Calculated *Observed Gamut* and *Test Set* using CIELAB and CIECAM02 Color Systems for Three Different Applications.

Application	**Color system**	***Observed Gamut* (pixels)**	***Test Set* (Selected Munsell Samples)**	**Average Multiplicity**
Meat	CIELAB	29.401	231	127
	CIECAM02	29.401	232	127
Fruit	CIELAB	134.207	170	789
	CIECAM02	134.207	174	771
Artwork	CIELAB	194.208	611	318
	CIECAM02	194.208	610	318

1.7(a)– 1.7(c), as derived from the measurements of the application in Fig. 1.7(a). The *Test Sets* of Figs. 1.7(a)– 1.7(c) show the two different angles of view depicted in Figs. 1.7(a)– 1.7(c) for the CIE-1931 xyY, CIELAB and CIECAM02 color spaces.

The *Test Set* for each application is obtained by evaluating the minimum Euclidean distances from each single pixel of the *Observed Gamut* to each element of the *Reference Set* (i.e. the closest Munsell sample to that pixel), in these cases using the cylindrical coordinates in CIELAB and CIECAM02. Figure 1.8 shows the 3-D xyY *Test Set* for the three example applications as seen in Figs. 1.6(a)– 1.6(c).

We now analyze three different light sources (with comparable CCT's and R_a's) as shown in Fig. 1.9 (left) by following the steps described above for the calculation of the *Test Set* and for the indices R_{as} and R_{am}. It can be seen (Fig. 1.9, left) that even though the R_a value remains essentially the same for each light source (and strictly the same for each application because it only depends on the spectral content of the light source), the R_{as} and R_{am} indices change from application to application. This demonstrates how the CRM and the derived indices constitute a useful tool for the lighting designer when personalizing scenes in specific applications. When high color rendering is of importance (i.e. retail, artwork, surgery , etc.), the use of customized indices such as R_{as} and R_{am} enables the user to establish specific threshold constraints which need to be met.

For the lamps studied in Fig. 1.9, the highest values of R_{as} and R_{am} are obtained for the artwork application, since artwork shows a *Test Set* with the widest range of hues.

Beyond the single-number indices R_{as} and R_{am}, a full description of the situation can be found in the next 3 figures, where the 3D-CRM has been

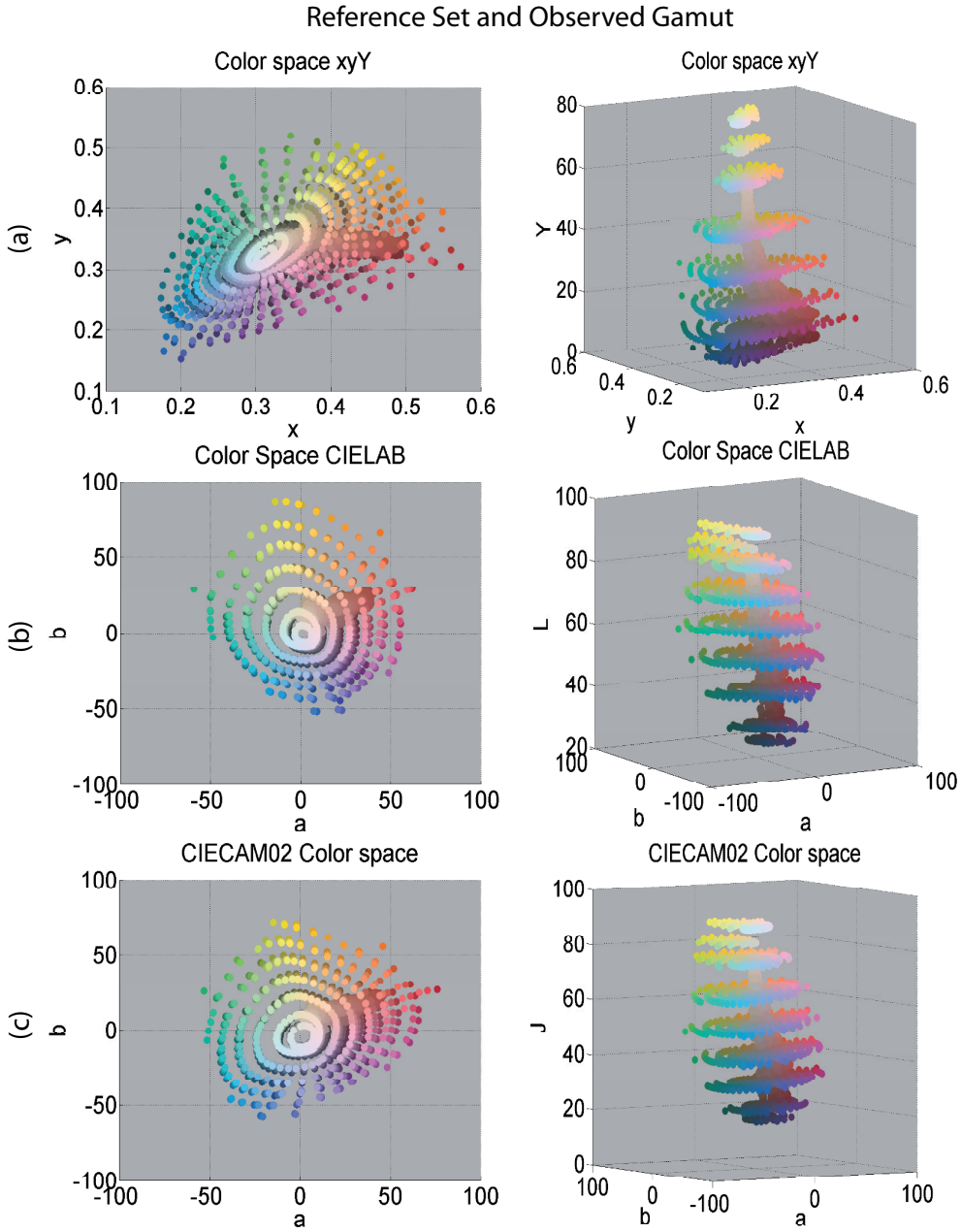

Figure 1.7: *Observed Gamut* data measured under a D65 simulator from the meat application shown in Fig. 1.6(a), in three versions of color space: CIE-1931 xyY (a), CIE-1976 L*a*b* (b) and CIECAM02 (c). These are seen in two views: Azimuth = 0°, Elevation = 90° (left column) and approximately Azimuth = -30°, Elevation = 10° (right column)

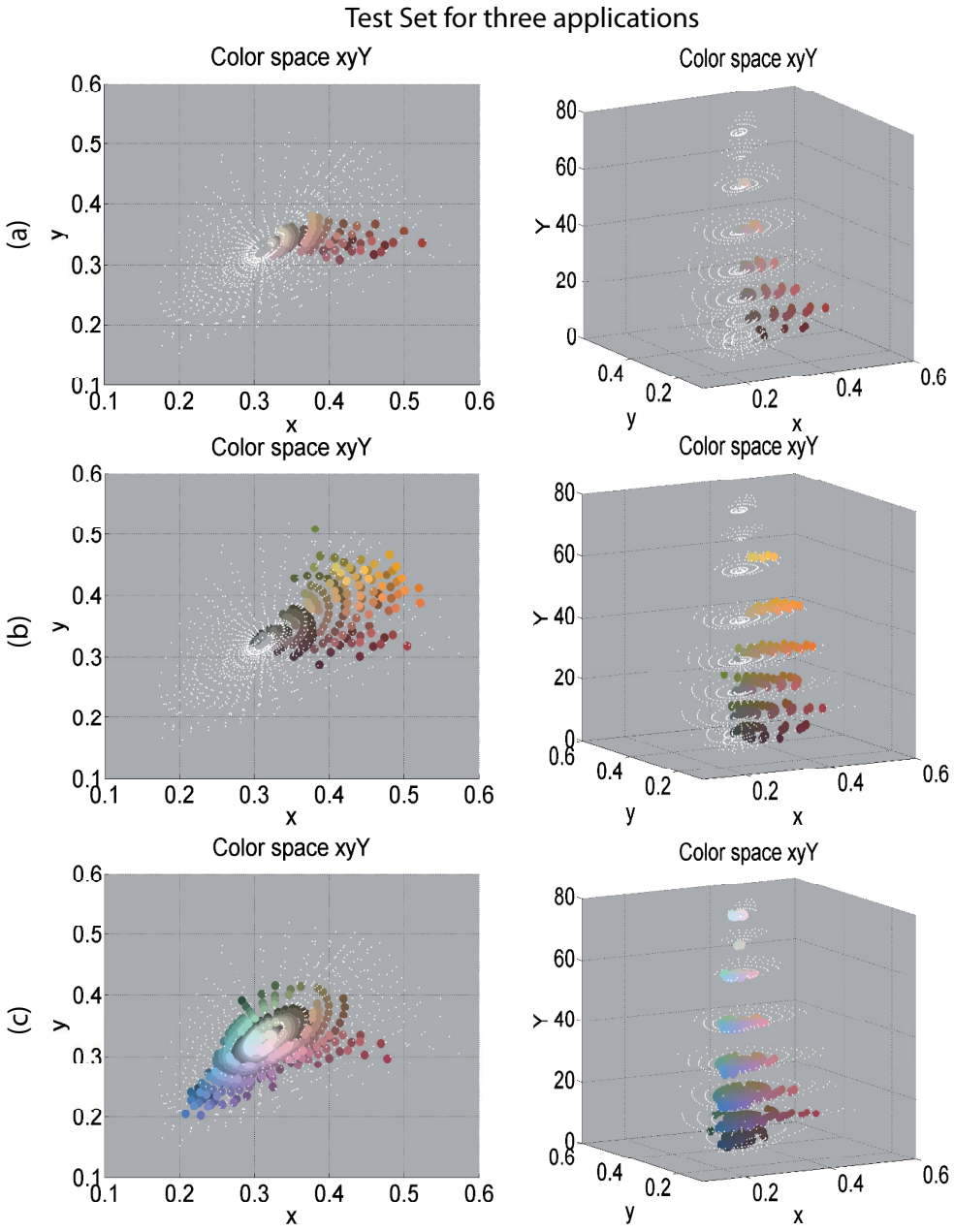

Figure 1.8: xyY representation of the *Test Set* found for the meat (a), fruit (b) and artwork (c) applications of Fig. 1.6.

evaluated and is shown for the different applications, i.e. meat (Fig. 1.10), fruit (Fig. 1.11), and artwork (Fig. 1.12).

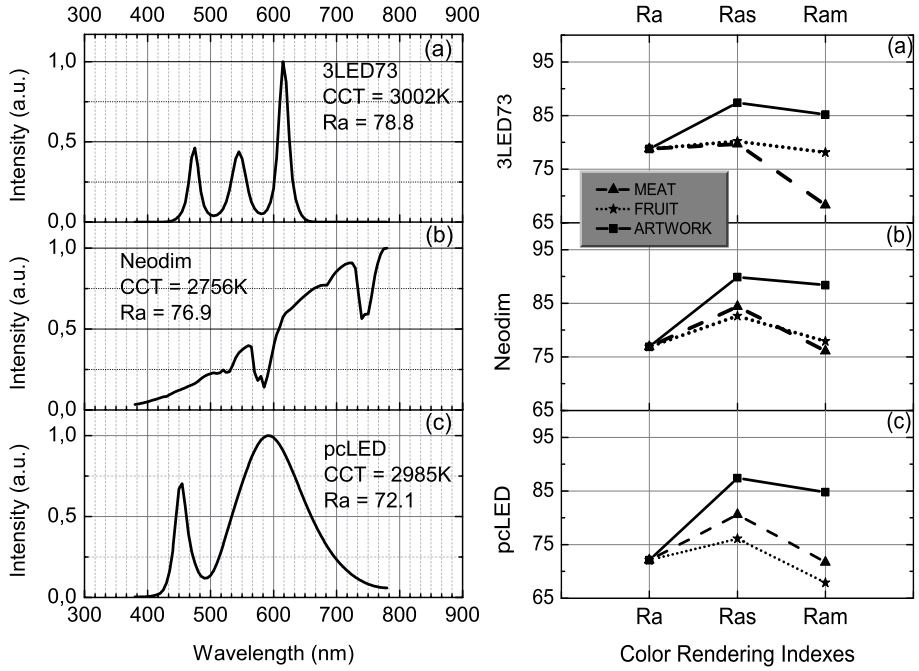

Figure 1.9: Left column: Three differing light sources, CCT=3000K , (a) R-G-B LED, (b) incandescent Neodimium lamp, and (c) Phosphor-converted LED. Right column: Corresponding color rendering indices CIE-R_a, R_{as} and R_{am}, for the three applications (*Test Set*) Meat, Fruit and Artwork.

Finally, by extracting the left column of Figs. 1.10– 1.12 and the R_{am} values from Fig. 1.9, we obtain Fig. 1.13, which is a useful in assessing the suitability of the three light sources for three different applications. Although each sub-plot in Fig. 1.13 shows just one angle of view of the 3D-CRM, this graphical representation along with the single-number R_{am} index, gives both intuitive (visual) and quantitative information. Our combined representation comes in handy when comparing the color rendering capabilities of different light sources for a specific application, or the suitability of a light source for different applications.

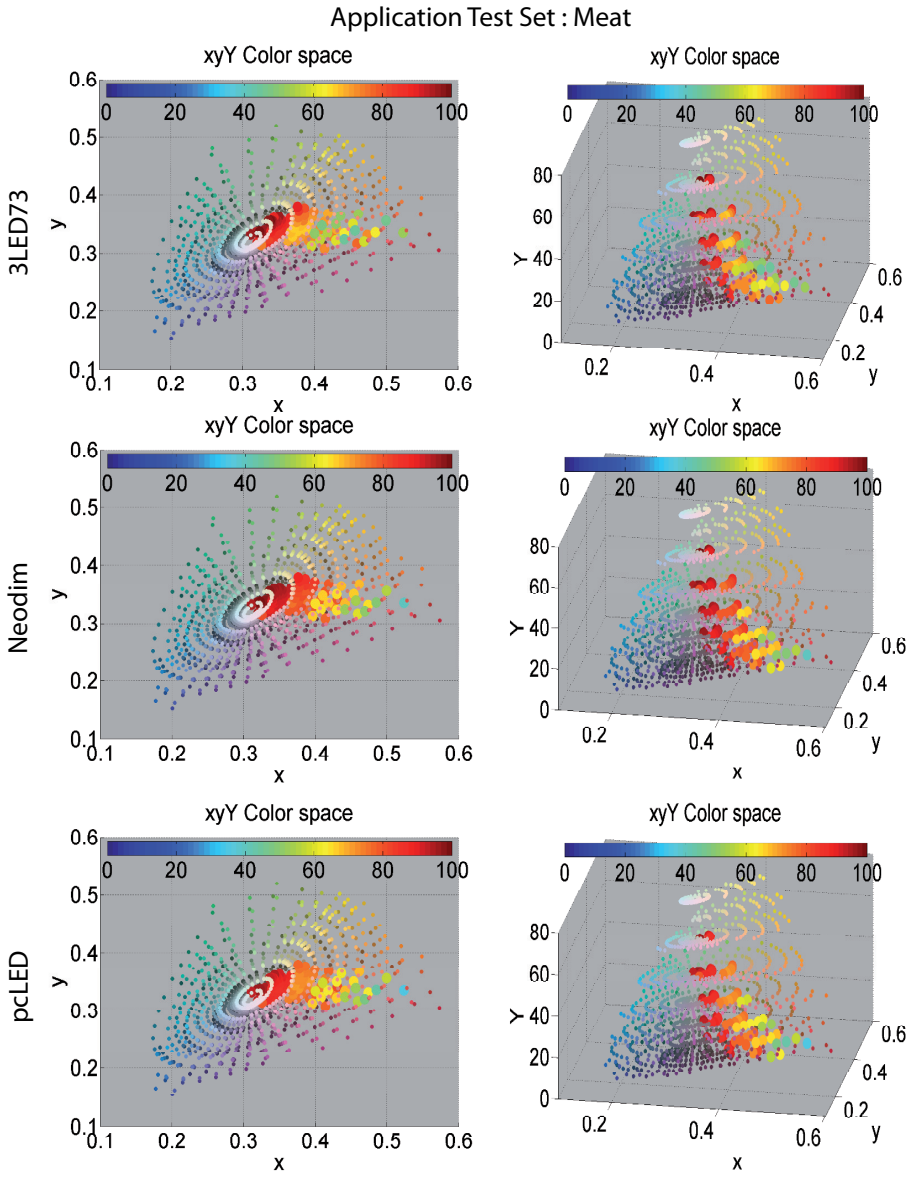

Figure 1.10: CRM representation in xyY color space of the *Test Set* found for the meat application of Fig. 1.6, and illuminated with the light sources of Fig. 1.9. R-G-B LED (upper row), Neodimium (middle row) and phosphor-converted LED (lower row). These are seen in two views: Azimuth = 0°, Elevation = 90° (left column) and Azimuth = 10°, Elevation = 24° (right column).

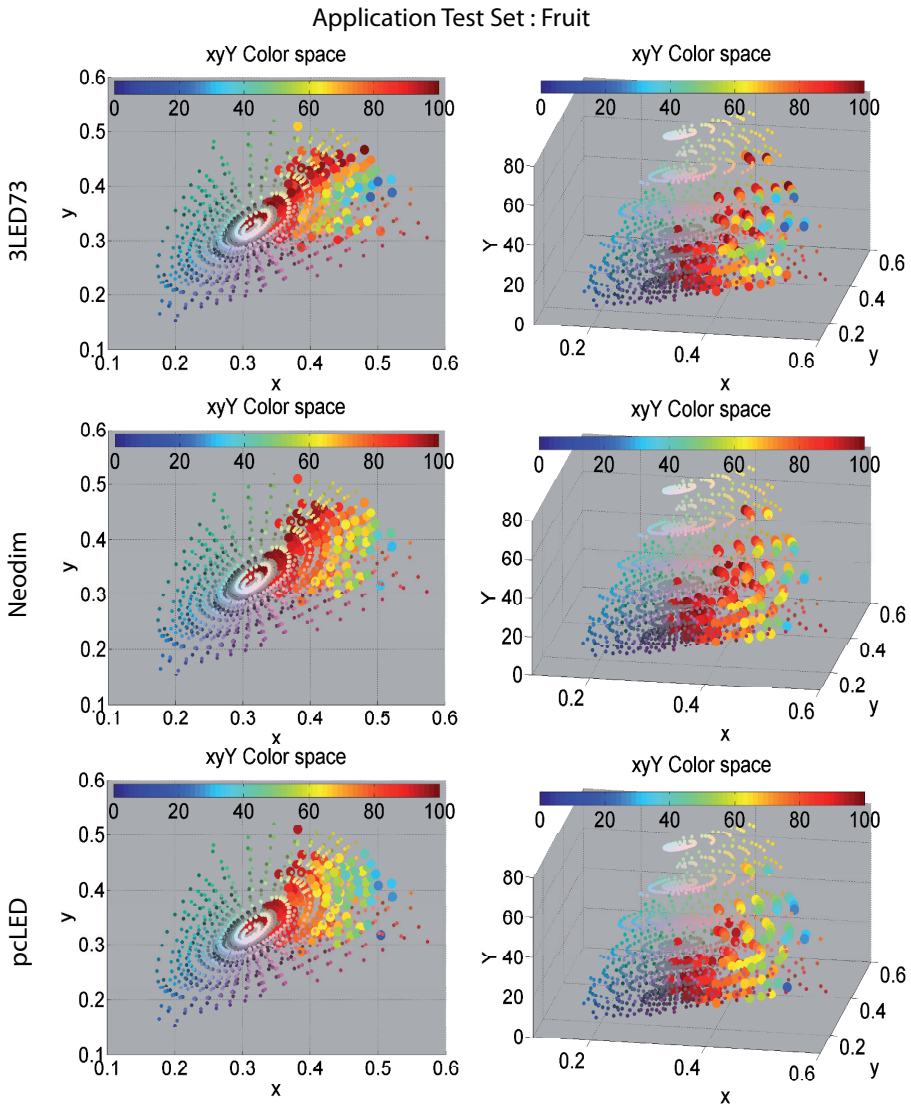

Figure 1.11: CRM representation in xyY color space of the *Test Set* found for the fruit application of Fig. 1.6, and illuminated with the light sources of the Fig. 1.9. R-G-B LED (upper row), Neodimium (middle row) and phosphor-converted LED (lower row). The same views as in Fig. 1.10 are shown.

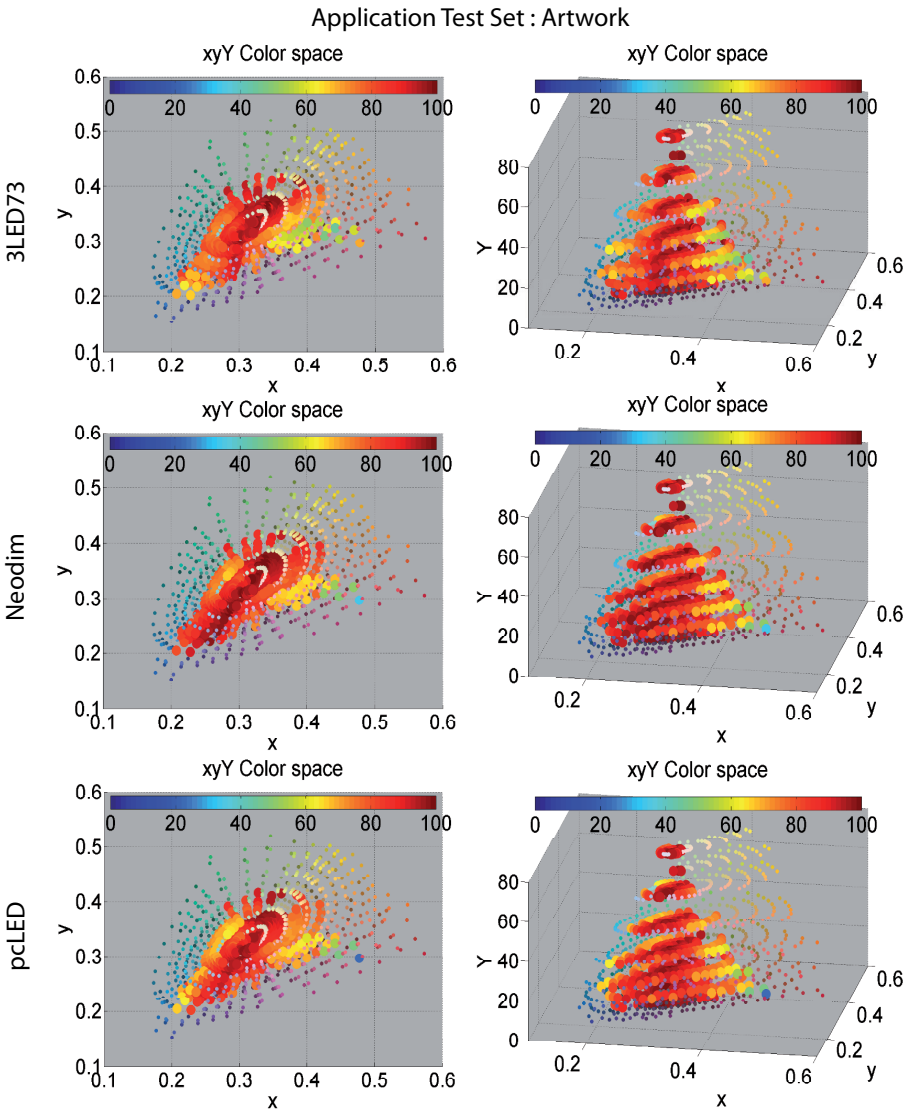

Figure 1.12: CRM representation in xyY color space of the *Test Set* found for the artwork application of Fig. 1.6, and illuminated with light sources of the Fig. 1.9. R-G-B LED (upper row), Neodimium (middle row) and phosphor-converted LED (lower row). The same views as in Fig. 1.10 are shown.

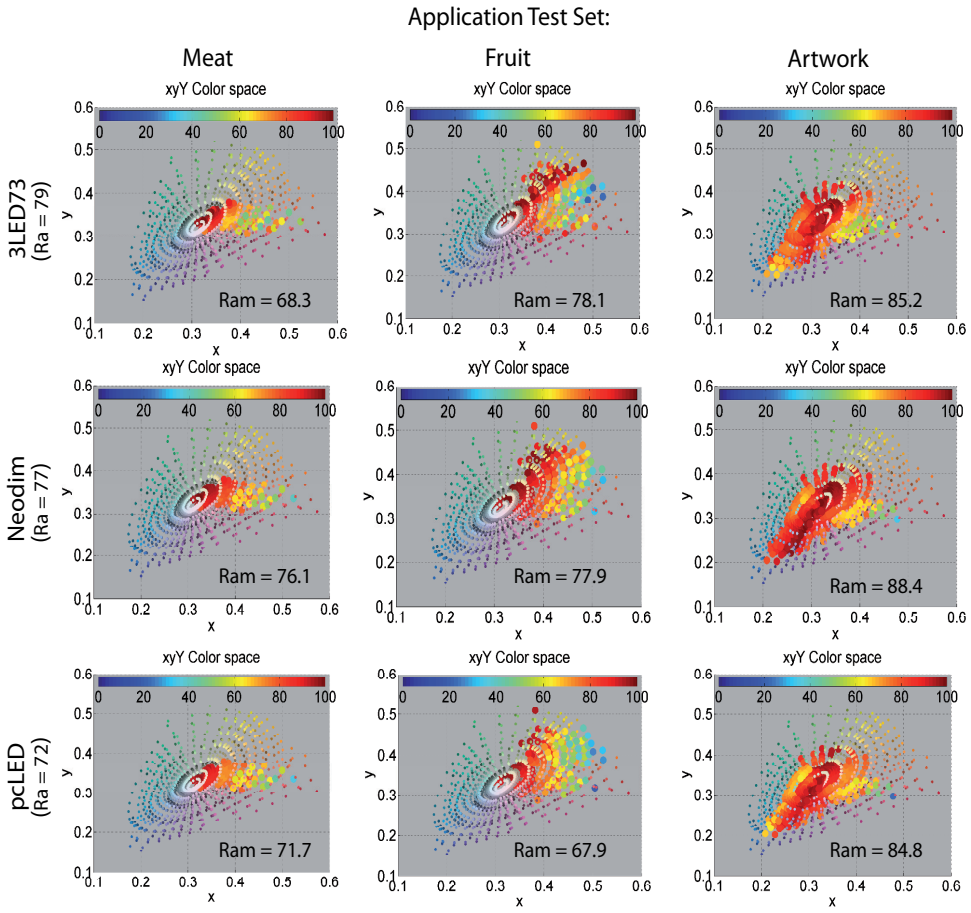

Figure 1.13: CRM representation in xyY color space of the *Test Set* for the three applications shown in Fig. 1.6, illuminated with light sources of Fig. 1.9. R-G-B LED (upper row), Neodimium (middle row) and phosphor-converted LED (lower row). Only one view is shown.

1.5 Discussion

With the advent of SSL and other new technologies to come (Quantum Dots, Nano-wires, OLEDs, etc.), a great revolution in the lighting industry is underway. This is not only due to their promised energy efficiency, but also because they offer us the flexibility to make spectral matching and tuned color reproduction a reality. In the same way the lighting designer

evaluates the position of the luminaires based on the desired illuminance and luminance levels of surfaces, another factor now comes into play: the color rendering of special or specific regions.

The CRM presented in this work constitutes a first attempt to develop a complete methodology that takes as an input not only the spectrum of the light source but also the color coordinates of the pixels of the scene involved, making it possible to find the best spectral content in illuminating different applications.

In the process of evaluating light sources, the 2-D CRM shows the user or lighting designer not only average, or weighted average of color rendering, but also, as is readily seen in Fig. 1.2, where the various deficiencies lie in the spectral content of any given light source. The CRMs of Figs. 1.2(a)–1.2(b) show clearly the expected red weaknesses in tri-junction LED lamps and trichromatic fluorescent sources. The restricted blackbody spectrum of Fig. 1.2(c), which is cut off at 450 and 650nm, has its saturated blue and red deficiencies immediately evident in the CRM. For a user who knows what part(s) of color space are important to a specific application, a 2-D CRM of any light source will immediately verify the applicability.

The 3-D CRM similarly allows a user to identify the areas of utility of color space, as well as lightness (volumes) within an application. Figures 1.10, 1.11 and 1.12 make the differences in the three demonstrated applications clear, not only in chromaticity and luminance; but also in diversity of color. This can be important if further metrics, such as efficacy or metamerism need to be considered in selecting a lamp for a chosen application: As we have seen, different light sources can have differing weak points, in luminous efficacy of radiation, over their spectral output. This inclusion of multiple metrics, and the level of sophistication required in the lighting design, become the indicators of what level of color appearance model (ie. simple, such as CIE-1931 xyY, versus complex, such as CIECAM02) ought to be employed in generating specific CRMs.

Also, although the Munsell gamut was used in this demonstration of the CRM, as the *Reference Set*, as well as the three well-known CIE color models, there is broad flexibility to expand or contract these, according the type of mapping which is desired. A *Reference Set* can range from a few hundreds of sample colors to a sophisticated color ordering system, such as the NCS or the OSA Uniform Color Scale, for a range of applications from illuminating highways to specialty lighting, such as used in medicine or cinematography. Also, a broad range of color appearance models, which also vary significantly in sophistication and power, can be used, as has been demonstrated here.

1.6 Conclusion

A method for evaluating light sources, and also for evaluating (and/or comparing) that source's desirability in specific applications using a graphical metric, the Color Rendering Map, has been described and demonstrated. A systematic method for evaluating light sources, regardless of application, has been shown using the 2-D CRM. The method of extending the evaluation to specific applications of any source has been described by using the 3-D CRM.

Solid State Lighting and the forthcoming emerging technologies will allow spectral reproduction in the near future. At that point, the Lighting Designer will be challenged by a situation in which the spectral content of a light will have to be adapted to its intended final application or space location. With this perspective in mind, the CRM constitutes an excellent tool for expanding illuminance and luminance-based designs to include color-based designs in the future.

The value of these methods is seen in their visual, graphical depiction in a map, as opposed to less descriptive, and potentially ambiguous, numeric metrics. The CRM also allows considerable flexibility in its implementation, both in limiting or expanding the palate of colors over which the user wishes to consider, or in limiting/expanding the color space for the graphical mapping.

Chapter 2

Color fidelity and Colorfulness as a description of color quality

In this chapter, the main attributes known to affect color quality are treated statistically over a set of 118 spectra representing the current mainstream lighting technology. The color rendering index (CRI) is used to assess color fidelity while colorfulness is used to complement CRI-R_a, supported by the growing evidence that assessment of light spectra cannot overlook color preference inputs. Colorfulness is evaluated by our optimal color (O_c) index, through a code that computes the (MacAdam) theoretical maximum volumetric gamut of objects under a given illuminant for all the spectra in our database. Pearson correlation coefficients for CRI-R_a, the (Y. Ohno's) color quality scale (CQS) and O_c show a high correlation (0.950) between CRI-R_a and CQS-Q_a, while O_c shows the lowest correlation (0.577) with CRI-R_a, meaning that O_c represents the best complement to CRI-R_a and Q_a for an in-depth study of color quality.

2.1 Introduction

Different quality color dimensions for light sources in general lighting have been studied for more than 40 years. Despite the fact that the CIE general color rendering index (CRI-R_a) [CIE13.3, 1995] is in a re-evaluation stage, it is widely accepted among the different players in the general lighting sector. The CIE-CRI-R_a index compares test and reference illuminants over 14 reflectance samples. However, beyond the CRI-R_a, there exists another dimension of color quality, colorfulness, that is being intensively studied in recent years due to the market growth of the LED technology, which is known to enhance object chroma. Chroma affects subjective aspects of color perception.

2.2 Color Fidelity and Colorfulness

Guo and Houser [Guo and Houser, 2004] made a comparison of nine color quality indices and Akashi (in his comment to this work [Akashi, 2004]) proposed dividing these nine indices into at least two groups: The first group would be driven by fidelity, i.e., how similarly test and reference illuminants render object colors, while the second relies on geometric attributes of objects in color spaces such as the gamut area or volume, as quantifiers of the colorfulness that the light source is able to provide. Subjacent to this is the idea that color fidelity schemes are not sufficient, and colorfulness information are required in order to have a complete description.

[Smet et al., 2011b] found that predictive performance in terms of naturalness is negatively correlated with the predictive performance for preference. Therefore, a metric that rates naturalness attributes well necessarily has to rate attractiveness poorly. This assertion confirms the finding of Rea and Freyssinier[Rea and Freyssinier, 2010], where a complete description of all aspects of color quality of a light source would likely require more than one metric. Previous results of [Smet et al., 2011a] are in agreement with Bartleson's findings [Bartleson, 1960] and several other studies, confirming that colors of familiar objects are remembered as being more vivid and saturated than in reality are, and that the recalled color (termed "memory color") is usually preferred than the real one.

In this way, the statistical analysis proposed by [Zukauskas et al., 2009] and [Žukauskas et al., 2011] through the use of color rendering vectors also concluded that color quality of solid state white lamps "should not be rated by a single figure of merit and require at least two: for color fidelity and saturation". Object color saturation indexes could also be a good complement to color rendering maps [Quintero et al., 2012e].

Further evidence in [Davis and Ohno, 2010] and [Ohno, 2004] suggests that increases in object chroma, as long as they are not excessive, are not detrimental to color quality and may even be beneficial. To quantify this, Davis and Ohno proposed the Gamut Area Scale (Q_g) [Davis and Ohno, 2010], as a support to the general color quality scale (Q_a). Figure 1 shows their color saturation icon for an RGB 3000K white LED that has a $Q_g = 111$. A Q_g greater than 100 reflects the ability of a light source to increase the object saturation in the regions where the plot exceeds the circumference boundary, as compared to the D65 CIE-standard illuminant ($Q_g = 100$),

represented by the white circumference in Fig.2.1(b).

2.3 Volume of Optimal colors boundaries as a Color Quality Index

It becomes clear that color quality has at least two quasi-orthogonal dimensions that give complementary information. The volume in the CIELAB space has been recently used to calculate spectra maximized for colorfulness in [Masuda and Nascimento, 2012]. The theory underlying the spectral properties of optimal colors, i.e., the colors with maximum purity for a given luminance factor, was developed by [Schrödinger, 1920], and their chromaticities were computed later by MacAdam in 1935. His theory of the maximum visual efficiency of colored materials in [MacAdam, 1935b] and [MacAdam, 1935a] resulted in what we now know as the MacAdam limits for optimal colors.

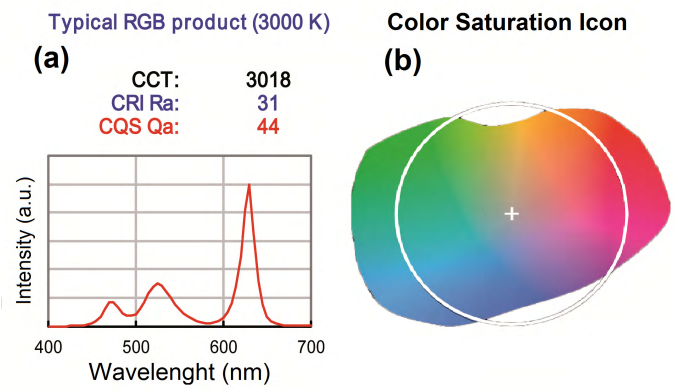

Figure 2.1: (a) Spectrum of a noncommercial 3000 K white RGB LED and (b) 2D saturation plot for the same 3000 K RGB LED with Q_g = 111 as compared to a CIE D65 standard illuminant (perfect circumference). Figure composed of images adapted from NIST spreadsheet Color Quality Scale ver 9.0.a 2011.

The development of indices to characterize the complex visual effects of illuminants is an actively studied topic that has been intensified by the need to characterize LEDs with almost arbitrary spectral profiles. In particular, the relationships between chromatic diversity and fidelity have been studied

computationally with outdoor and indoor scenes by [Linhares and Nascimento, 2012] and with artistic paintings by [Linhares et al., 2009]. Psychophysical studies have been also carried out for naturalness and chromatic diversity by [Nascimento and Masuda, 2012]. An explicit relationship between CRI and the MacAdam volume was derived by [Martínez-Verdú et al., 2007] for a set of selected illuminants.

2.4 Defining the O_c index

In this chapter, by using the convex hull method, we calculate the volume of the optimal colors of all light sources contained in a 118 spectra database (from Ohno's spreadsheet v9.0.a 2011). This database is large enough to represent all the currently available technologies, and will help us in the determination of the limits of the proposed index.

For each spectral power distribution of the 118-spectra database, we start from the the calculation of the optimal colors solid through the computational method proposed by [Masaoka, 2010]. Figure 2 shows the optimal color solid calculated for a 3000 K RGB-LED light source.

The method in [Masaoka, 2010] provides a relatively fast and accurate manner to calculate the solid comprised within the MacAdam limits. After obtaining the 118 optimal color solids, the convex hull volume (V_{ch}) subtended within the CIELAB color boundaries is calculated. The Vch ratio between the test light source and its reference light source as defined in CIE-CRI-R_a [CIE13.3, 1995] was calculated (and termed O_c), in analogy to the CQS-Q_g that is calculated in a similar manner from gamut areas, as seen in Eqs.2.1 and 2.2:

$$Q_g = 100 \left(\frac{GamutArea_{test}}{GamutArea_{ref}} \right)_{CIELAB} \tag{2.1}$$

$$O_c = 100 \left(\frac{V_{ch_{test}}}{V_{ch_{ref}}} \right)_{CIELAB} \tag{2.2}$$

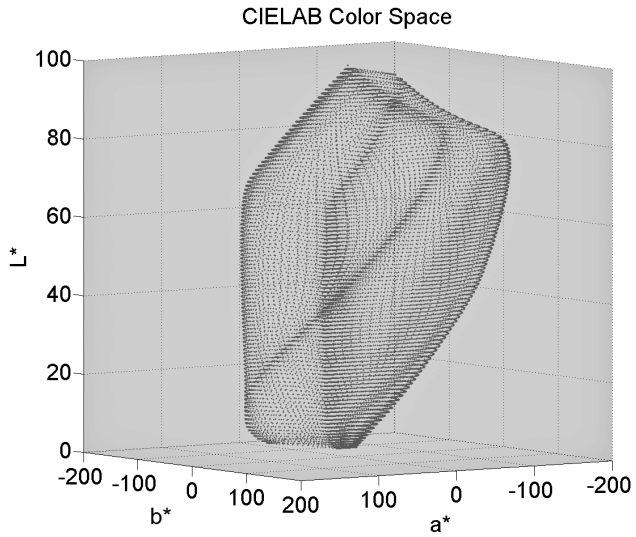

Figure 2.2: Optimal color volume (V_{ch}) for the 3000K-typical RGB light source of Fig.2.1.

2.5 Statistical analysis

In order to unravel the statistical correlation hidden into the variables CRI-R_a, Q_a, Q_g, O_c and V_{ch}, a statistical study was performed. This approach will allow us to find a minimal set of uncorrelated variables that optimally describe all the attributes of color quality.

Figure 2.3(a) shows that R_a and Q_a follow an almost identical trend as a function of the statistical percentiles (quantil function or inverse cumulative distribution function). This is manifested through a nearly constant Qa-R_a function on the right axis. On the contrary, Oc-R_a [see Fig.2.3(b)] presents a nonlinear relationship, meaning that O_c and R_a provide information about different attributes of color quality.

Statistical Pearson correlations along with their level of significance of the 118-spectra are summarized in "Table 1". The high similarity between CRI-R_a and Q_a observed in Fig.2.3 is confirmed by a correlation coefficient of 0.950. Thus, these two indexes do not complement each other, even when the CQS-Q_a was designed with a clear motivation of mixing color fidelity and people's preference for chroma enhancement, by using more saturated

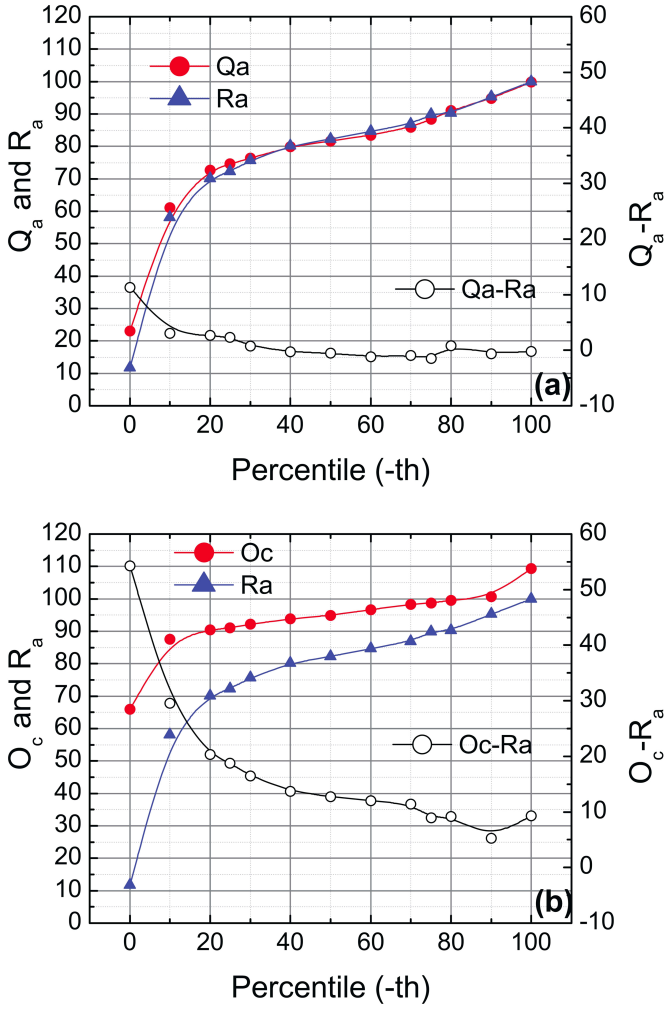

Figure 2.3: (a) Qa, Ra (left axis) and $Qa - Ra$ (right axis) as a function of the statistical percentiles and (b) O_c, Ra (left axis) and $O_c - R_a$ (right axis) as a function of the statistical percentiles.

Table 2.1: Pearson Coefficients of Correlation Between Different Pairs of Color-Related Indexes for the 118-Spectra Database

	R_a	Q_a	Q_g	O_c	V_{ch}
R_a	1	0.950*[a]	0.619*	0.577*	0.589*
Q_a		1	0.732*	0.606*	0.616*
Q_g			1	0.791*	0.784*
O_c				1	0.992*
V_{ch}					1

[a]Significance values (p-values) lower than 0.001 are indicated with an asterisk symbol.

test-color samples and not penalizing for increased chroma.

In "Table 1", it is seen that the less-correlated pair of variables are R_a and O_c. This means that maximal information of color quality is obtained when both variables are used in the assessment of light sources. It is worth noting that these two decorrelated indicators precisely correspond to the fidelity and colorfulness dimensions, respectively, in agreement with the results obtained through psychophysical studies.

2.6 Conclusion

The application of Pearson correlation coefficients of different attributes of color quality over an extensive database consisting of 118 spectra that represent the vast majority of different lighting technologies currently available in the market confirms that a joint specification of a fidelity index (R_a) along with a colorfulness index (our proposed O_c) is required for a complete statistical specification of color quality. This statistical approach reinforces a series of psychophysical studies performed recently such as [Guo and Houser, 2004], [Smet et al., 2011b], [Rea and Freyssinier, 2010], [Smet et al., 2011a], [Bartleson, 1960], and [Zukauskas et al., 2009], indicating that the colorfulness dimension of color quality is the best complement to indexes based on fidelity schemes (color differences from a reference source) such as CQS-Q_a or CIE-CRI-R_a.

From this chapter it becomes clear (both from psychophysical and statis-

tical standpoints) that a meaningful indicator of color quality should be a weighted function of R_a and O_c. Although it could be proposed for correlation coefficients to be the weighting factors for the definition of an ultimate color quality index, psychophysical tests would be required to support such a statement, reinforcing the need for future field works to quantify the role played by both color dimensions.

Chapter 3

Color quality and luminous efficacy ranking for light sources

A method for calculating two indexes that involves both luminous efficacy of radiation (LER) and colour quality (CQ) is presented. The generic name of these new indexes is Efficacy and Colour Quality (ECQ) and they are designed to classify groups of light sources in a ranking by analysing several of their spectrum features. With this calculation the optimal CQ/LER trade-off can be defined through the value given to a coefficient representing the weight that colour quality should have in the ranking established. Using a linear combination between the General Colour Quality Scale - Q_a proposed in [Davis and Ohno, 2010] and the Gamut Volume index O_c proposed in [Quintero et al., 2012c], we obtained an suitable ranking over the 121-spectra database studied. Furthermore, it was demonstrated that the Gamut Volume index O_c has a very similar behaviour to the Gamut Area Scale index - Q_g also proposed in [Davis and Ohno, 2010], indicating that both indexes are good predictors for object colour saturation of a light source.

3.1 Introduction

The selection of an adequate light source for a specific application involves the assessment of multiple factors, both subjective and objective, including colour temperature, preference for chroma enhancement (an increase of object colour saturation), and the well-known trade-off between Colour Quality (CQ) and Luminous Efficacy of Radiation (LER) required for each specific application. Currently, the only CIE standard index representing colour quality of a light source is the Colour Rendering Index CRI [CIE13.3, 1995]. However, because this index has several limitations in correctly predicting colour rendering of emerging light sources such as LED,

there is a general consensus about its re-evaluation. For these reasons, there have been several proposals to complement or replace this index which has not been updated since 1974. One of these proposals was presented by the author in [Quintero et al., 2012e], consisting in a graphical representation of the colour rendering of a light source that can be accompanied with a numerical index such as the ECQ proposed here. In a preceding analysis [Quintero et al., 2012c], the authors found that a good predictor for colour quality of a light source should have at least two components or indexes representing colour rendering and object colour saturation in order to deliver optimum colour fidelity and colour preference. With the aim to proposing an index to value colour quality of a light source, we start by calculating the optimal colour volume generated by the optimal colours solid limit proposed by [MacAdam, 1935b] and [MacAdam, 1935a]. This optimal colour volume is calculated over the 121-spectra light sources of Davis and Ohno work [Davis and Ohno, 2010] by using the algorithm proposed by [Masaoka, 2010]. In these terms, we calculate O_c, presented in [Quintero et al., 2012c] as the ratio between optimal colour volumes of test and reference light sources.

Since O_c is similar to $CQS - Q_g$ proposed by [Davis and Ohno, 2010], but calculated using theoretical maximum values for the object colour saturation, we can say that both are good indexes representing object colour saturation of a light source.

In order to find an adequate expression for colour quality to calculate the indexes Efficacy and Colour Quality (ECQ) and Efficacy and Colour Quality with Colour Temperature (ECQ_t) that combine both luminous Efficacy of radiation and Colour Quality, we evaluate different combinations between two indexes that predict colour rendering, i.e. CIE-CRI and $CQS - Q_a$, and two indexes that represent the object colour saturation: $CQS - Q_g$ and O_c. To meet the requirement, the Colour Quality equation has to give the highest score to well-recognized light sources having high colour quality. We used various math expressions to find an average between CIE-CRI and O_c using a trial and error process. We found a linear combination satisfying this requirement by using the square of the coefficients of correlation given in 3.1. Finally, after having defined indexes to be used and how to calculate colour quality, it is possible to calculate ECQ and ECQ_t indexes based on weight functions of light source indexes, such as LER, CRI, Q_a, Q_g, O_c, and CCT. Thus, the indexes ECQ and ECQ_t can serve as a tool for the selection or analysis of a spectra collection of light sources in order to choose a light source with specific characteristics in the balance between colour quality,

luminous efficacy of radiation and colour temperature. In this way, these indexes also can be useful as objective functions in optimization algorithms intended to synthesize light sources spectra with specific characteristics of colour quality, luminous efficiency of radiation and colour temperature of light sources based on monochromatic clusters of LEDs.

3.2 Method

In order to define and validate the behaviour of the ECQ and ECQ_t indexes we used the 121-spectra database taken from the spread sheet supplied courtesy of Wendy Davis and Yoshi Ohno from [Davis and Ohno, 2010]. We calculated the following indexes: The Gamut Volume O_c - calculated applying the model presented in [Masaoka, 2010], general colour Quality Scale ($CQS-Q_a$), Gamut Area Scale ($CQS-Q_g$), $CIE-CRI$, Correlated Colour Temperature (CCT) and Luminous Efficacy of Radiation (LER). Moreover, statistics such as 100 percentiles were also calculated for the first five indexes mentioned above.

3.2.1 Definition of the weight functions

Prior to defining the basic equations for ECQ and ECQ_t, we have to define the weight function for six indexes: LER, $CIE-CRI$, $CQS-Q_a$, $CQS-Q_g$, O_c and CCT. Each weight function defined for these indexes has an input range that covers all possible values of the respective index, and the output range goes from 0 to 1. They are intended to give more or less influence to the corresponding index according to their frequency distribution, or what the user or lighting application requires. Five weight functions were created by following the curve generated by 100 percentiles for these indexes calculated over the 121-spectra database and shown in Fig.1-(a) to Fig.1-(e). In contrast to these functions, the sixth weight function that corresponds to CCT is a Gaussian function with parameters T_d and σ.

$$f_{wt}(CCT, T_d, \sigma) = e^{-\left(\frac{CCT-T_d}{\sigma}\right)^2} \tag{3.1}$$

application, and σ represents the weight that user want to give to the desired temperature T_d. Figure 1-(f) represents this function with the parameters of $T_d = 4000K$, and σ taking values 1000, 5000 and 100000.

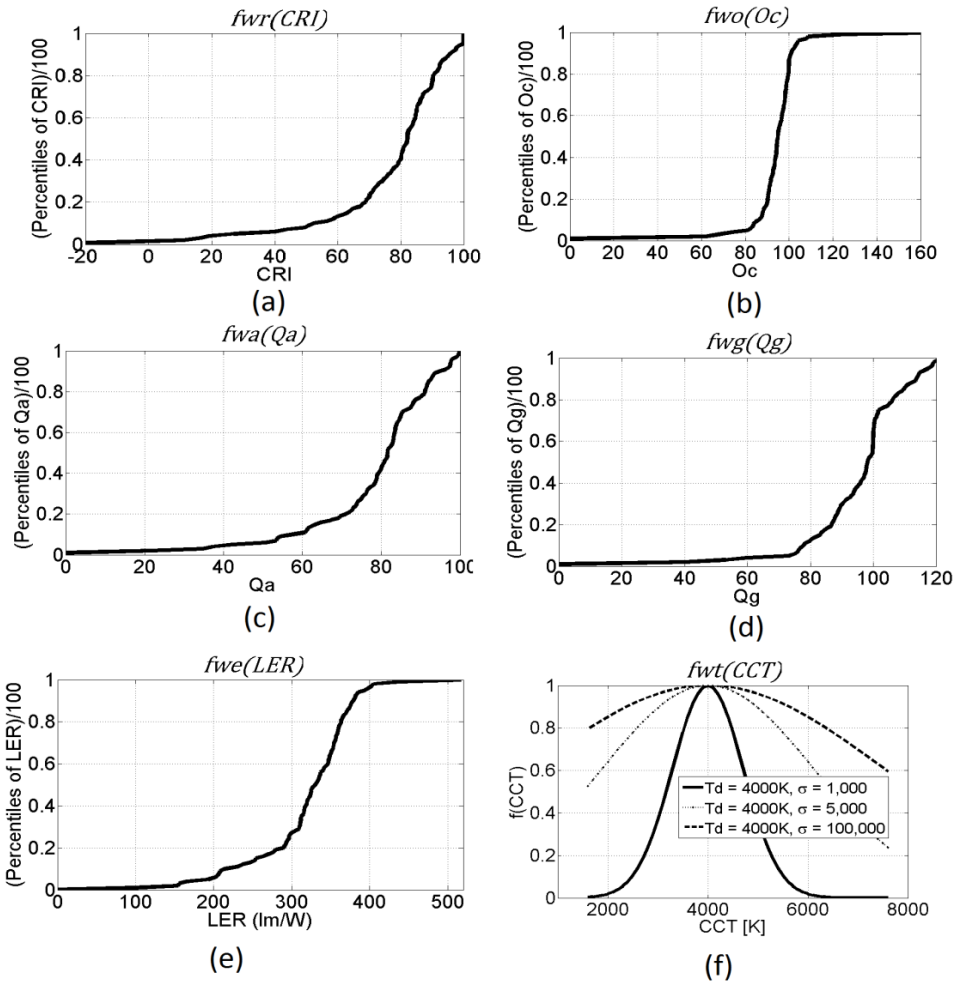

Figure 3.1: The weight functions based on 100 percentiles for parameters CRI, O_c, Q_a, O_c and LER, (a) to (e). Sub-plot (f) represents the weight function for CCT based in a Gaussian function plotted for $Td = 4000K$ and σ taking values: 1000; 5000 and 100000.

3.2.2 Definition of the colour quality term

As was shown in 2, a good index for colour quality of a light source should involve at least two indexes: One showing the colour rendering, i.e. by colour comparison (or colour fidelity), and another representing the object colour saturation that involves a subjective issue of colour preference.

In order to obtain the terms that can properly represent quality colour of a light source, we found the coefficients to calculate a weighted average between the CIE-CRI and Oc indexes, as explained above. We also wanted to evaluate other possibilities for this colour quality expression by using other three possible combinations including CQS-Qa and CQS-Qg indexes and the coefficients of correlation between these four parameters, as shown in Table 3.1.

Table 3.1: Pearson coefficients of correlation of color rendering and object color saturation for the 121-spectra database.

	$CIE-CRI$	$CQS-Q_a$	$CQS-Q_g$	O_c
CRI	1	**0,9496**	**0,6188**	**0,5773**
Q_a		1	**0,7319**	**0,6064**
Q_g			1	0,7913
O_c				1

Note: All values from this table have p-values for significance of correlation less than 0.001.

Now, we can formulate four options for a colour quality equation ranging between 0 to 1, by keeping the same structure of the equation found to evaluate colour quality by trial and error process and using the weight functions with their coefficients of correlation in Table 3.1.

$$f_1(CQ) = \frac{0,9496^2 f_{wa} + 0,6188^2 f_{wg}}{0,9496^2 + 0,6188^2} \tag{3.2}$$

$$f_2(CQ) = \frac{0,9496^2 f_{wa} + 0,5773^2 f_{wo}}{0,9496^2 + 0,5773^2} \tag{3.3}$$

$$f_3(CQ) = \frac{0,9496^2 f_{wr} + 0,7319^2 f_{wg}}{0.9496^2 + 0.7319^2} \tag{3.4}$$

$$f_4(CQ) = \frac{0,9496^2 f_{wr} + 0,6064^2 f_{wo}}{0,9496^2 + 0,6064^2} \tag{3.5}$$

Where f_w are weight functions defined by 100 percentiles of the metrics

calculated over the 121-spectra database and showed in figure 3.1, as follows:

$f_{wa} =$ *Weight function for* Q_a.
$f_{wr} =$ *Weight function for* CRI.
$f_{wg} =$ *Weight function for* Q_g.
$f_{wo} =$ *Weight function for* O_c.

In these terms we have to analyse four options, in order to conclude which one is the best option for the term corresponding to "Colour Quality" in the calculus of ECQ and ECQ_t indexes.

3.2.3 Definition of ECQ and ECQ_t indexes

As it was mentioned above, ECQ and ECQt indexes are intended to generate a ranking of several light source spectra. In this ranking the user has the possibility to choose the desired trade-off between luminous efficacy and colour quality by varying the value assigned to a input coefficient called kcq (coefficient of colour quality); the user can give to it values from 0 to 1, where kcq = 0 means zero importance to the colour quality in the ranking generated, while kcq = 1 means 100% of importance to the colour quality, Equations 3.6 and 3.7 show the basic form, or rms value, of the indexes ECQ and ECQ_t respectively.

$$ECQ_{rms} = \frac{1}{\sqrt{2}}\sqrt{[k_{cq} \times f(CQ)]^2 + [(1 - k_{cq}) \times f_{we}(LER)]^2} \tag{3.6}$$

$$ECQ_{trms} = \frac{1}{\sqrt{3}}\sqrt{[k_{cq} \times f(CQ)]^2 + [(1 - k_{cq}) \times f_{we}(LER)]^2 + [f_{wt}(CCT, T_d, \sigma)]^2} \tag{3.7}$$

Where:
$k_{qc} =$ *Coefficient of Colour Quality, it can take values from 0.0 to 1.0.*
$T_d =$ *Desired colour temperature in Kelvin..*
$\sigma =$ *Wide of the weight function for CCT, by default this parameter is set to 1000.*
$f(CQ) =$ *One of the four Colour Quality functions equation 3.2 to equation 3.5.*
$f_w =$ *One of the six weight functions in figure 3.1.*

From equations (3.6) and 3.7, we can see that when the coefficient kcq increases, the weight to the Color Quality term also increases, but the weight of the LER term decreases. In these terms, when k_{cq} equals zero, the output value of the ECQ, depends exclusively on the weight function for LER. In

other words, the ECQ index gives ranking to the spectra database, based only on their luminous efficacy of radiation value. The other extreme is presented when k_{cq} equals to one, in this case, the output ranking generated depends exclusively on the colour quality function.

In order to adjust the output values of ECQ and ECQ_t indexes to a range between 0 and 100, an extensive calculation of the equations 3.6 and equation 3.7 was performed using the four options for the colour quality term, equations 3.2 to 3.5, and varying values of Td from 1700K to 7500K in steps of 10K, k_{cq} from 0 to 1 in steps of 0.01 and σ from 1000K to 7000K in steps of 200K. Table 2 shows the maximum and minimum values found for the 121-spectra database. These values are used to define the intercept and scale factor (slope) of the linear equation for calculating ECQ and ECQ_t indexes.

Table 3.2: Maximum and minimum values found for ECQ_{rms} and ECQ_{trms} over the 121-spectra database

	ECQ_{rms}	ECQ_{trms}
$(Max) * 100$	70,71	81,65
$(Min) * 100$	0,15	0,15

Finally, equations 3.8 and 3.9 show how to calculate indexes ECQ and ECQ_t respectively. The use of these equations over the 121-spectra database guarantees that their output values are in the range from 0 to 100

$$ECQ = \frac{(ECQ_{rms} - 0,0015)}{(0,7071 - 0,0015)} * 100 \tag{3.8}$$

$$ECQ_t = \frac{(ECQt_{rms} - 0,0015))}{(0,7071 - 0,0015)} * 100 \tag{3.9}$$

3.3 Results

3.3.1 ECQ and ECQ_t with $k_{cq} = 0,0$ (full luminous efficacy required)

The score for the first 15 items ranked by ECQ and ECQt with $k_{cq} = 0,0$ (ECQ_0, ECQ_{t0}), $Td = 4500K$ and $\sigma = 1000$ calculated over the 121-spectra database are shown in 3.3. Here we can see that the score of the ECQ column is defined entirely by the values of the parameter LER, regardless

of the colour quality function $f(CQ)$ and CCT values. While the values of the ECQ_t column are affected by the CCT values, giving higher scores to light source with colour correlated temperature close to 4500K.

Here we have to highlight that the value of the ECQ_0 for a specific light source gives an idea of its position in the group respect to the maximum efficacy attainable ($ECQ_0 = 100$). For example, from the values of ECQ_0 in Table 3.3, we can say that all 15th light sources are approximately in the fourth quartile of the luminous efficacy of radiation for the 121-spectra database.

Table 3.3: First 15 items of the ranking defined by ECQ and ECQt with $k_{cq} = 0,0$; $T_d = 4500K$ and $\sigma = 1000$ for the 121-spectra database.

Lamp_Type	**Efficacy**	**CCT**	**CRI**	**ECQ0**	**ECQt0**
(#_ Description)	**lm/W**	**K**	—	—	—
013_LPS	516,9	1720	-47	100	70,7
014_457-540-605	408,3	3303	80	98	71,3
068_RGB(Ra=67)	404,8	3304	67	98	71,3
070_RGB(Ra=80)p.c	402,6	3304	80	97	70,6
018_3-LED-2Yellow	399,9	3306	85	96	69,9
032_Ide_Prim_Col	393	4240	69	95	94,2
082_Duv=+0.010(47	396,1	3005	86	95	67,5
081_Duv=+0.006(47	383,9	3003	85	93	66,1
093_4peak3012Kds4	382,6	2981	70	93	66,1
047_C100S54(HPS)	381,9	1970	16	92	65
062_F34T12/LW/RS	380,5	4165	50	91	90,2
009_HPS	380,9	2074	20	91	64,3
072_RGB_CRI_optim	378,3	3302	90	90	65,8
055_F34T12WW/RS/E	376,5	3013	50	89	63,3
094_4peak3020Kds3	375,6	2986	76	88	62,6

3.3.2 ECQ for $k_{cq} = 1.0$ (full colour quality required)

In this case, a comparison between the results of using each one of the colour quality function in equations 3.2 to 3.5 was performed. As a result, Table 3.4 shows the first 15 items ranked by ECQ with $k_{cq} = 1.0$ (ECQ100) using the four options for the colour quality term in equation 3.8.

Table 3.4: First 15 items of the ranking defined by ECQ with $k_{cq} = 1,0$ ($ECQ100$) using four different options for the colour quality term and evaluated over the 121-spectra database

Lamp_Type	$f_4(CQ)$; eq. 3.5 using CRI & O_c		$f_2(CQ)$; eq.3.3 using Q_a & O_c		f1(CQ); eq. 3.2 using Q_a & Q_g		f3(CQ); eq. 3.4 using CRI & Q_g	
(Description)	ECQ100	Ranking	ECQ100	Ranking	ECQ100	Ranking	ECQ100	Ranking
126_CIE_illum_A	83,9	1	92,5	5	86,1	9	86,2	2
131_CIE_illum_D75	83,6	2	94,2	4	87,5	3	85,6	6
127_CIE_illum_D65	83,2	3	94,5	3	87,2	4	84,6	8
130_CIE_illum_D55	83,1	4	95,8	2	87,1	6	82,8	11
129_CIE_illum_D50	82,2	5	96,2	1	87,2	5	81,4	15
011_Incandescent	80,5	6	91,5	6	84,8	12	82,3	13
046_60A/W(SofW	80,5	7	91,5	7	84,8	13	82,3	14
102_Broad4030Kref	79	8	89	9	86,6	7	85,9	4
041_CIE-F8	78,9	9	90,9	8	82,1	**16**	78,4	**17**
092_Broad3050	77,9	10	87,7	12	80,2	**20**	78,2	**18**
128_CIE_illum_C	77,2	11	88,6	11	88	2	85,9	5
031_EEW(380-780nm	76,1	12	88,7	10	88,2	1	85,1	7
057_F40/C75	74,5	13	86,7	13	82,5	15	78,8	**16**
019_461-526-576-6	74,1	14	81,7	**18**	84,8	11	86,3	1
097_4peak3000Kneu	73,9	15	82,6	15	85,2	10	86	3

If we take as a reference the ranking given by ECQ100 calculated by using equation 3.5, i.e. by using $CIE - CRI$ and O_c, as Table 3.4 shows, we can see that several differences exist with the ranking established using the other functions for colour quality. To evaluate these differences over the 121-spectra database, we calculated the average of the ranking number difference ($D_{j,k}$), as is expressed in equation 3.10.

$$D_{j,k} = \frac{1}{121} \sum_{i=0}^{121} \sqrt{(R_{ij} - R_{jk})^2} \tag{3.10}$$

Where:

j and k can take values: $1, 2, 3$ or 4 (four different options for the colour quality term in ECQ).
$R_{i,j}$ is the ranking number assign by $ECQ100$ for the i-th spectrum of the 121-spectra database with the j-th option for colour quality term.

From Table 3.5, we can determine how different the ranking established are over the 121-spectra using the four options presented in Chapter 2.2 for calculation of ECQ. We can take as a reference the function $f_4(CQ)$, with the CRI is a CIE standard, Oc is a value based on a theoretical maximum and the first seven items of its ranking generated by ECQ_{100} correspond to light sources that are well-recognized having high colour quality. Therefore, we can conclude by the difference of ranking with $f_4(CQ)$ and because the

Table 3.5: Average differences of the ranking between the four options for $ECQ100$ in Table 3.4 calculated over the 121-spectra database

	$f_1(CQ)$ $Q_a\&Q_g$	$f_2(CQ)$ $Q_a\&O_c$	$f_3(CQ)$ $CRI\&Q_g$	$f_4(CQ)$ $CRI\&O_c$
$f_1(CQ); Q_a\&Q_g$	0	5,3	8,5	10,6
$f_2(CQ); Q_a\&O_c$	5,3	0	10,9	**8,7**
$f_3(CQ); CRI\&Q_g$	8,5	10,9	0	**8**
$f_4(CQ); CRI\&O_c$	10,6	8,7	8	0

light sources ranked in the first 7 positions, that $f_2(CQ)$, using weight functions of $CQS - Q_a$ and O_c, works adequately as a colour quality term for the calculation of ECQ and ECQ_t.

In addition, we can see that the lowest difference in ranking is presented between $f_1(CQ)$ and $f_2(CQ)$ functions; since both of them have as common factor $CQS - Q_a$, we can infer that $CQS - Q_g$ and O_c indexes have very similar performance, as was demonstrated in 2.6.

3.3.3 Representation of ECQ

Figure 3.2 shows a 3D representation of ECQ index that was calculated by using equations 3.8 and 3.3 with $\sigma = 1000$, and varying parameters k_{cq} and T_d. Here we can highlight that the light source with the maximum LER in the 121-spectra database (517 lm/W and $CCT = 1700K$) obtain a $ECQ = 100$ when the colour quality coefficient, $k_{cq} = 0.0$ (only the luminous efficacy term is taken into account), while this same light source got an $ECQ = 0$, for $k_{cq} = 1.0$ (only the colour quality term is taken into account), because its $CQS - Q_a$ and O_c are zero.

In general terms, we can say that this graphical representation of the ECQ index gives a quick and general idea of how well a ligh source can perform for its luminous efficacy of radiation and/or quality color characteristics. This could be useful in the process of selecting a light source for a especific aplication, in other words, a defined balance between luminous efficacy and color quality.

3.3.4 ECQ_{50}, ECQ_0 and ECQ_{100}

Table 3.6 shows the first 15th items ranked by $ECQ_{50}(k_{cq} = 0.5)$ using the selected colour quality function $f_2(CQ)$ that involve the weight functions $CQS - Q_a$ and O_c.

We have to highlight here, that using only the ECQ index, with different values of the coefficient k_{cq} (0,0; 0,5 and 1,0; in the case of Table 3.6), it

Table 3.6: First 15 items of the ranking defined by ECQ with $k_{cq} = 0,5$ (ECQ_{50}), and its values with $k_{cq} = 0$ and 1 (ECQ_0 and ECQ_{100}) using the selected colour quality function $f_2(CQ)$ evaluated over the 121-spectra database

Lamp_Type	LER	CCT	CRI	Q_a	Q_g	O_c
(Description)	lm/W	K	—	—	—	—
019_461-526-576-6	360	3300	98	93	102	97
022_4LEDwith_ yel	359	3300	94	91	106	98
071_RGB(Ra=80)	375	3303	80	85	108	97
021_4LED_no_yel	354	3304	92	92	97	98
081_Duv=+0.006(47	384	3003	85	81	95	95
018_3-LED-2Yellow	400	3306	85	77	90	96
032_Ide_Prim_Col	393	4240	69	69	115	167
082_Duv=+0.010(47	396	3005	86	78	91	95
124_CreeF	357	3036	90	87	100	98
078_TriDuv=+0.010	371	3010	84	79	94	109
097_4peak3000Kneu	342	2950	95	93	107	98
020_4-LED-2(447	347	3300	91	92	98	98
125_CreeF2	353	3062	90	88	101	99
014_457-540-605	408	3303	80	74	95	90
073_4-color(Ra=90	349	3300	90	91	97	98

Lamp_Type	ECQ_{50}	R	ECQ_0	R	ECQ_{100}	R
(Description)	—	#	—	#	—	#
019_461-526-576-6	56	1	77	28	82	18
022_4LEDwith_ yel	54,4	2	76	30	78	26
071_RGB(Ra=80)	54,2	3	87	16	65	44
021_4LED_no_yel	52,3	4	70	37	78	27
081_Duv=+0.006(47	52,2	5	93	8	48	65
018_3-LED-2Yellow	51,7	6	96	5	39	77
032_Ide_Prim_Col	51,5	7	95	6	40	74
082_Duv=+0.010(47	51,4	8	95	7	40	75
124_CreeF	50,6	9	72	34	71	35
078_TriDuv=+0.010	50,5	10	85	18	55	54
097_4peak3000Kneu	50,4	11	58	51	83	15
020_4-LED-2(447	50,4	12	61	47	81	22
125_CreeF2	50,2	13	67	40	75	32
014_457-540-605	50,2	14	98	2	23	99
073_4-color(Ra=90	49,9	15	64	44	77	28

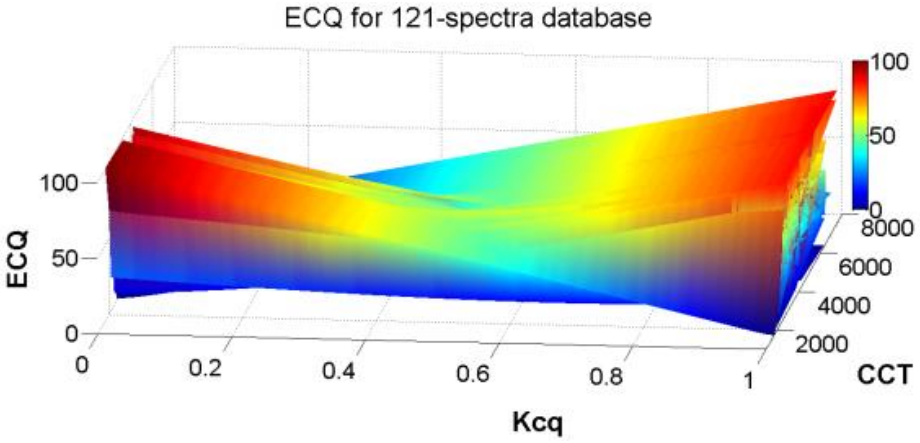

Figure 3.2: 3D representation for ECQ calculated over the 121-spectra database.

is possible to obtain a quick idea of how a light source behaves for luminous efficacy and colour quality; this characteristic could be very useful in spectrum synthetizing algorithms, in order to match a light source spectrum with specific characteristics of colour quality and luminous efficacy.

3.3.5 ECQ_{t50}, ECQ_{t0} and ECQ_{t100} with $T_d = 3000K$ and $\sigma = 1000$.

Table 3.7 shows the first 15 items ranked by $ECQ_{t50}(k_{cq} = 0.5)$ using the selected colour quality function $f_2(CQ)$, and parameters $T_d = 3000K$ and $\sigma = 1000$ (high weight to the correlated colour temperature).

From the data of Table 3.7, we can see that ECQ_t has higher values than ECQ, because the third CCT term increases the score. The ranking of Table 3.7 is quite influenced by the Correlated Colour Temperature of the light source, so it is evident that the highest score of ECQ_{t50} is given to the light source having the highest luminous efficacy and colour quality with the closest CCT to 3000K.

Table 3.7: First 15 items of the ranking defined by ECQ_t with $k_{cq} = 0,5$ (ECQ_t50), and its values with $k_cq = 0$ and 1 (ECQ_0 and ECQ_{100}) using the selected colour quality function $f_2(CQ)$ with parameters $T_d = 3000K$ and $\sigma = 1000$ evaluated over the 121-spectra database

Lamp_Type	LER	CCT	CRI	Qa	Qg	Oc
(Description)	lm/W	K	—	—	—	—
081_Duv=+0.006(47	384	3003	85	81	95	95
082_Duv=+0.010(47	396	3005	86	78	91	95
078_TriDuv=+0.010	371	3010	84	79	94	109
124_CreeF	357	3036	90	87	100	98
079_Duv=0.000(474	367	3003	82	83	100	94
097_4peak3000Kneu	342	2950	95	93	107	98
125_CreeF2	353	3062	90	88	101	99
095_4peak3022Kds2	363	2984	84	84	96	94
096_4peak3000Kds1	357	2964	90	88	99	95
092_Broad3050	325	3037	97	96	100	100
098_4peak3000Kst1	334	2952	88	91	111	100
093_4peak3012Kds4	383	2981	70	74	87	90
094_4peak3020Kds3	376	2986	76	78	90	91
077_TriDuv=+0.006	361	3008	85	82	99	96
099_4peak3010Kst2	327	2956	81	88	114	101

Lamp_Type	ECQ_{t50}	R	ECQ_{t0}	R	ECQ_{t100}	R
(Description)	—	#	—	#	—	#
019_461-526-576-6	79,8	1	97	2	78	31
022_4LEDwith_ yel	79,5	2	98	1	76	33
071_RGB(Ra=80)	79,2	3	93	10	81	26
021_4LED_no_yel	79,2	4	87	18	87	10
081_Duv=+0.006(47	79	5	92	12	81	25
018_3-LED-2Yellow	79	6	82	31	92	5
032_Ide_Prim_Col	78,9	7	85	24	88	9
082_Duv=+0.010(47	78,8	8	91	14	82	22
124_CreeF	78,8	9	87	19	86	14
078_TriDuv=+0.010	78,8	10	78	38	94	2
097_4peak3000Kneu	78,4	11	80	33	91	6
020_4-LED-2(447	78,3	12	97	3	73	43
125_CreeF2	78	13	94	7	74	40
014_457-540-605	78	14	90	15	80	28
073_4-color(Ra=90	77,9	15	79	37	90	7

Data from Table 3.7 shows that ECQ_t index could be very useful in the process of selection a light source for a specific application that defines the "level" of colour quality and the colour temperature of the light source desired.

3.4 Conclusion

It was demonstrated that similar behaviour exist between $CQS - Q_g$ and Gamut volume O_c indexes; since the latter is based on the maximum theoretical object colour saturation of a light source. We could infer that both indexes are good predictors for this feature. Moreover, it was found that a combination of $CQS - Q_a$ and Gamut Volume O_c indexes that represents quite well the colour quality term in the calculus of the ECQ and ECQ_t indexes. Finally the usefulness of the ECQ and ECQ_t indexes was demonstrated by establish an appropriate ranking for light sources that meets user and/or specific lighting application requirements and achieves a balanced trade-off between luminous efficacy and colour quality.

Part II

Mesopic Photometry and Street Lighting

Chapter 4

Near field and far field goniophotometry

One of the most important issue related with street lighting is the measurement of the Light Intensity Distribution (LID) of a fixture or luminary, since it is basic for the designing process and lighting design in any application. The standard and well known equipment for measuring LID is the far field goniophotometer with its different types classified according [LM75-01, 2001]. Near-field goniophotometry is a recent promising measurement technique to determine the photometric characteristics of light sources. This type of goniophotometers are used to determine luminous intensity distributions of a wide variety light sources of various dimensions. In this chapter results obtained with the near field goniophotometer are compared with photometric data obtained with a far field goniophotometer.

The near-field goniophotometers allow to obtain information about both the luminous flux and the luminous intensity of light sources. The main characteristic, in comparison with far field ones, is the small footprint even for that intended to measure large fixtures or light sources (up to 2.0 m long). In this chapter luminous flux and LID parameters are investigated for a calibrated incandescent source and for a remote phosphor LED source. An assessment of luminous flux and LID obtained from both lamps are performed for both near and far field goniophotometers. We will see that small deviations appeared during far field goniophotometry due to the lamp motion in this equipment.

4.1 Comparison between near field and far field goniophotometer measurements

Near field goniophotometry is a recent promising measurement technique to determine the photometric characteristics of light sources. This technique makes use of a photometer and an camera with a 2-dimensional CCD array,

which are both mounted on the frame of the goniophotometer so that both devices can rotate on a virtual sphere around the light source. The camera is used to measure the relative luminance distribution of the light source from all light emitting directions, while normalization of the data is obtained from the additional luminous flux determination with the photometer. The application of imaging luminance cameras allows for a compact set-up of a near field goniophotometer and consequently smaller room dimensions compared to the conventional far field goniophotometers.

Since a far field goniophotometer experiment yields the luminous intensity data obtained in all light emitting directions, these data can be used to construct the luminous intensity distribution (LID) of the source. In addition, integration of the luminous intensity data yields the luminous flux of the light source [CIE84, 1989]. In the following section, luminous intensity and luminous flux data obtained from near field goniophotometer measurements at the Light and Lighting Laboratory of the KaHo Sint Lieven Catholic University (Ghent, Belgium) are compared to data obtained from the CIE type II far field goniophotometer at the same laboratory.

4.2 Near field goniophotometers

The near field goniophotometer at the Light & Lighting Laboratory are installed in a room acclimatized at 25 °C. The camera moves around the geometrical centre located at the intersection of the two rotation axes of the goniophotometer at a distance of 1.50 m. Various optical lenses can be mounted on the camera resulting in a maximum diameter of the luminous area of 2.00 m. The missing solid angle fraction due to the lamp holder for this goniophotometer is only 0.3 %. The CCD camera is equipped with several neutral density filters to increase its dynamic range. Several objectives can be mounted on the camera so that luminaires of a wide range of dimensions can be characterized. The photometer is a 18 bit illuminance meter with 8 measuring ranges, $V(\lambda)$ calibration ($f1^{'} < 1.5$ %) and cosine adaptation. As reference a luminous flux standard incandescent lamp traceable to PTB standards was used.

The far field goniophotometer at the Light & Lighting Laboratory is a CIE type II goniophotometer [CIE121, 1996], with a moving source mounted in a rotating frame and a luminance probe as a detector positioned at a distance of 9 m from the light source. The frame limits the maximal dimensions of the sources to 55 cm. Here a spectral irradiance standard incandescent lamp traceable to NPL standards was used.

4.3 Light sources

In order to compare near and far field goniophotometer experiments, stable light sources are required, especially since the far field goniophotometer has a stationary detector while the light source is rotating around two different axes. Two kind of light sources are selected:

- A calibrated incandescent lamp, with traceability to PTB, operated in DC mode at 75 W.
- A remote phosphor high power LED module, operated in AC mode at 47 W.

Since both sources have small dimensions less than 15 cm, the point source approximation is also valid during measurement with the near field goniophotometer. This permits to make a additional comparison with results obtained solely with the photometer of the near field goniophotometer.

4.4 Results

4.4.1 Luminous flux measurements

The luminous flux of the calibrated incandescent lamp has been determined by an accredited third party laboratory as 1334 lm with an uncertainty of ±1.2 % (k = 2). For luminous flux measurements a complete spherical surface was scanned with steps of 1° for both polar and azimuth angles. The luminous flux, Φ, can be calculated from the photometer measurements as 4.1:

$$\Phi = \int_0^{\pi} \int_0^{2\pi} E \cdot d\phi d\gamma \tag{4.1}$$

From the measurements with the near field goniophotometer values of 1338,2 lm and 1335,1 lm were obtained. These values were obtained with the photometer and differ only by 0,31 % and 0,08 % from the value from the calibration sheet.

Since the far field goniometer allows only measurements in 4 C-planes, the luminous flux of light sources can only be calculated from the radiation pattern in case of light sources having rotational symmetry along the first axis of the luminaire. Although the incandescent lamps are frosted, it will be illustrated in section 3.2 that their radiation pattern is not symmetrical.

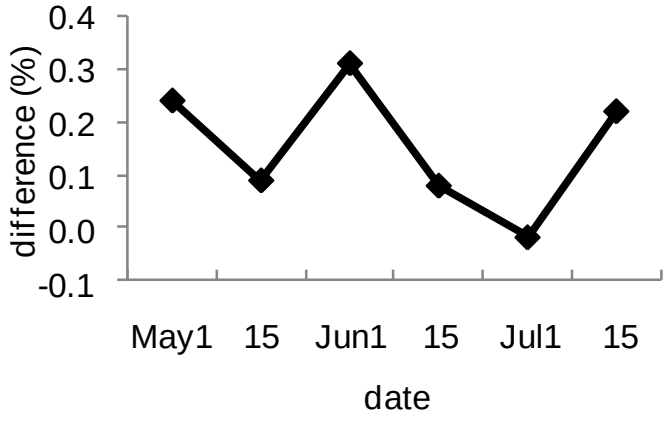

Figure 4.1: Luminous flux measurement control chart.

4.4.2 Control chart

In the period from May to July 2010 a luminous flux control measurement is performed twice a month in order to track the behaviour of the near field goniophotometer equipment. For this experiment three incandescent lamps are tested and the differences from the luminous flux values as stated in the calibration certificate are reported. The variations in luminous flux are as small as 0,3 % or less, as can be seen in Figure 1. These differences are less than the uncertainty of the calibrated lamps, which means that the goniophotometer equipment has been stable during the testing period.

4.4.3 LED module

With the photometer of the near field goniophotometer luminous flux values of 1744,3 lm and 1745,2 lm were obtained for the remote phosphor LED module. Since the radiation pattern of the LED module has rotational symmetry along the first axis of the luminaire, the luminous flux can be calculated from the luminous intensity values as obtained with the far field goniometer. The luminous flux for this LED module is calculated according equation 4.4. In these terms $\Phi \approx 1721\ lm$. Considering the expanded uncertainty of 44 lm (k = 2) this result corresponds well with the results from the measurements obtained using the near field goniophotometer.

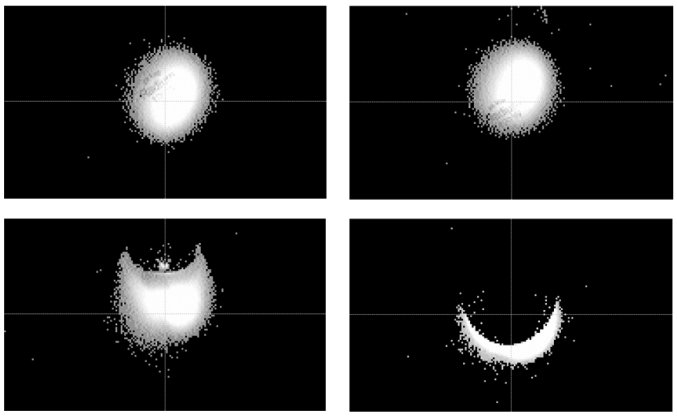

Figure 4.2: Camera images of the incandescent lamp in one C-plane.

$$\Phi = \int_{\phi=0}^{2\pi} \int_{\gamma=0}^{\pi} I(\gamma) d\Omega \tag{4.2}$$

$$\Phi = \int_{\phi=0}^{2\pi} \int_{\gamma=0}^{\pi} I(\gamma) \sin(\gamma) d\gamma d\phi \tag{4.3}$$

$$\Phi \approx \frac{\pi}{2} \sum_{Cplanes} I(\gamma) \sin(\gamma) \Delta\gamma \tag{4.4}$$

4.5 Luminous intensity measurements

4.5.1 Calibrated incandescent lamp

The luminous intensity values of the incandescent lamp have been determined with the near field goniophotometer both with camera and photometer. The camera with a 25 mm lens (and a field of view of 48 cm x 36 cm at a distance of 1,5 m) took 64358 images of the incandescent lamp as is illustrated in Figure 2, where 4 images in an arbitrary C-plane are shown. From the camera images the relative luminous intensity distribution in any direction can be calculated, while the absolute values are obtained with the help of the integrated photometer readings.

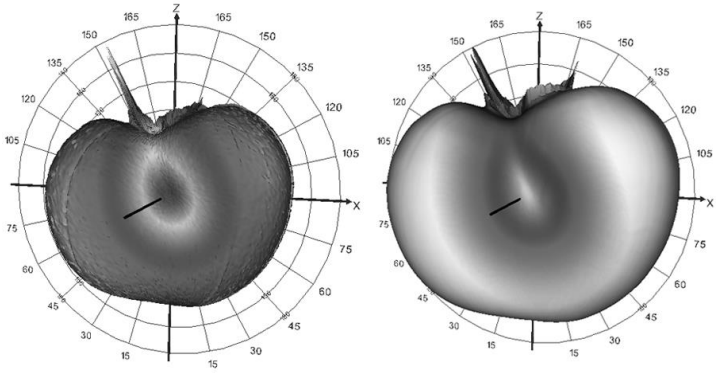

Figure 4.3: Radiation pattern of an incandescent lamp as registered with camera (left side) and with photometer (right side).

From the luminous intensity distribution a potato shaped radiation pattern was found as shown in the left part of Figure 3. Since this pattern has relatively smooth shape and the small dimensions of 5 cm of the lamp the point source approximation is valid and the luminous intensity values can be calculated from the measured illuminance values as well. In the right part of Figure 3 this pattern is also shown. The luminous intensity values as obtained with camera and with photometer correspond well. In the normal ($C = 0°$,$\gamma = 0°$) direction that is located along the first axis of the luminaire and that corresponds to the first photograph of Figure 72, the respective values are 115 cd and 112 cd.

In order to compare these near field luminous intensity values with the results as obtained with the far field goniophotometer, a far field luminous intensity measurement is made in the horizontal ($\gamma = 0°$) plane perpendicular to the first axis of the lamp. From Figure 4 a good agreement can be observed between both type of measurements in almost all C-planes. Differences are less than 2 %. No correct far field measurements were possible around ($C = 120°$) and ($C = 300°$) planes due to the shadowing effect of the frame with respect to the detector, yielding differences up to 9%.

4.5.2 LED Module

Similar tests are also performed on the remote phosphor LED module. The camera images are illustrated in Figure 5, while the radiation pattern as registered by camera and by photometer are shown in Figure 6. From these

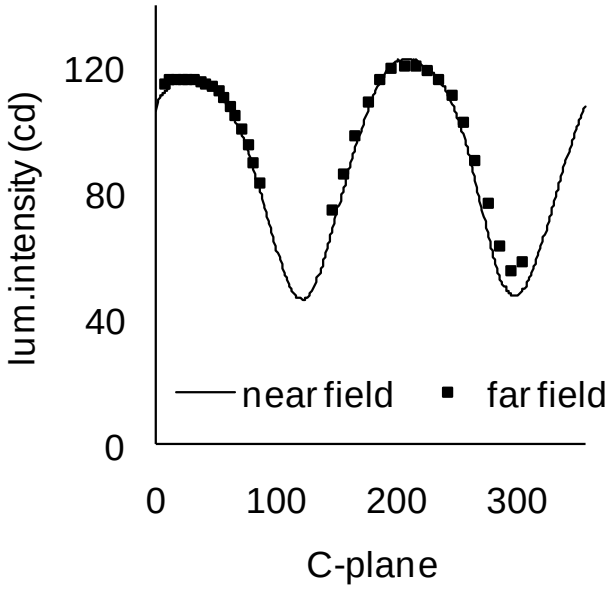

Figure 4.4: Luminous intensity in the ($\gamma = 90°$) plane of the incandescent lamp obtained from near field (solid line) and far field (dots) measurements

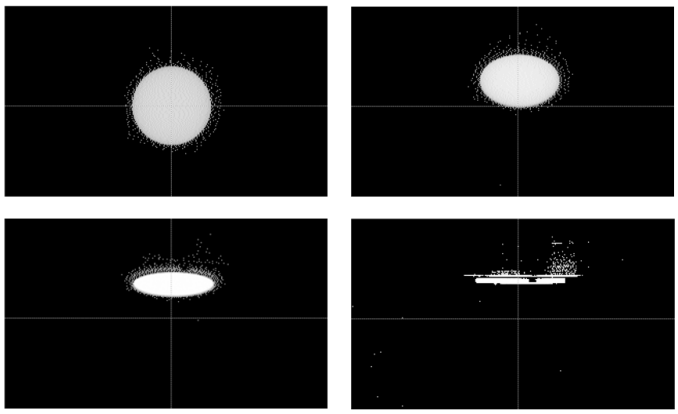

Figure 4.5: Camera images of the LED module in one C-plane.

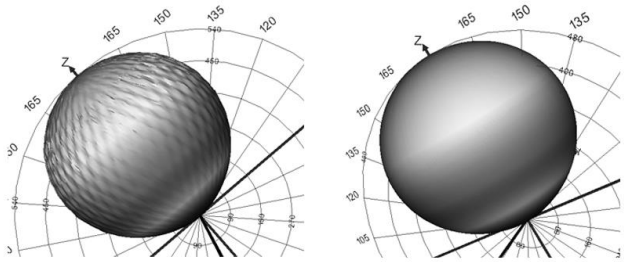

Figure 4.6: Radiation pattern of a LED module as registered with camera (left side) and with photometer (right side).

figures it can be seen that this hemispherical LED module radiates almost like a lambertian source.

However the radiation pattern found with the photometer is somewhat elliptical, since near the equatorial plane ($\gamma = 90°$) the photometer detects still some radiation, while the camera does not. Since total luminous flux is similar in both measurement, a lower value of 557 cd versus 582 cd in the normal ($C = 0°$,$\gamma = 0°$) direction was registered. These differences are illustrated for the ($C = 0°$) plane in Figure 7. For comparison the theoretical luminous intensity of a lambertian source is also shown. Due to the alignment of the LED module 7 cm below the goniometer's centre, the luminous intensity as registered with photometer will be lower than the

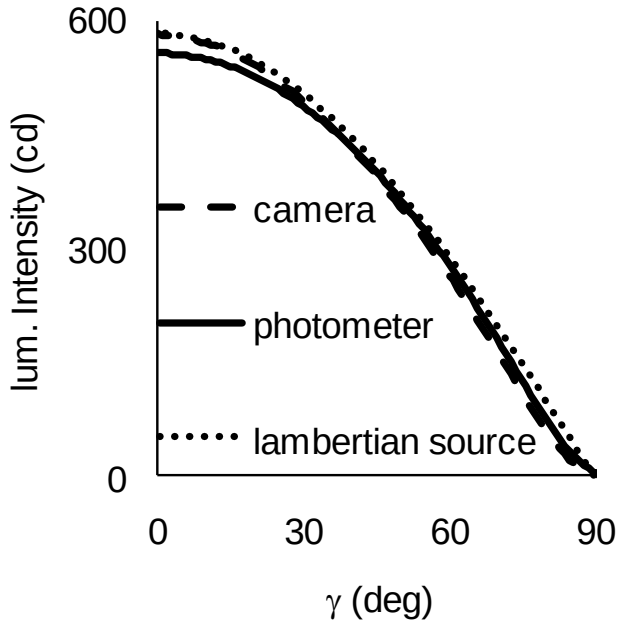

Figure 4.7: Luminous intensity of a LED module in C = 0Â° plane as registered with camera (dashed line) and with photometer (solid line)

value obtained from the camera measurement.

Luminous intensity values have also been determined with the far field goniophotometer in 4 C-planes. These results are shown in Figure 8. In the normal ($C = 0°$,$\gamma = 0°$) direction a value of 610 cd was registered. This values is higher than the value obtained during the near field measurement. This difference is assigned to the different lamp position in the far field goniometer, in which the lamp is mounted in a vertical plane.

Besides this, in non-normal directions differences between different planes up to 40 cd were observed for identical γ angles. Here too it is an reasonable assumption that the different rotations in horizontal and vertical planes may affect the luminous output of the LED module. To check the influence of the light source rotations additional measurements are planned with a far field goniophotometer with rotating mirror where the orientation of light source remains fixed.

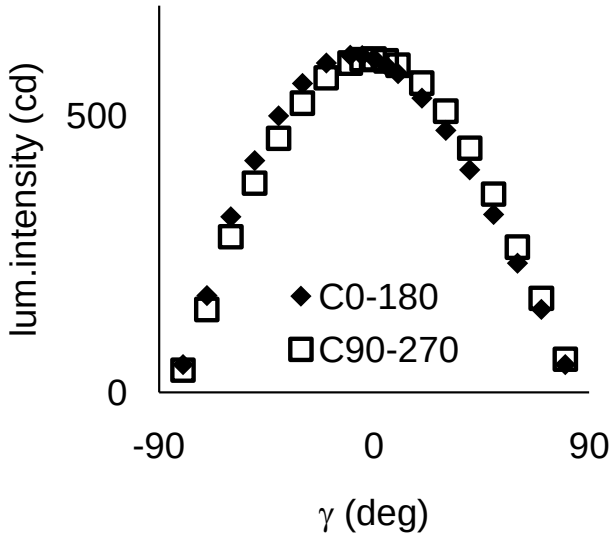

Figure 4.8: Luminous intensity of a LED module in 4 C-planes as registered with a far field goniophotometer.

4.6 Recent findings

In a research developed recently at the Light and Lighting laboratory at K. U. Leuven-KaHo Sint Lieven in Ghent, [Acuña et al., 2014] found a substantial difference in the luminous intensity measured by Near-field and Far-field goniophotometers when the fixture has a sharp pattern in the LID. In this case measurements of the Luminous intensity performed by Near-field goniophotometer are near to zero while the far-field gonio are not. This is due to the narrower dymanic range of the CCD camera than the photometer of the far-field goniophotometer.

4.7 Conclusion

In this chapter the possibilities near field goniophotometers are illustrated. Measurements were performed on various light sources and results are compared to photometric data obtained during traditional far field goniophotometer tests. The luminous flux and the luminous intensity were investigated. The luminous flux has been determined using the photometer, resulting in a good agreement with far field data.

On the contrary luminous intensity should be determined with the camera, even when the dimensions of the light sources are small. Luminous intensities as obtained from the test lamps are comparable for both near and far field goniophotometers. Deviations may appear during far field goniophotometry due to the lamp motion in this equipment.

There are a substantial difference in the luminous intensity measurements between near-field and far-field goniophotometers when the LID pattern is sharp, e.g. a PAR 30 spot light bulb. In this case, CCD camera measures zero luminous intensity while the photometer of the far-field goniophotometer measures values higer but near zero due to their higher dynamic range.

Chapter 5

CIE system for mesopic photometry and street lighting

The most relevant technical aspects of mesopic photometry system based on visual performance recommended in a recent technical report of the International Committee on Illumination, CIE 191:2010 are presented. Applying the recommended system (equations and method of calculus) and using a spectra collection of more than 100 different real and theoretical light sources a graphical representation of the correction factor to convert standard photopic luminance values into their respective mesopic values was made. To contrast these results and to gain insight on the recommended CIE system, the same graphical representation was made by using a sliding Gaussian spectrum as a light source and obtaining similar results to that provided in table 11 of the CIE technical report 191:2010. Finally, an application example is done to illustrate some hints and the impact that this recent recommended CIE system of mesopic photometry can have on designs for outdoor lighting.

5.1 Introduction

The current practice in most of lighting applications is based primarily on the function of photopic spectral luminous efficiency $V(\lambda)$, which was defined by the International Committee on Illumination (CIE) in the early 1900s and characterizes the sensitivity of the foveal cones when adaptation luminance is higher than 10 cd/m^2. A function was also defined for scotopic spectral luminous efficiency $V'(\lambda)$ for the eye's adaptation luminance near total darkness or luminance levels less than 0.001 cd/m^2 where the rods sensors of the retina define the non-color sensitivity of the eye. However, when the luminance of adaptation levels are between 10 cd/m^2 and $0,001$ cd/m^2, which defines the mesopic zone, where foveal cones and rods are active, the spectral luminous efficiency function is not adequately defined by

$V(\lambda)$ nor by $V'(\lambda)$. Currently the CIE technical committee $TC1-37$ is developing an alternative and unique photometric system in order to evaluate lighting at all levels (photopic, mesopic and scotopic) based on the brightness equalization as a visual criterion of comparison. Since the late 1990's a mesopic photometry method based on visual performance [Goodman, 1997], [McGowan and Rea, 1994] has become increasing standard in the scientific community. Additionally, given that the majority of the international average luminance levels required for street lighting and other specific applications such as emergency, security, navy and air transport lighting are between 0.3 cd/m^2 and 10 cd/m^2, a CIE technical committee, $TC1-58$, was created within CIE Division 1, in order to generate a recommendation system for mesopic photometry based on visual performance. As a result, technical report [CIE191, 2010], "Recommended system for mesopic photometry based on visual performanc" was published in 2011. Among other things, this technical report studies four different systems for mesopic photometry i.e. UPS [Rea et al., 2004], MOVE [Goodman et al., 2007], and intermediate systems MES1, MES2 proposed by the members of TC1-58. After a detailed analysis of the measured performance for these four systems, the main conclusion was to recommend System MES2 with photopic luminance limits between 0.005 cd/m^2 and 5 cd/m^2. In addition to the equations and method for calculus of the correction luminance levels, the technical report gives a table with the correction factors to convert the photopic luminance levels into their equivalent mesopic ones depending on the S/P ratio of the light source.

5.2 CIE system for mesopic photometry

In general terms the recommended system in [CIE191, 2010] consists in finding a spectral luminous efficacy for the mesopic zone $V_mes(\lambda)$. This function depends on the photopic luminance of the visual adaptation field L_p, and the S/P ratio and in turn, the latter depends on the spectral power distribution (SPD) of the light source. This model defines $V_mes(\lambda)$ as a linear combination of the photopic $V(\lambda)$, and scotopic $V'(\lambda)$ spectral luminous efficacies. In these terms, after having $V_mes(\lambda)$ defined, the mesopic luminance L_{mes} can be calculated as the integral of the product between the spectral radiance $L_mes(\lambda)$ of the light source and the function $V_mes(\lambda)$. In addition, this model imposes limits for L_{mes}, i.e. when the calculus corresponds entirely to the photopic zone ($L_{mes} \geq 5.0\ cd/m^2$), or completely to the scotopic zone ($L_{mes} \leq 0.005\ cd/m^2$).

A brief description preserving the sequence of calculation on how the mesopic luminance is calculated in this chapter is given bellow.

(i) To calculate the S/P ratio by using eq. 5.1.

$$S/P = \frac{K'_m \int_0^\infty S_\lambda(\lambda)V'(\lambda)d\lambda}{K_m \int_0^\infty S_\lambda(\lambda)V(\lambda)d\lambda} \tag{5.1}$$

Where:

- $K'_m \approx 1700\ lm \cdot W^{-1}$) is the maximum spectral luminous efficacy for scotopic vision, $K'(\lambda)$.
- $K_m \approx 683\ lm \cdot W^{-1}$) is the maximum spectral luminous efficacy for photopic vision, $K(\lambda)$.
- $S_\lambda(\lambda)$ is the spectral distribution of the light source.
- λ is the wavelength.
- L_p and L_s are the photopic and scotopic luminance of the visual adaptation field.

(ii) To find the coefficient m (level of the visual adaptation field), by using the iterative approximation showed in eq. 5.2 and 5.3.

$$L_{mes\_ad,n} = \frac{m_{(n-1)} \cdot L_p + (1 - m_{(n-1)}) \cdot L_s \cdot V'(\lambda_0)}{m_{(n-1)} \cdot (1 - m_{(n-1)}) \cdot V'(\lambda_0)} \tag{5.2}$$

Given $m_0 = 0.5$

$$m_n = 0.7670 + 0.3334 \cdot log(L_{mes\_ad,n}) \tag{5.3}$$

With $0 \leq m_n \leq 1$

Where:

- n is the iteration step. In average, eight iterations ($n = 8$) are enough to obtain an accurate value of m.

- $L_{mes\_ad,n}$ is the mesopic luminance of the visual adaptation field.

(iii) To calculate $V_{mes}(\lambda)$ and L_{mes} by using eq. (5.4) to 5.6.

$$V_{mes,m}(\lambda) = m \cdot V(\lambda) + (1 - m) \cdot V'(\lambda) \tag{5.4}$$

With $0 \leq m_n \leq 1$

$$V_{mes}(\lambda) = \frac{V_{mes,m}(\lambda)}{M(m)} \tag{5.5}$$

$$L_{mes} = \frac{683}{V_{mes,m}(\lambda_0)} \int V_{mes}(\lambda) \cdot L_e(\lambda) \cdot d\lambda \tag{5.6}$$

Where:

- $M(m) = max(V_{mes,m}(\lambda))$, is the normalization value for the function $V_{mes,m}(\lambda)$ evaluated at the m value.

- $V_{mes,m}(\lambda_0)$ is the value of $V_{mes,m}(\lambda)$ at 555 nm.

- L_{mes} is the mesopic luminance

- $L_e(\lambda)$ is the spectral radiance of the light source.

If $L_{mes} \geq 5.0\ cd/m^2$, then $m = 1$.(photopic zone).
If $L_{mes} \leq 0.005\ cd/m^2$, then $m = 0$.(scotopic zone).

5.2.1 SPD, S/P Ratio and CCT of a light source

The SPD of a light source, also called spectral distribution S_λ, when absolute values of the radiant power are not given, determines several characteristics of a light source such as Color Rendering Index, S/P ratio, Correlated

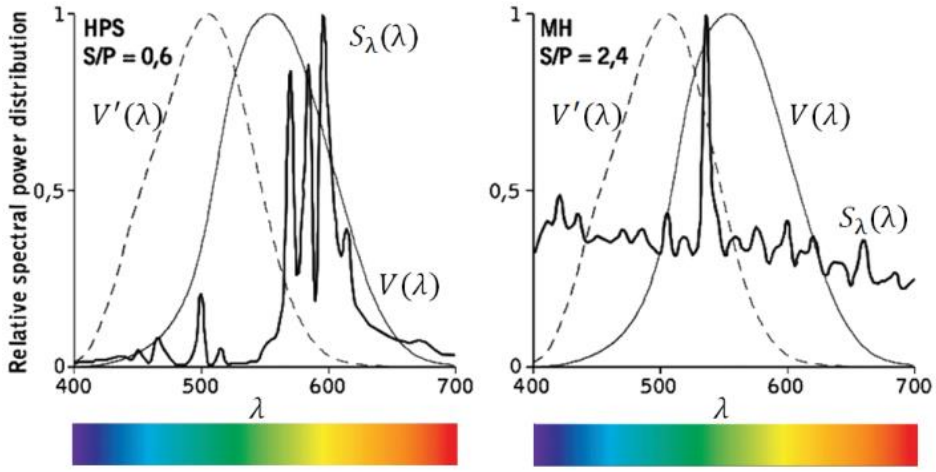

Figure 5.1: Visual comparison of how S/P ratio varies due to spectral distribution of the light source.

Color Temperature (CCT), luminous efficacy of radiation (LER), etc. From eq. 5.1 it can be inferred that the S/P ratio could reach high values when spectral distribution of the light source is concentrated mainly under the wavelength region covered by the scotopic spectral luminous efficacy. On the other hand, the S/P ratio gives low values when the spectral distribution is concentrated under the photopic zone. This effect can be visualized in Fig. 5.1. Moreover, the CCT is sensible to this characteristic of the spectral distribution. See Fig. 5.2.

Fig. 5.2 shows how CCT and S/P ratio vary for four SPD of fluorescent lamps; while CCT moves from 2900K to 6500K, the S/P ratio goes from 1.3 to 2.2.

5.2.2 Simplified calculus of mesopic luminance

In order to make the recommended CIE system [CIE191, 2010] easy to use, this technical recommendation gives a table with the percentage of differences between photopic and mesopic luminance depending on the S/P ratio of the light source, see Table 5.1. In these terms, to calculate the mesopic luminance, the input values required are just the photopic luminance and the S/P ratio of the light source.

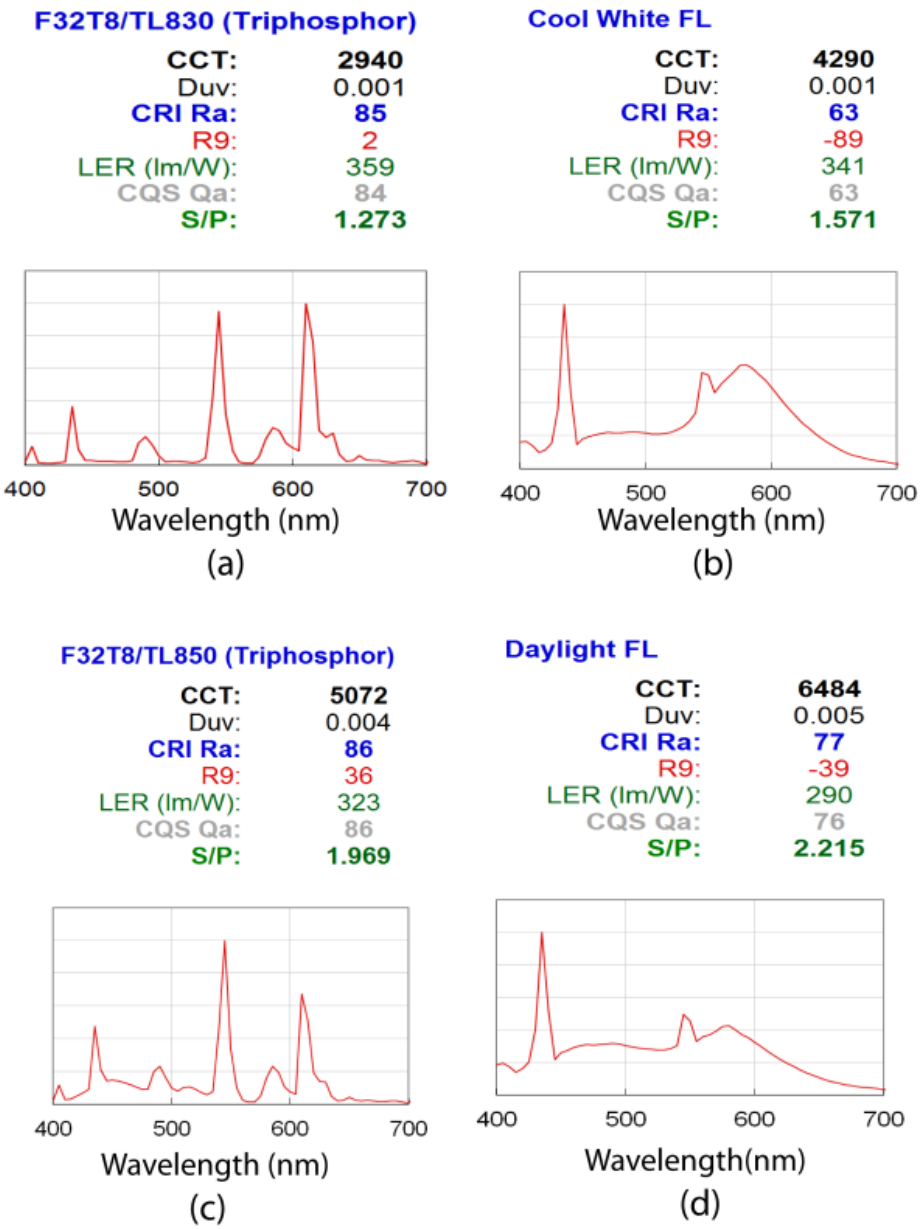

Figure 5.2: Colorimetric and spectral characteristics for four SPD of commercially available fluorescent light sources. Note: Created using NIST Color Quality Scale ver 9.0.a, courtesy of Yoshi Ohno and Wendy Davis (2012) [Davis and Ohno, 2010].

Table 5.1: Percentage difference between mesopic and photopic luminance calculated for an S/P ratio range from 0.25 to 2.65. (Data taken from [CIE191, 2010])

	Photopic Luminance[cd·m^{-2}]									
S/P	**0,01**	**0,03**	**0,1**	**0,3**	**0,5**	**1**	**1,5**	**2**	**3**	**5**
0,25	**-75%**	**-52%**	**-29%**	**-18%**	**-14%**	**-9%**	**-6%**	**-5%**	-2%	0%
0,45	**-55%**	**-34%**	**-21%**	**-13%**	**-10%**	**-6%**	-4%	-3%	-2%	0%
0,65	**-31%**	**-20%**	**-13%**	**-8%**	**-6%**	-4%	-3%	-2%	-1%	0%
0,85	**-12%**	**-8%**	**-5%**	-3%	-3%	-2%	-1%	-1%	0%	0%
1,05	4%	3%	2%	1%	1%	1%	0%	0%	0%	0%
1,25	**18%**	**13%**	**8%**	**5%**	4%	3%	2%	1%	1%	0%
1,45	**32%**	**22%**	**15%**	**9%**	**7%**	**5%**	3%	3%	1%	0%
1,65	**45%**	**32%**	**21%**	**13%**	**10%**	**7%**	**5%**	4%	2%	0%
1,85	**57%**	**40%**	**27%**	**17%**	**13%**	**9%**	**6%**	**5%**	3%	0%
2,05	**69%**	**49%**	**32%**	**21%**	**16%**	**11%**	**8%**	**6%**	3%	0%
2,25	**80%**	**57%**	**38%**	**24%**	**19%**	**12%**	**9%**	**7%**	4%	0%
2,45	**91%**	**65%**	**43%**	**28%**	**22%**	**14%**	**10%**	**8%**	4%	0%
2,65	**101%**	**73%**	**49%**	**31%**	**24%**	**16%**	**12%**	**9%**	**5%**	0%

Table 5.1 clearly shows three groups of values: (i) At the upper-left part there are negative differences, meaning very poor performance of these light source types at photopic luminance levels lower than 1.0 cd/m^2. (ii) At the central-right part values are close to zero, meaning that performance of this light sources at luminance levels higher than 2.0 cd/m^2 are similar in both photometry systems: Photopic and mesopic. And (iii) the zone at the lower-left part shows high and positive differences, meaning quite good performance of these light sources at photopic luminance lower than 1.5 cd/m^2. The four columns of Table 5.1 that are marked with a square represent the standard photopic luminance levels commonly used in street lighting.

5.2.3 Rule of thumb that link luminance and illuminance levels in street lighting

In street lighting design it's well known that conversion from luminance to illuminance values depends on the specific mounting conditions of the light source, the reflectance factor of the pavement and observers' positioning. However, by using typical values for these variables it is possible to get the rule of thumb show in eq. 5.7.

$$E = L_p \cdot 15 \left[\frac{lx}{cd/m^2} \right] \tag{5.7}$$

Where:
E is the illuminance in lux and Lp is the luminance in cd/m^2.

This rule of thumb can be used in outdoor lighting design in order to use the CIE system [CIE191, 2010], when the only available input data are the average illuminance levels (lx).

5.3 Using the CIE mesopic photometry system

In order to study how the CIE recommended system [CIE191, 2010] works and to assess their performance with different SPD of light sources, algorithms were developed in Matlab®using two collections of light source spectra. One consists in a Gaussian sliding function, and another that corresponds to the 121-spectra database of theoretical and commercially available light sources, taken from the work from Davis and Ohno in [Davis and Ohno, 2010].

5.3.1 Graphical representation of the mesopic luminance

Fig. 5.3 shows the percentage difference between mesopic and photopic luminance calculated for a Gaussian curves collection (obtained by shifting a Gaussian function). It should be lighted that the 3D shape of Fig. 5.3 is quite similar to that obtained with data from Table 5.1.

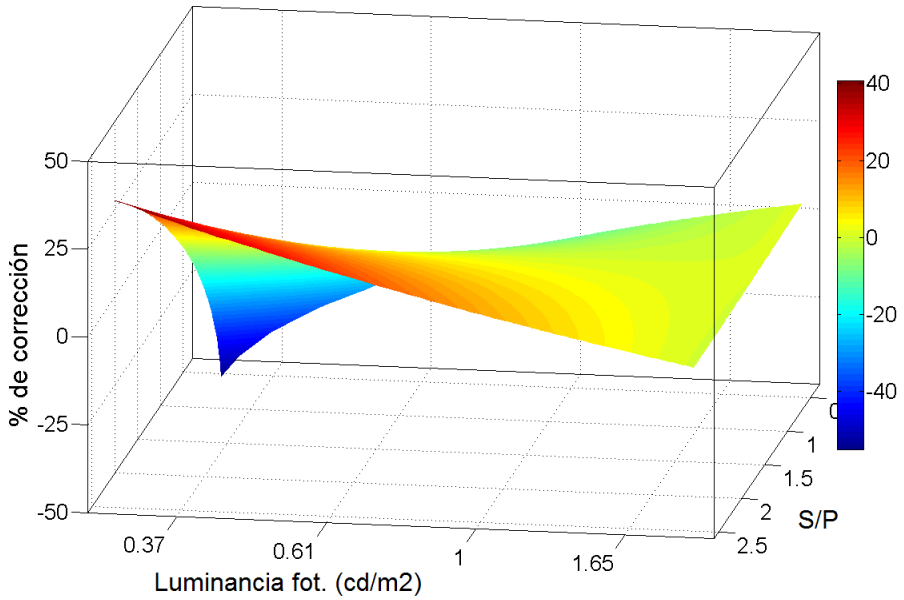

Figure 5.3: Graphical representation of the difference between mesopic and photopic luminance. Mesopic luminance was calculated using the CIE recommended system [CIE191, 2010] and a sliding Gaussian curve as a light source spectrum.

In the same way, the mesopic luminance differences represented in Fig. 5.3 and Fig. 5.4 are dissimilar. This subject can be due to the shape types of the Spectral Distributions of the two groups of light sources studied.

Fig. 5.5 depicts the mesopic luminous efficiency function (Vmes) obtained by using [CIE191, 2010] for the fluorescent light source presented in Fig. 5.2-(c) and calculated for a input photopic luminance of 1.0 cd/m^2. Data provided by Fig. 5.5 shows that mesopic luminance increase 9.81% respect to the photopic luminance.

Fig. 5.7 shows difference of the mesopic luminance calculated with the CIE system [CIE191, 2010] over the Fluorescent and LED light sources depicted

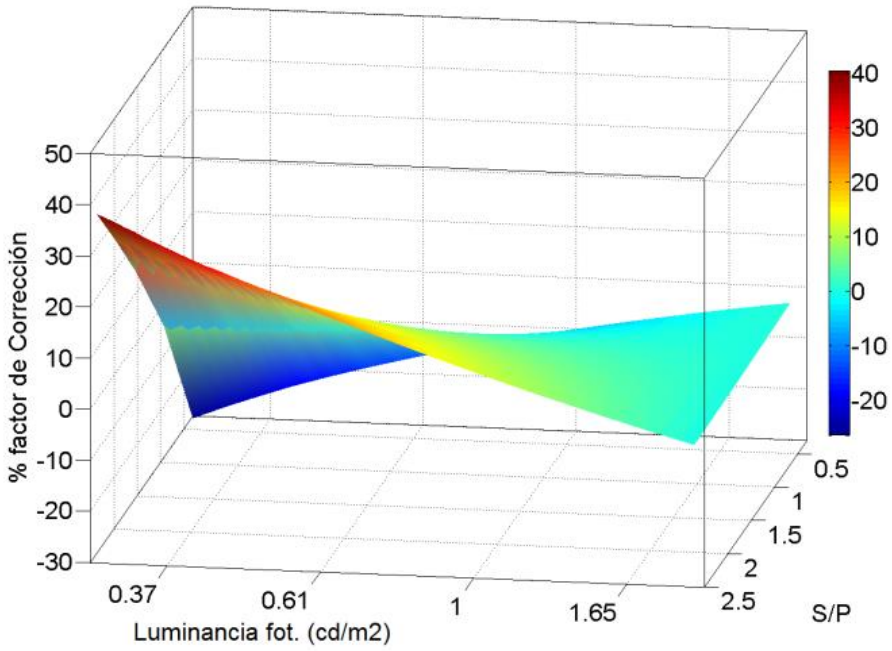

Figure 5.4: (Color online) Graphical representation of the difference between mesopic and photopic luminance. Mesopic luminance was calculated using the CIE recommended system [CIE191, 2010] over a 121-spectra database, from the Davis and Ohno work [Davis and Ohno, 2010] (spreadsheet NIST CQS ver 9.0.a 2011).

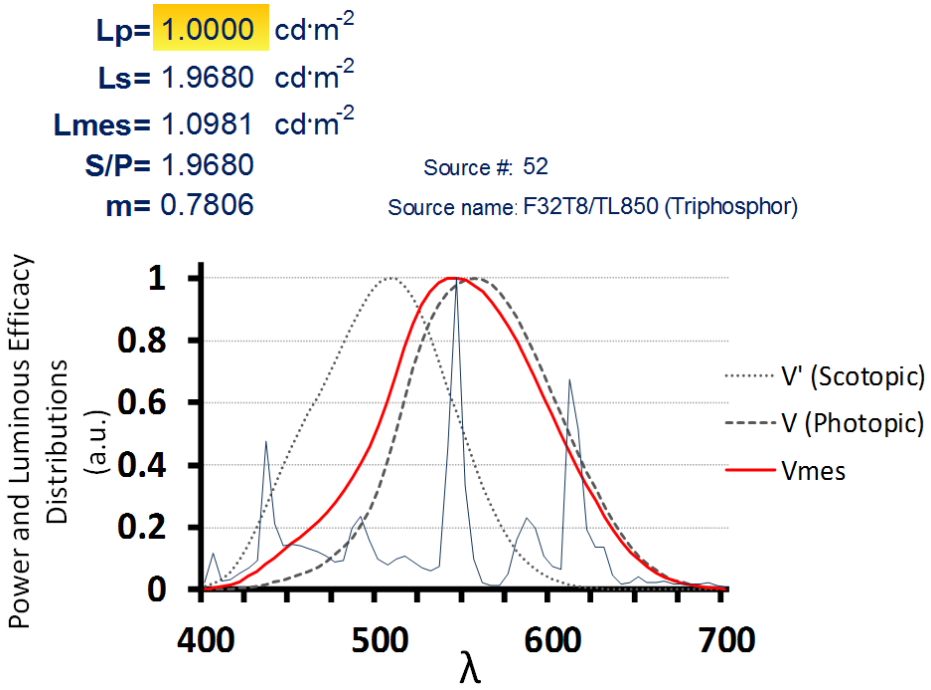

Figure 5.5: Mesopic relative luminous efficiency Vmes, found for SPD of the light source in Fig.5.2-(c), with photopic luminance $L_p = 1.0$ cd/m^2 using the CIE System [CIE191, 2010]. (Image taken from modified Spreadsheet NIST CQS ver 9.0.a from Davis and Ohno work [Davis and Ohno, 2010].)

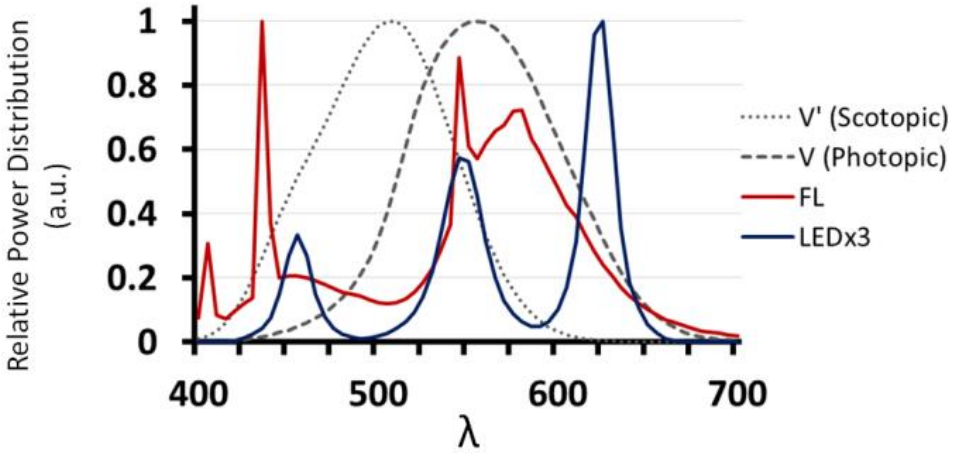

Figure 5.6: SPD of Fluorescent and LED light sources having S/P ratio of 1.3502 and 1.3535 respectively.

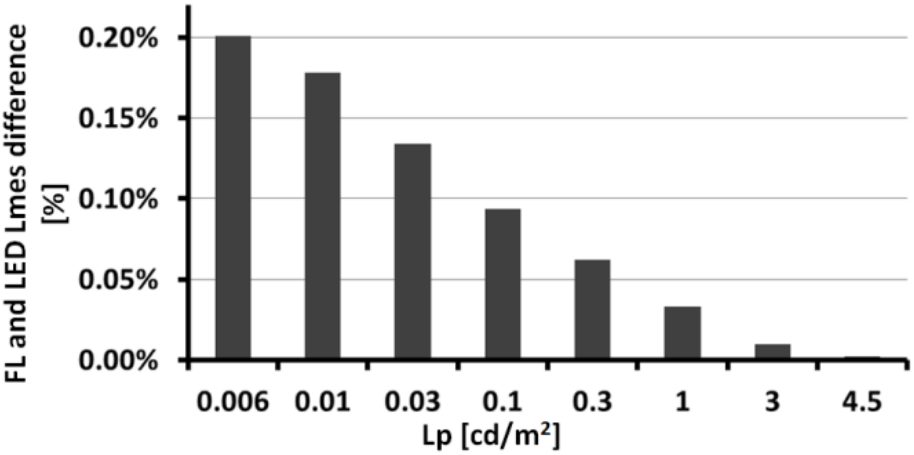

Figure 5.7: Difference in mesopic luminance calculated by using CIE system [CIE191, 2010] over the two SPD presented in Fig. 5.6.

in Fig. 5.6. The maximum difference found in the range of 0.005 cd/m^2 and 5.0 cd/m^2 for photopic luminance (Lp) was 0.2%.

5.4 Conclusion

From Table 5.1, Fig. 5.3 and Fig. 5.4 it can be inferred that a significant enhancement of the light source performance in mesopic photometry for street lighting applications can be obtained when the S/P ratio of the light source is higher than 1.8 and photopic luminance is less than 2 cd/m^2.

It was found that the spectral distribution of a light source has a considerable effect in the mesopic luminance calculated by using the CIE recommended system [CIE191, 2010]. Moreover, from differences between Fig. 5.3 and Fig. 5.4 it can be inferred that using two light source groups with unrelated shape of the SPD, substantial differences of the mesopic luminance can be obtained. However, negligible differences (less than 0.2%) for the mesopic luminance were obtained for two SPD corresponding to fluorescent and LED light sources with similar S/P ratio (1.35).

Table 1 supplied by [CIE191, 2010] gives an easy-to-use tool in order to calculate approximated values of mesopic luminance, although it is recommended to use the complete CIE model to avoid have significant errors due to shape of the SPD and approximations for the input L_p in this table.

Chapter 6

The Street lighting energy consumption index

In order to quantify possible energy savings in street lighting systems by using mesopic photometry combined with fixture luminous flux control, in this chapter it is presented a useful index intended to predict the annual average energy consumption per illuminated street area. This index called Q_{sa} involves the main parameters used in the street lighting design i.e. maintenance factor f_m, utilization factor f_u, nominal luminous efficacy of the light source K_{nl}, and include our two new features: Luminous Flux control factor f_{cf} and mesopic correction factor f_{cm}. This latter takes into account the improvement of visual performance by correcting the standard photometry system (photopic) by the recommended system (mesopic) in the [CIE191, 2010]. It is also demonstrated how this index works for three different and possible street lighting scenarios by assessment their energy consumption using both: photopic and mesopic photometry and three fixture control flux types. Most of the information and data presented in this chapter is the contribution of the author to the oral presentation by [Sánchez-Balvás et al., 2012a].

6.1 Introduction

Urban lighting, as an element of the public space design and a large energy consumer, is the subject of study in this chapter. It is worth noting that a poor lighting design can lead to a waste of energy, light pollution as well as to a deterioration of the visual comfort and security of the inhabitants living in an urban area.

The Energy Consumption Index Q_{sa} presented in this chapter, can be easily applied and read by the non-expert and shows the potential savings that can be achieved by using different lamp technologies, luminous flux controls and the correction to the mesopic photometry.

In the following sections, a brief description of the mesopic photometry system is briefly described, a number of important lighting design criteria based on visual performance are given and an example of application of the Q_{sa} in three different urban lighting scenarios based on standard parameters and recommended design values given by [Real-Decreto1890, 2008] closes the analysis.

6.2 Mesopic photometry on street lighting

As it was investigated in 5,the luminance levels in the edges of the mesopic region are 0.001 and 10 cd/m2 . This range covers, among others, street luminance levels, emergency lighting, security lighting and public lighting for crime prevention purposes [Fotios and Goodman, 2012].

The recommended CIE photometric system [CIE191, 2010] showed in Table 2 gives the correction factors that have to be applied in order to obtain the equivalent mesopic luminance level. These correction factors depend on the standard photopic luminance level and the so-called S/P ratio of the light source, which is essentially the ratio of the spectral energies lying within the scotopic and the photopic regions. For example, high pressure sodium lamps (HPS) have a S/P ratio from 0.65 to 1.05, while Metallic Halide lamps (MH) are from 1.25 to 2.45 [CIE191, 2010].

A capital application of the mesopic system of photometry is road lighting, since the luminance levels at night fall into the mesopic region [CIE191, 2010]. In this zone, both rods and cones in the retina are activated, which increases peripheral vision and enhances visual performance in specific tasks such as driving at night.

6.3 Definition of the Energy Consumption Index

Let us call Q_{sa} the total energy consumption during one year per unit of illuminated area. The basic equation to calculate this is obtained from [Real-Decreto1890, 2008]. To obtain the general energy consumption Q'_{sa}, we cleared this equation for power and multiply it by the average number of hours that the light system is turned on. Doing so, the resulting equation reads,

$$Q'_{sa} = \left(\frac{E_m \cdot t_{ua}}{\eta_{aux} \cdot K_{nl} \cdot f_m \cdot fu} \right) \frac{1}{1000} [kWh/m^2] \tag{6.1}$$

Where: E_a: Average illuminance level (lux); t_a: Annual time of operation of the lighting system (h); η_{aux}: Efficiency of auxiliary elements (W/W); K_{nl}: Nominal efficacy of lamps (lm/W); f_m: Maintenance factor; f_u: Utilization factor.

From 6.1, it can be inferred that a reduction of the energy consumption in practical terms can be obtained by two ways:

- Reducing the annual equivalent operation time of the lamp (tua). Alternatively, this can be achieved by using different flux control techniques.
- By improving the luminous efficacy of the lamp, i.e. applying a correction factor associated with an improvement of the user's visual performance in the mesopic region.

Figure 6.1 shows trhee possible profiles for controlling the luminous flux in a street lighting system. The correction factor f_{cf} for each profile of luminous flux control is obtained as the ratio of area covered by the luminous flux profile to the area covered by full flux profile, i.e case (a) in 6.1.

Once the type of lamp, level of photopic luminance and type of luminous flux control have been defined, two correction factors can be calculated: f_{cm} and f_{cf}. The correction factor for the luminance in the mesopic region f_{cm} is obtained from Table 6.1, while f_{cf} is calculated from the control flux profile selected, as shown in Figure 6.1.

Table 6.1: Correction factors for mesopic photometry

HPS S/P= 0,65		MH S/P= 1,85		LED S/P= 2,25		FL S/P= 2,45	
Lp	Δ Lmes	Lp	Δ Lmes	Lp	Δ Lmes	Lp	Δ Lmes
0,5	-6	0,5	13	0,5	19	0,5	22
0,75	-5	0,75	11	0,75	15	0,75	20
1	-4	1	9	1	12	1	14
1,5	-3	1,5	6	1,5	9	1,5	10
2	-2	2	5	2	7	2	8

Finally, Equation 2 shows how to calculate the total energy consumption during one year per unit of illuminated area considering corrections for mesopic photometry and the profile of the luminous flux control.

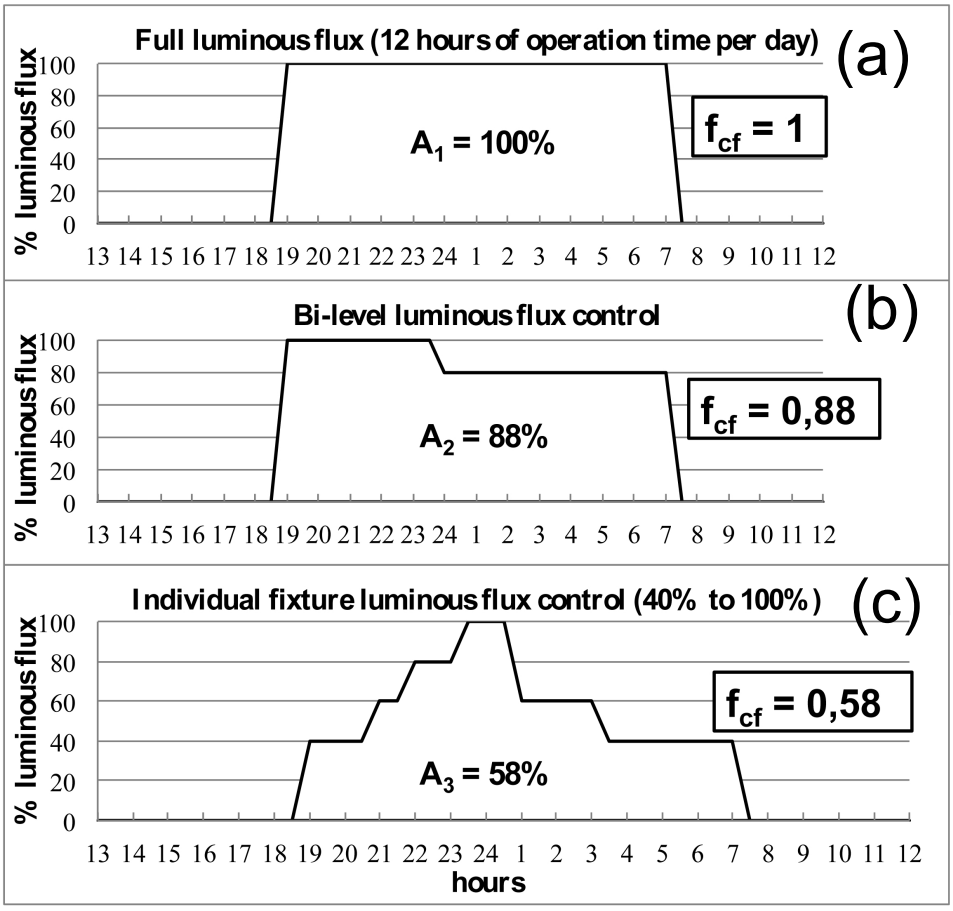

Figure 6.1: (a) Control profile for a non-reduction of luminous flux, (b) Two-level control profile and (c) multi-level control profile of the luminous flux. Control flux factor f_{cf} is calculated as the percentage of the area covered by the profile control flux

$$Q_{sa} = \left(\frac{E_m \cdot (t_{ua} \cdot f_{cf})}{\eta_{aux} \cdot (K_{nl} \cdot f_{cm}) \cdot f_m \cdot fu} \right) \frac{1}{1000} [kWh/m^2] \tag{6.2}$$

The nominal luminous efficacy of the lamp (K_{nl}), utilisation factor (f_u) and three factors needed to calculate the luminaire maintenance factor (f_m), i.e. Lamp Lumen Depreciation Factor (LLD), Lamp Survival Factor (LSF) and Luminaire Dirt-Depreciation Factor (LDF) are showed in Table 6.2.

Table 6.2: Values for nominal luminous efficacy, utilisation and maintenance factors for four different light sources

		Lamp Type			
		HPS	MH	LED	FL
K_{nl}	[lm/W]	86.69	79.5	80.95	72.73
f_u	Road	0.38	0.28	0.55	0.22
	Pedes.	0.28	0.30	0.65	0.22
LLD	Road	0.94	0.76	–	0.93
	Pedes.	0.94	0.76	–	0.93
LSF	Road	0.94	0.94	–	0.99
	Pedes.	0.94	0.94	–	0.99
LDF	Road	0.89	0.89	–	0.89
	Pedes.	0.86	0.86	–	0.86
f_m	Road	0.79	0.64	0.80	0.82
	Pedes.	0.76	0.61	0.80	0.79

6.4 How the energy comsumption index works

As an example of application, Q_{sa} was calculated in three different scenarios described in Table 6.3, 6.4 and 6.5. Each scenario represents a type of city with 8 different categories of streets: ME1, ME2, ME3, Historical Centre, Combined commercial and residential, only residential, and squares or places with low luminous flux. In addition, their percentage of the total street area of the city it is specified.

6.4.1 Scenario no. 1

Lighting in road and pedestrian areas with HPS lamps. HPS lamps are highly efficient and have relatively long lifetimes ($\geq$ 16000 hours. Implementation of illuminance levels given by [Real-Decreto1890, 2008] and full

luminous flux control is defined (the most popular and inexpensive one).

Table 6.3: Components description for scenario no.1 of a studied urban lighting system

Street Type	Ea[a] [lux]	Street area [%]	Lamp type	Flux Control Type
ME1	30	5	HPS	Full flux
ME2	20	5	HPS	Full flux
ME3	15	5	HPS	Full flux
ME4	10	20	HPS	Full flux
Hist. Centre	20	5	HPS	Full flux
Res-Comer	15	30	HPS	Full flux
Residential	10	20	HPS	Full flux
Squares	7,5	10	HPS	Full flux

[a]Average illuminance level (Ea) and road types are taken from [Real-Decreto1890, 2008]

6.4.2 Scenario no. 2

Installation of different lamps and luminous flux control for each type of road and pedestrian area could be a faithful representation of a real city. Places with intensive pedestrian activity should be illuminated by white light sources characterized by excellent colour rendering.

6.4.3 Scenario no. 3

Lighting in road and pedestrian areas with LED lamps with excellent colour rendering and a relatively high efficacy. Implementation of illuminance levels given by [Real-Decreto1890, 2008] and the luminous flux control type is performed individualy to each Fixture (the most expensive gear and control system).

Table 6.4: Components description for scenario no.2 of a studied urban lighting system

Street Type	Ea[a] [lux]	Street area [%]	Lamp type	Flux Control Type
ME1	30	5	HPS	Bi-level
ME2	20	5	MH	Bi-level
ME3	15	5	MH	Bi-level
ME4	10	20	LED	Indiv. Fixture
Hist. Centre	20	5	MH	Bi-level
Res-Comer	15	30	MH	Bi-level
Residential	10	20	LED	Indiv. Fixture
Squares	7,5	10	FL	Full flux

[a]Average illuminance level (Ea) and road types are taken from [Real-Decreto1890, 2008]

Table 6.5: Components description for scenario no.3 of a studied urban lighting system

Street Type	Ea[a] [lux]	Street area [%]	Lamp type	Flux Control Type
ME1	30	5	LED	Indiv. Fixture
ME2	20	5	LED	Indiv. Fixture
ME3	15	5	LED	Indiv. Fixture
ME4	10	20	LED	Indiv. Fixture
Hist. Centre	20	5	LED	Indiv. Fixture
Res-Comer	15	30	LED	Indiv. Fixture
Residential	10	20	LED	Indiv. Fixture
Squares	7,5	10	LED	Indiv. Fixture

[a]Average illuminance level (Ea) and road types are taken from [Real-Decreto1890, 2008]

6.5 Results

In scenario no. 1, where HPS lamps are used, a negative performance is obtained when evaluated in the mesopic region, i.e. mesopic Q_{sa} is higher than standard photopic energy consumption as seen in Table 6.6. This is explained by an S/P ratio for HPS lamps lower than 1.8, making them unsuitable for energy savings using mesopic photometry.

Table 6.6: Scenario no. 1. Energy consumption index Q_{sa} $[kWh/m^2]$ calculated for photopic and mesopic zone

Street Type	Q_{sa} Phot.	$[kWh/m^2]$ Mes.
ME1	5.072	5.176
ME2	3.381	3.522
ME3	2.536	2.642
ME4	1.691	1.799
Hist. Centre	4.749	4.947
Res-Comer	3.562	3.710
Residential	2.375	2.526
Squares/Low flux	1.781	1.895
Weighted Ave.Values	**2.847**	**2.982**

The results of scenario 2 indicate that the diversity of luminous flux controls and lamps in an urban lighting system reduces the energy consumption (Table 6) and therefore the energy consumption using the Q_{sa} is lower than the scenario 1. See table 6.7.

Although the luminous efficacy of LED lamps is lower than that for HPS lamps (80.95 lm/W vs. 86.69 lm/W, respectively) major savings are obtained with the LED lamps, see Table 6.6 and 6.8, two reasons explain this situation: The individual and multilevel control of the luminous flux in scenario no.3, see figure 6.1 where scenario no.3 is just 58% of the energy consumption of scenario no.1. On the other hand, the utilization factor (fu) on LEDs is higher compared to HPS lamps 0,55 vs. 0,38, respectively, as it can see in Table 6.2.

Without considering the costs of implementation for different lamp technologies and luminous flux control systems, it is clear that LED technology with individual fixture luminous flux control provides maximum energy savings. Although it is important to highlight that such type of luminous flux

Table 6.7: Scenario no. 2. Energy consumption index Q_{sa} $[kWh/m^2]$ calculated for photopic and mesopic zone

Street Type	Q_{sa} Phot.	$[kWh/m^2]$ Mes.
ME1	4.464	4.555
ME2	4.013	3.682
ME3	3.010	2.761
ME4	0.708	0.595
Hist. Centre	5.261	4.826
Res-Comer	3.946	3.620
Residential	0.599	0.504
Squares /Low flux	2.593	2.125
Weighted Ave.Values	**2.542**	**2.309**

Table 6.8: Scenario no. 3. Energy consumption index Q_{sa} $[kWh/m^2]$ calculated for photopic and mesopic zone

Street Type	Q_{sa} Phot.	$[kWh/m^2]$ Mes.
ME1	2.125	1.986
ME2	1.417	1.265
ME3	1.062	0.949
ME4	0.708	0.595
Hist. Centre	1.199	1.070
Res-Comer	0.899	0.803
Residential	0.599	0.504
Squares/ Low flux	0.450	0.378
Weighted Ave. Values	**0.866**	**0.762**

Table 6.9: Summary of average values of the energy consumption index Q_{sa} $[kWh/m^2]$ calculated for the three scenarios studied

Scenario No.	Average Q_{sa} Phot.	$[kWh/m^2]$ Mes.
1: HPS - Full Flux	2.847	2.982
2: Combined Lamps - Bilevel	2.542	2.309
3: LEDs - Indiv. Fixture	0.866	0.762

Table 6.10: Summary of percentual energy consumption Q_{sa} referenced to scenario No. 1 with photopic photometry

Scenario No.	Average Q_{sa} Phot.	Mes.
1: HPS - Full Flux	100%	104.7%
2: Combined Lamps - Bilevel	89.3%	81.1%
3: LEDs - Indiv. Fixture	30.4%	26.8%

control could imply a re-categorization of the streets because of the high reduction of the luminous flux at low traffic hour.

6.6 Conclusion

Through an application example, it was demonstrated that the energy consumption index is an easy-to-use tool to assess urban lighting systems. Using the Q_{sa}, it is possible to know in a simple way, the energy savings that can be obtained in different urban lighting systems depending on the type of road, light sources, luminous flux control and photometry system that is used. The application of this indicator comes in handy either for the lighting industry or decision makers, whenever the most efficient and sustainable lighting system has to be chosen for a city. Nevertheless, as a subsequent study, the Q_{sa} should be complemented taking into account the economic cost of acquisition, implementation and management of the different urban lighting systems analysed.

Bibliography

[Acuña et al., 2014] Acuña, P., Quintero, J. M., Losada, D. F., Leloup, F. B., and Hanselaer, P. (2014). Inter-laboratory comparison of luminous intensity distribution and total luminous flux measurements with far field and near field goniophotometers. In *Anais do XII Conferência Latino-Americana De Iluminação*, pages 127 – 131. 62, 99

[Acuña et al., 2010] Acuña, P., Quintero, J. M., and Parra, E. E. (2010). Impacto del alumbrado público con tecnología led en la emisión de armónicos en la red de distribución. In *X Congreso Panamericano de Iluminación - Luxamérica 2010*. 99

[Akashi, 2004] Akashi, Y. (2004). Comments about: A review of colour rendering indices and their application to commercial light sources. Personal comunication from: LRC Rensselaer Polytechnic Institute, 110 Eighth Street, Troy, New York 12180, USA. 30

[Bartleson, 1960] Bartleson, C. J. (1960). Memory colors of familiar objects. *J. Opt. Soc. Am.*, 50(1):73–77. 30, 35

[Carreras and Hunt, 2012] Carreras, J. and Hunt, C. E. (2012). Efficacy and color rendering limits in artificial light sources emulating natural illumnation. Publication at IREC, Barcelona, Catalonia.

[Carreras et al., 2010] Carreras, J., Quintero, J. M., and Hunt, C. E. (2010). Theoretical maximum efficacy and color rendering assessment of energy-efficient light sources. In *2nd CIE Expert Symposium on Appearance, When Appearance meets Lighting Book of Abstracts*. 98

[CIE121, 1996] CIE121, T. R. (1996). The photometry and goniophotometry of luminaries. Technical report, International Commission on Illumianation, Central Bureau of the CIE, Vienna, Austria. 54

[CIE13.3, 1995] CIE13.3, T. R. (1995). Method of specifying and measuring color rendering properties of light sources. Technical report, International Commission on Illumianation, Central Bureau of the CIE, Vienna, Austria. 5, 6, 7, 13, 29, 32, 37

Bibliography

[CIE177, 2007] CIE177, T. R. (2007). Color rendering of white led light sources. Technical report, International Commission on Illumianation, Central Bureau of the CIE, Vienna, Austria. 5

[CIE191, 2010] CIE191, T. R. (2010). Recommended system for visual performance based mesopic photometry. Technical report, International Commission on Illumianation, Central Bureau of the CIE, Vienna, Austria. xvi, xvii, 66, 69, 71, 72, 73, 74, 75, 76, 77, 79, 80

[CIE84, 1989] CIE84, T. R. (1989). The measurement of luminous flux. Technical report, International Commission on Illumianation, Central Bureau of the CIE, Vienna, Austria. 54

[Corredor et al., 2014] Corredor, D. A., Ochoa, M., and Quintero, J. M. (2014). Software multiplataforma para cálculos colorimétricos y de eficacia lumínica de las fuentes de luz. In *Anais do XII Conferência Latino-Americana De Iluminação*, pages 182– 187. 100

[Davis and Ohno, 2010] Davis, W. and Ohno, Y. (2010). Color quality scale. *Optical Engineering*, 49(3):033602–033602–16. xvi, 6, 30, 37, 38, 39, 70, 72, 74, 75

[Fairchild, 2005] Fairchild, M. D. (2005). *Color Appearance Models*, chapter 10–16. Wiley. 10

[Fotios and Goodman, 2012] Fotios, S. and Goodman, T. (2012). Proposed uk guidance for lighting in residential roads. *Lighting Research and Technology*, 44(1):69–83. 80

[Goodman, 1997] Goodman, T. (1997). Workshop making measurements in the mesopic region: Photometric and colorimetric aspects. In *Proceedings of the NPL-CIE-UK Conference Visual Scales*. 66

[Goodman et al., 2007] Goodman, T., Forbes, A., Walkey, H., Eloholma, M., Halonen, L., Alferdinck, J., Freiding, A., Bodrogi, P., VÃ¡rady, G., and Szalmas, A. (2007). Mesopic visual efficiency iv: a model with relevance to nighttime driving and other applications. *Lighting Research and Technology*, 39(4):365–392. 66

[Guo and Houser, 2004] Guo, X. and Houser, K. (2004). A review of colour rendering indices and their application to commercial light sources. *Lighting Research and Technology*, 36(3):183–197. 30, 35

[Gutierrez et al., 2014a] Gutierrez, J. F., Chávez, M. A., Cabra, M. S., and Quintero, J. M. (2014a). Calibración de monitores para estudio de percepción de color. In *Anais do XII Conferência Latino-Americana De Iluminação*, pages 171 – 177. 100

[Gutierrez et al., 2014b] Gutierrez, J. F., Hunt, C. E., and Quintero, J. M. (2014b). Visible light communication led based on luminary for general lighting: State of the art. In *Anais do XII Conferência Latino-Americana De Iluminação*, pages 163– 170. 99

[Gutierrez and Quintero, 2014] Gutierrez, J. F. and Quintero, J. M. (2014). Planteammiento procedimiento para verificación de luminancímetros. In *Anais do XII Conferência Latino-Americana De Iluminação*, pages 114 – 118. 100

[Gutierrez et al., 2014c] Gutierrez, J. F., Quintero, J. M., and Sudrià-Andreu, A. (2014c). VLC: Fuentes de luz led para comunicación inalámbrica. Revista Automática e Instrumentación. No. 466. 101

[Hertog et al., 2014] Hertog, W., Llenas, A., Quintero, J. M., Hunt, C. E., and Carreras, J. (2014). Energy efficiency and color quality limits in artificial light sources emulating natural illumination. *Opt. Express*, 22(S7):A1659–A1668. 14, 98

[Hunt et al., 2011] Hunt, C. E., Carreras, J., and Quintero, J. M. (2011). Appearance degradation and chromatic shift in energy-efficient lighting devices. In *Nineteeth Color Imaging Conference: Color Science and Engineering Systems, Technologies, and Applications*. 99

[Linhares and Nascimento, 2012] Linhares, J. M. M. and Nascimento, S. M. C. (2012). A chromatic diversity index based on complex scenes. *J. Opt. Soc. Am. A*, 29(2):A174–A181. 32

[Linhares et al., 2009] Linhares, J. M. M., Pinto, P. D. A., and Nascimento, S. M. C. (2009). Color rendering of art paintings under cie illuminants for normal and color deficient observers. *J. Opt. Soc. Am. A*, 26(7):1668–1677. 32

[LM75-01, 2001] LM75-01, I. (2001). Goniophotometer types and photometric coordinates. Technical report, Illuminating Engineering Society of North America - IESNA, New York City, USA. 53

[Luo, 2011] Luo, M. R. (2011). The quality of light sources. *Coloration Technology*, 127:75–87. 6, 12

[MacAdam, 1935a] MacAdam, D. L. (1935a). Maximum visual efficiency of colored materials. *J. Opt. Soc. Am.*, 25(11):361–367. 31, 38

[MacAdam, 1935b] MacAdam, D. L. (1935b). The theory of the maximum visual efficiency of colored materials. *J. Opt. Soc. Am.*, 25(8):249–249. 31, 38

[Malacara, 2002] Malacara, D. (2002). *Color Vision and Colorimetry theory and Applications*, chapter 4. SPIE. 10

[Martínez-Verdú et al., 2007] Martínez-Verdú, F., Perales, E., Chorro, E., de Fez, D., Viqueira, V., and Gilabert, E. (2007). Computation and visualization of the macadam limits for any lightness, hue angle, and light source. *J. Opt. Soc. Am. A*, 24(6):1501–1515. 32

[Masaoka, 2010] Masaoka, K. (2010). Fast and accurate model for optimal color computation. *Opt. Lett.*, 35(12):2031–2033. 32, 38, 39

[Masuda and Nascimento, 2012] Masuda, O. and Nascimento, S. M. C. (2012). Lighting spectrum to maximize colorfulness. *Opt. Lett.*, 37(3):407–409. 31

[McGowan and Rea, 1994] McGowan, T. and Rea, M. (1994). Visibility and spectral composition, another look in the mesopic. In *Proceedings of the CIE Symposium on Advances in Photometry*, pages 107–109. 66

[Nascimento and Masuda, 2012] Nascimento, S. M. C. and Masuda, O. (2012). Psychophysical optimization of lighting spectra for naturalness, preference, and chromatic diversity. *J. Opt. Soc. Am. A*, 29(2):A144–A151. 32

[Ochoa et al., 2014] Ochoa, M., Corredor, D. A., and Quintero, J. M. (2014). Comparación de pinturas para aplicaciones en fotometría. In *Anais do XII Conferência Latino-Americana De Iluminação*, pages 127 – 131. 100

[Ohno, 2004] Ohno, Y. (2004). Color rendering and luminous efficacy of white led spectra. 6, 30

[Ohta and Robertson, 2005] Ohta, N. and Robertson, A. R. (2005). *Colorimetry: Fundamentasl and Applications*, chapter 6. Wiley. 10

[Pérez-Carpinell et al., 1998] Pérez-Carpinell, J., de Fez, M. D., Baldoví, R., and Soriano, J. C. (1998). Familiar objects and memory color. *Color Research & Application*, 23:416–427. 14

[Quintero and Carreras, 2012] Quintero, J. M. and Carreras, J. (2012). *CIE* recommended mesopic photometry system and implications in outdoor lighting design. In *Memorias XI Congreso Iberoamericano de Iluminación, Luxamérica Cartagena Colombia 2012*. 99

[Quintero et al., 2010] Quintero, J. M., Carreras, J., Sudrià-Andreu, A., and Ramírez-Pisco, R. (2010). Led: ¿la nueva generación en fuentes de luz ?. Revista Automática e Instrumentación. No. 422. 100

[Quintero and Forment, 2010] Quintero, J. M. and Forment, S. (2010). Comparison of measures using a far field and near field goniophotometer. In *Proceedings of the CIE Expert Symposium on Spectral and Imaging Methods for Photometry and Radiometry*. 98

[Quintero et al., 2014] Quintero, J. M., Gutierrez, J. F., and Sudrià-Andreu, A. (2014). Necesidad de nuevos indicadores de calidad de color en fuentes de luz. Revista Automática e Instrumentación. No. 466. 101

[Quintero et al., 2012a] Quintero, J. M., Hunt, C. E., and Carreras, J. (2012a). The $3D$-color rendering map. In *Memorias XI Congreso Iberoamericano de Iluminación, Luxamérica Cartagena Colombia 2012*. 99

[Quintero et al., 2012b] Quintero, J. M., Hunt, C. E., and Carreras, J. (2012b). Comparison of $CQS(Qg)$ and optimal color volume for the evaluation of color saturation. In *13th International Light-Source Symposium, LS13*. 100

[Quintero et al., 2012c] Quintero, J. M., Hunt, C. E., and Carreras, J. (2012c). De-entangling colorfulness and fidelity for a complete statistical description of color quality. *Opt. Lett.*, 37(23):4997–4999. 37, 38, 98

[Quintero et al., 2012d] Quintero, J. M., Hunt, C. E., and Carreras, J. (2012d). Method to establish a color quality and luminous efficacy ranking for light sources. In *Lighting quality and energy efficiency CIE conference*. 98

[Quintero et al., 2012e] Quintero, J. M., Sudrià-Andreu, A., Hunt, C. E., and Carreras, J. (2012e). Color rendering map: a graphical metric for assessment of illumination. *Opt. Express*, 20(5):4939–4956. 30, 38, 98

[Quintero et al., 2009] Quintero, J. M., Sudrià-Andreu, A., and Ramírez-Pisco, R. (2009). Barreras en la sustitución masiva de bombillas incandescentes. Revista Automática e Instrumentación. 100

[Rea et al., 2004] Rea, M., Bullough, J., Freyssinier-Nova, J., and Bierman, A. (2004). A proposed unified system of photometry. *Lighting Research and Technology*, 36(2):85–109. 66

[Rea and Freyssinier, 2010] Rea, M. and Freyssinier, J. (2010). Color rendering: Beyond pride and prejudice. *Color Research & Application*, 35(6):401–409. 30, 35

[Rea and Freyssinier-Nova, 2008] Rea, M. S. and Freyssinier-Nova, J. P. (2008). Color rendering: A tale of two metrics. *Color Research & Application*, 33(3):192–202. 6

[Real-Decreto1890, 2008] Real-Decreto1890, S. (2008). Reglamento de eficiencia energética en instalaciones de alumbrado exterior. Technical report, Ministerio de Industria, Turismo y Comercio, Madrid, Spain. 80, 83, 84, 85

[Rodríguez et al., 2014] Rodríguez, C., Zapata, M. A., Amórtegui, F. J., and Quintero, J. M. (2014). Diseño de luminaria para intecomparación de goniofotómetros. In *Anais do XII Conferência Latino-Americana De Iluminação*, pages 278 – 281. 100

[Sánchez-Balvás et al., 2012a] Sánchez-Balvás, L. A., Quintero, J. M., Sudrá-Andreu, A., de Felipe Blanch, J. J., and Carreras, J. (2012a). Toward a new model of sustainable urban lighting. In *Congreso Iberoamericano de Iluminación Luxamérica 2012, Cartagena Colombia.* 79, 99

[Sánchez-Balvás et al., 2012b] Sánchez-Balvás, L. A., Quintero, J. M., Sudriá-Andreu, A., de Felipe Blanch, J. J., and Carreras, J. (2012b). General guidelines for efficient and comfortable urban lighting. In *III European Conference on Energy Eficiency and Sustainability in Architecture and Planning.* 99

[Schanda, 2011] Schanda, J. (2011). Getting color right: Improved visual matching with led light sources. In *The Professional Lighting Design Convention 2011.* 14

[Schrödinger, 1920] Schrödinger, E. (1920). Theorie der pigmente von gröster leuchtkraft. *Annalen der Physik*, 367(15):603–622. 31

[Smet et al., 2011a] Smet, K., Ryckaert, W. R., Pointer, M. R., Deconinck, G., and Hanselaer, P. (2011a). Colour appearance rating of familiar real objects. *Color Research & Application*, 36(3):192–200. 30, 35

[Smet et al., 2011b] Smet, K., Ryckaert, W. R., Pointer, M. R., Deconinck, G., and Hanselaer, P. (2011b). Correlation between color quality metric predictions and visual appreciation of light sources. *Opt. Express*, 19(9):8151–8166. 30, 35

[Smet and Whitehead, 2011] Smet, K. and Whitehead, L. A. (2011). Consideration of meta-standards for color rendering metrics. In *Proceedings of the 19th Color Imaging Conference*. 12

[Smet et al., 2014] Smet, K. A., Lin, Y., Nagy, B. V., Németh, Z., Duque-Chica, G. L., Quintero, J. M., Chen, H.-S., Luo, R. M., Safi, M., and Hanselaer, P. (2014). Cross-cultural variation of memory colors of familiar objects. *Opt. Express*, 22(26):32308–32328. 98

[Smet et al., 2010] Smet, K. A. G., Ryckaert, W. R., Pointer, M. R., Deconinck, G., and Hanselaer, P. (2010). Memory colours and colour quality evaluation of conventional and solid-state lamps. *Opt. Express*, 18(25):26229–26244. 6

[van der Burgt and van Kemenade, 2010] van der Burgt, P. and van Kemenade, J. (2010). About color rendition of light sources: The balance between simplicity and accuracy. *Color Research & Application*, 35:85–93. 7

[Žukauskas et al., 2011] Žukauskas, A., Vaicekauskas, R., Tuzikas, A., Vitta, P., and Shur, M. (2011). Statistical approach to color rendition properties of solid state light sources. 30

[X-Rite®, 2012] X-Rite® (2012). *The Munsell Book of Color (Glossy Collection)*. X–rite. 12

[Zukauskas et al., 2009] Zukauskas, A., Vaicekauskas, R., Ivanauskas, F., Vaitkevicius, H., Vitta, P., and Shur, M. (2009). Statistical approach to color quality of solid-state lamps*. *Selected Topics in Quantum Electronics, IEEE Journal of*, 15(6):1753–1762. 30, 35

Appendix A

Curriculum Vitae of the Author

A.1 Brief Biography

Jesús M. Quintero received the degree of Specialist in Industrial Automation and Control from the National University of Colombia in 2007, a B.S.E.E. degree from the National University of Colombia in 1992 and a Specialist degree in Informatics and Communications Technology from Los Andes University, Colombia in 2002. He worked from 1991 to 2003 as a Leader Engineer for a Colombian company devoted to desing and manufacturing of power electronics equipment. Since 2004, he has been at the National University of Colombia in Bogotá, where he is a Senior Lecturer on Electrical and Electronics Engineering, with appointments in analog electronics and the Light and Lighting program. He is in his fifth year of Ph.D. Program in Electrical Engineering at the Universitat Politecnica de Catalunya (UPC) in Barcelona, Spain. He worked as a doctoral fellow at the Institute for Energy Research of Catalonia (IREC) from 2009 to 2012 and did his staying as a doctoral fellow for three months in 2010 at the Light and Lighting Laboratory of the KaHo Sint-Lieven University in Ghent, Belgium. His research centers on high-power light-emitting diodes, luminescent materials, color quality of light sources and power electronics.

A.2 List of publications

A.2.1 Journal papers

- [Quintero et al., 2012e] Quintero, J. M., Sudrià-Andreu, A., Hunt, C. E. and Carreras, J. (2012b). Color rendering map: A graphical metric for assessment of illumination. Opt. Express, 20(5):4939-4956.

- [Quintero et al., 2012c] Quintero, J. M., Hunt, C. E., and Carreras, J.(2012a). De-entangling colorfulness and fidelity for a complete statistical description of color quality. Opt. Lett., 37(23):4997-4999.

- [Hertog et al., 2014] Hertog, W., Llenas, A., Quintero, J. M., Hunt, C. E.,and Carreras, J. (2014). Energy efficiency and color quality limits in artificial light sources emulating natural illumination. Opt. Express, 22(S7):A1659-A1668.

- [Smet et al., 2014] Smet, K. A., Lin, Y., Nagy, B. V., Németh, Z., Duque-Chica, G. L., Quintero, J. M., Chen, H.S., Luo, R. M., Safi, M., and Hanselaer, P. (2014). Cross-cultural variation of memory colors of familiar objects. Opt. Express, 22(26):32308-32328.

A.2.2 CIE Conference proceedings

- [Quintero et al., 2012d] Quintero, J. M., Hunt, C. E., and Carreras, J. (2012). Method to establish a color quality and luminous efficacy ranking for light sources. In Lighting quality and energy efficiency CIE conference. Hangzhou, China

- [Quintero and Forment, 2010] Quintero, J. M. and Forment, S. (2010). Comparison of measures using a far field and near field goniophotometer. In Proceedings of the CIE Expert Symposium on Spectral and Imaging Methods for Photometry and Radiometry. Bern, Switzerland

- [Carreras et al., 2010] Carreras, J., Quintero, J. M., and Hunt, C. E. (2010). Theoretical maximum efficacy and color rendering assessment of energy efficient light sources. In 2nd CIE Expert Symposium on Appearance, When Appearance meets Lighting Book of Abstracts. Ghent, Belgium

A.2.3 International Conference Proceedings

- [Sánchez-Balvás et al., 2012a] Sánchez-Balvás, L. A., Quintero, J. M., Sudrià-Andreu, A., de Felipe Blanch, J. J., and Carreras, J. (2012a). Toward a new model of sustainable urban lighting. In Memorias XI Congreso Iberoamericano de Iluminación, Luxamérica 2012, Cartagena - Colombia

- [Quintero and Carreras, 2012] Quintero, J. M. and Carreras, J. (2012). CIE recommended mesopic photometry system and implications in outdoor lighting design. In Memorias XI Congreso Iberoamericano de Iluminación, Luxamérica 2012, Cartagena - Colombia

- [Quintero et al., 2012a] Quintero, J. M., Hunt, C. E., and Carreras, J. (2012). The 3D-color rendering map. In Memorias XI Congreso Iberoamericano de Iluminación, Luxamérica 2012, Cartagena - Colombia

- [Sánchez-Balvás et al., 2012b] Sánchez-Balvás, L. A., Quintero, J. M., Sudrià-Andreu, A., de Felipe Blanch, J. J., and Carreras, J. (2012). General guidelines for efficient and comfortable urban lighting. In III European Conference on Energy Efficiency and Sustainability in Architecture and Planning. San Sebastian, Spain

- [Hunt et al., 2011] Hunt, C. E., Carreras, J., and Quintero, J. M. (2011). Appearance degradation and chromatic shift in energy-efficient lighting devices. In Nineteeth Color Imaging Conference: Color Science and Engineering Systems, Technologies, and Applications. San José, California - USA

- [Acuña et al., 2010] Acuña, P., Quintero, J. M., and Parra, E. E. (2010). Impacto del alumbrado público con tecnología led en la emisión de armónicos en la red de distribución. In X Congreso Panamericano de Iluminación - Luxamérica 2010. Valparaiso, Chile

- [Acuña et al., 2014] Acuña, P., Quintero, J. M., Losada, D. F., Leloup, F. B., and Hanselaer, P. (2014). Inter-laboratory comparison of luminous intensity distribution and total luminous flux measurements with far field and near field goniophotometers. In Anais do XII Conferência Latino-Americana De Iluminação, pages 127 - 131.

- [Gutierrez et al., 2014b] Gutierrez, J. F., Hunt, C. E., and Quintero, J. M. (2014b). Visible light communication led based on luminary

for general lighting: State of the art. In Anais do XII Conferência Latino-Americana De Iluminação, pages 163 - 170.

- [Gutierrez and Quintero, 2014] Gutierrez, J. F. and Quintero, J. M. (2014). Planteammiento procedimiento para verificación de luminancímetros. In Anais do XII Conferência Latino-Americana De Iluminação, pages 114 - 118.

- [Gutierrez et al., 2014a] Gutierrez, J. F., Chávez, M. A., Cabra, M. S., and Quintero, J. M. (2014a). Calibración de monitores para estudio de percepción de color. In Anais do XII Conferência Latino-Americana De Iluminação, pages 171 - 177.

- [Corredor et al., 2014] Corredor, D. A., Ochoa, M., and Quintero, J. M.(2014). Software multiplataforma para cálculos colorimétricos y de eficacia lumínica de las fuentes de luz. In Anais do XII Conferência Latino-Americana De Iluminação, pages 182 - 187.

- [Ochoa et al., 2014] Ochoa, M., Corredor, D. A., and Quintero, J.M. (2014). Comparación de pinturas para aplicaciones en fotometría. In Anais do XII Conferência Latino-Americana De Iluminação, pages 127 - 131.

- [Rodríguez et al., 2014] Rodríguez, C., Zapata, M. A., Amórtegui, F. J., and Quintero, J. M. (2014). Diseño de luminaria para intecomparación de goniofotómetros. In Anais do XII Conferência Latino-Americana De Iluminação, pages 278 - 281.

A.2.4 Conference abstracts with (poster) presentation

- [Quintero et al., 2012b] Quintero, J. M., Hunt, C. E., and Carreras, J. (2012b). Comparison of CQS(Qg) and optimal color volume for the evaluation of color saturation. In 13th International Light-Source Symposium, LS13. Troy, New York. USA

A.2.5 Publication in national journals

- [Quintero et al., 2009] Quintero, J. M., Sudrià-Andreu, A., and Ramírez-Pisco, R. (2009). Barreras en la sustitución masiva de bombillas incandescentes. Revista Automática e Instrumentación. Spain

- [Quintero et al., 2010] Quintero, J. M., Carreras, J., Sudrià-Andreu, A., and Ramírez-Pisco, R. (2010). Led: ¿la nueva generación en

fuentes de luz ?. Revista Automática e Instrumentación. No. 422. Spain

- [Quintero et al., 2014] Quintero, J. M., Gutierrez, J. F., and Sudrià-Andreu, A. (2014). Necesidad de nuevos indicadores de calidad de color en fuentes de luz. Revista Automática e Instrumentación. No. 466. Spain

- [Gutierrez et al., 2014c] Gutierrez, J. F., Quintero, J. M., and Sudrià-Andreu, A. (2014b). VLC: Fuentes de luz led para comunicación inalámbrica. Revista Automática e Instrumentación. No. 466. Spain

Appendix B

Journal Publications

B.1 Publication No. 1

ATTENTION ¡

Pages 104 to 136 of the thesis are available at the editor's web

- **Quintero, J. M., Sudrià-Andreu, A., Hunt, C. E. and Carreras, J**. *Color rendering map: A graphical mètric for assessment of illumination*. Optics Express, 2012, vol. 20 #5, p. 4939-4956. doi 10.1364/OE.20.004939 http://www.opticsinfobase.org/oe/abstract.cfm?uri=oe-20-5-4939

- **Quintero, J. M., Hunt, C. E., Carreras, J**. *De-entangling colorfulness and _delity for a complete statisticaldescription of color quality*. Optics Letters, 2012. vol 37 #23, p.4997-4999 doi: 10.1364/OL.37.004997 http://www.opticsinfobase.org/ol/abstract.cfm?uri=ol-37-23-4997

- Hertog, W., Llenas, A., Quintero, J. M., Hunt, C. E.,and Carreras, J. *Energy efficiency and color quality límits in artificial light sources emulating natural illumination* Optics Express, 2014, vol. 22, S7, p. A1659-A1668 doi: 0.1364/OE.22.0A1659 http://www.opticsinfobase.org/oe/abstract.cfm?uri=oe-22-S7-A1659

Appendix C

Matlab code

In this apendix there are parts of the Matlab code generated to calculate Color Rendering Map, 3D-CRM in chapter 1, Efficacy and color quality, ECQ in chapter 2, and Optimal Colors Solid Volume, V_{ch} in chapter 3.

```
% Approach based on color diffences in the CIELAB and CIECAM02
Color spaces

function importgamut_Callback(hObject, eventdata, handles)
%{
%Calculate white point of the iluminant light source
XYZ=handles.data.XYZ;
wavelength=handles.data.wavelength;

Xw=trapz(wavelength,handles.data.illuminant.psd.*XYZ(:,1));
Yw=trapz(wavelength,handles.data.illuminant.psd.*XYZ(:,2));
Zw=trapz(wavelength,handles.data.illuminant.psd.*XYZ(:,3));
Xn = 100 * Xw / Yw;
Yn = 100;
Zn = 100 * Zw / Yw;
%}
%%%%%%%%%%%%%%%%%%%%%%%%%%%%%%%%%%%%%%
%%%%%
[file,path]=uigetfile('*.txt','Load Gamut');
if  isfloat(file),  return; end
aux=load([path file]);

Lm=aux(:,1); %luminances measured
x=aux(:,2);
y=aux(:,3);
%Luminance scale factor validate with real Macbeth D65 light
source

% ---------------------- Input Values ----------------------------
% -------------------- of measurement ----------------------------

Lw = 400; % average measured luminance [cd / m2] of the white
patch No. 19

XnYnZn = [95.87 100 111.48]; %Illuminant light source used in
measurements.
% [95.87 100 111.48] ref white of Spectralight III
% [95.048 99.998 108.9] ref. white of transformation Matrix sRGB
% [95.04 100 108.88] ref. white standar CIE D65 illuminante
%-----------------------------------------------------------------
maxmunsell = 100;      % Factor to obtain XYZ values in [0 - 1] range.
                        % (based on maximun of XYZ values of
munsell samples).
%----------------------------------------------------------------
% -- Parameters to obtain the input-gamut volume ----------------
RY = 100;       % No of desided steps in Y axis; Recommended: 100.
Rx = 50;        % No of desided steps in x axis; Recommended: 50.
% ---------------------------------------------------------------
scalefactor = 91 / Lw; % Luminace value(Y) that should gives p 19
                  % under illuminant D65 over Luminance (Lw)
                  % measured (cd/m^2) on this patch.

Ym = Lm * scalefactor; % Y from 0 to aprox. 100
xyY = [x y Ym];
xyYvol = volumegamut(xyY, RY, Rx);

xvol = xyYvol(:,1);
yvol = xyYvol(:,2);
Yvol = xyYvol(:,3);
Xvol = Yvol ./ yvol .* xvol;
Zvol = Yvol ./ yvol .* (1 - xvol - yvol);
XYZvo = [Xvol Yvol Zvol];         % XYZ of input-gamut volume
XYZvol = XYZvo / maxmunsell;

RGBvo = XYZ2sRGB(XYZvol,XnYnZn);
RGBvol = RGBvo / 255;            % RGB colors of input-gamut volume
labvol = XYZ2Lab(XYZvo, XnYnZn);  % CIELAB of input-gamut
volume

JChvol = XYZ2CIECAM02(XYZvo,Lw);  % CIECAM02 of input-
gamut volume
                    % Lw = measured luminance white patch.[cd/m2]
Chrvol = JChvol(:,2);
Jvol = JChvol(:,1);
acvol = Chrvol .* cos( pi/180 * JChvol(:,3));
bcvol = Chrvol .* sin( pi/180 * JChvol(:,3)); % rectangular
coordinates of
                    % CIECAM02 input-gamut volume
% ---------------------------------------------------------
%{
% To clamp the input gamut
indexx=find(Ym < 150);
x=x(indexx);
y=y(indexx);
Lm=Lm(indexx);
Ym=Ym(indexx);
%}

%{
%%  Obtaining Vm from Ym by generating table V, Y %%%%%
%Equation from book: Colorimetry - by Ohta/Robertson, pg. 122

V=0:0.01:10;
Y=1.2219*V-0.23111*V.^2+0.23951*V.^3-
0.021009*V.^4+0.0008404*V.^5;

for i=1:length(Ym)
   [minvalue index]=min(abs(Y-Ym(i)));
   Vm(i)=V(index);
end   %Input Ym, output Vm with values taken from table V, Y

%%% Another aproach to obtain Vm, using a direct equation:
%%% Equation taken from ASTM-D1535-08

for i=1:length(Ym)
    if Ym(i)<=0.9 Vm(i)=0.87445*Ym(i)^0.9967;
    else Vm(i)=2.49268*Ym(i)^(1/3)-1.5614-0.985/((0.1073*Ym(i)-
3.084)^2+7.54)+0.0133/Ym(i)^2.3+0.0084*sin(4.1*Ym(i)^(1/3)+1)+
(0.0221/Ym(i))*sin(0.39*(Ym(i)-2))-
(0.0037/(.44*Ym(i)))*sin(1.28*(Ym(i)-0.53));
    end
end

for i=1:length(handles.data.munsell.names)
   [a1 a2 a3
a4]=parseMunsellName(handles.data.munsell.names(i,:));
   Vmunsell(i)=a3;
end
%}

% Munsell Lab
x1=handles.data.munsell.xyY(:,1);
y1=handles.data.munsell.xyY(:,2);
Y1=handles.data.munsell.xyY(:,3);

%%%%%%%%%%%%%%%%%%%%   CIELAB of Munsell samples
%%%%%%%%%%%%%%%%%%%%%
X1=Y1./y1.*x1;
Z1=Y1./y1.*(1-x1-y1);
XYZ1=[X1 Y1 Z1];
%----------------------------------------------------------------

XYZ1s = XYZ1 / maxmunsell;  % scale XYZ1 to [0,1]
RGB1 = XYZ2sRGB ( XYZ1s, XnYnZn ); % conversion to sRGB
```

```
RGB1 = RGB1 / 255;        % scale RGB to [0,1]
%--------------------------------------------------------------------

lab1=XYZ2Lab(XYZ1, XnYnZn); %


% Chroma of Munsell samples

C1=sqrt(lab1(:,2).^2+lab1(:,3).^2);

% Hue of Munsell samples

b1=lab1(:,3);
a1=lab1(:,2);
h1=atan2(b1,a1);
index1 = find( h1 < 0 );
h1(index1) = h1(index1)+ 2 * pi;

%%%%%%%%%%%%%%%%%%   CIELAB of input Gamut
%%%%%%%%%%%%%%%%%%%%%%%%%
R=0;
h2=waitbar(0, 'Calculating input gamut in CIELAB....please wait.');
for i=1:length(Ym)

   X=Ym(i)/y(i)*x(i);
   Z=Ym(i)/y(i)*(1-x(i)-y(i));

   XYZi=[X Ym(i) Z];

   lab=XYZ2Lab(XYZi,XnYnZn);% light source used in measurements.

   % XYZinput(i,:) = XYZi;

   gamutlab(i,:)=lab;

%%%%%%%%%%    approach using differences in cilindrical
coordinates

   % Chroma
   C=sqrt(lab(2)^2+lab(3)^2);

   % Hue
   b=lab(:,3);
   a=lab(:,2);
   h = atan2( b, a );
   if h < 0
     h = h + 2 * pi;
   end

   deltaL = lab1(:,1) - lab(1);
   deltaC = C1 - C;
   deltaH = h1 - h;
   distance= sqrt( (deltaL).^2 + C1.^2+C.^2 -2.*C1.*C.*cos(deltaH));
   [mindistance(i) index] = min(distance);
   R = R + handles.data.munsell.Rm(index);
   selectedmunsell(i) = index;

 waitbar(i/length(Ym));
end
close(h2);

R = R / length(Ym);

% input gamut to RGB colors
%--------------------------------------------------------------------
   % XYZs = XYZinput / maxmunsell;  % scale XYZ (input gamut) to
[0,1]
   % RGB = XYZ2sRGB ( XYZs, XnYnZn );% conversion to sRGB
   % RGB = RGB / 255;                  % scale RGB to [0,1]
%--------------------------------------------------------------------

Rmun = 0;
j=1;
for i=1:1269
   index=find( selectedmunsell == i);
   if ~isempty(index)
      string(j,:)=[handles.data.munsell.names(i,:) '        '...
                sprintf('%5d',length(index)) '        '...
                sprintf('%7.3f',handles.data.munsell.Rm(i))];
      labselindex(j,:) = [i length(index)]; %index of CIELAB selected
munsell and repetitions
      labsel(j,:) = lab1(i,:);    % CIELAB of selected Munsell
      RGBlabsel(j,:) = RGB1(i,:); % RGB color of selected Munsell
      xmunsellselected(j)=handles.data.munsell.xyY(i,1);
      ymunsellselected(j)=handles.data.munsell.xyY(i,2);
      Ymunsellselected(j)=handles.data.munsell.xyY(i,3);
      j=j+1;
      Rmun = Rmun + handles.data.munsell.Rm(i);

   end
end
Rmun = Rmun / j;

handles.data.labselindex=labselindex;
%save ('labselindex')
% ------------------------------------------------------------
% save 'pixelsinfo.txt' string -ASCII; % Information of the Selected
Munsell
% R     % Weighted average of R.
% Rmun    % simple average of R.
maxdist = max(mindistance);  % max.of the min.dist.found from input
gamut to munsell
mindist = min(mindistance);  % min.of the min.dist.found from input
gamut to munsell
meandist = mean(mindistance);

Rinfo = [sprintf('%s','CIELAB') '    ' sprintf('%5d',length(Ym))...
'    ' sprintf('%5d',size(labselindex,1))  '    ' sprintf('%7.3f', R) ...
'    ' sprintf('%7.3f',Rmun) '    ' sprintf('%7.3f',maxdist) ...
'    ' sprintf('%7.3f',mindist) '    ' sprintf('%7.3f',meandist)];
%string  % selected munsell table.

%{
%%%%  plot of the gamut of the munsell samples at the Horseshoe
(tongue)%%%

figure;
set(gca,'XColor','y','YColor','y');
try
   load('munsellxytongue.mat');
   var=load('xyz.mat');
   minx=xytongue{1}(1); maxx=xytongue{1}(2);
   miny=xytongue{2}(1); maxy=xytongue{2}(2);
   C=xytongue{3};
   image([minx maxx],[miny maxy],C);
   set(gca,'YDir','normal');
   hold on
   plotxyboundary(var.wavelength,var.XYZ,'ciecolor',1);
   axis([minx-.05 maxx+.05 miny-.05 maxy+.05])
   set(gca,'Color',handles.background);
   text(0.5,0.7,'CIE Diagram over','Color','w')
   text(0.5,0.65,'Munsell Region','Color','w')
catch
   [minx, maxx, miny, maxy, C]=plotxytongue(handles);
   axis([minx-.05 maxx+.05 miny-.05 maxy+.05])
   xytongue{1}=[minx maxx];
```

Appendix C Matlab code

```
   xytongue{2}=[miny maxy];
   xytongue{3}=C;
   save munsellxytongue.mat xytongue;
   text(0.45,0.7,'CIE Diagram over','Color','w')
   text(0.45,0.65,'Munsell Region','Color','w')
end

hold on
plot(x1,y1,'k.');                    % munsell samples
plot(x,y,'w.');                      % input gamut
plot(xmunsellselected,ymunsellselected,'.'); % selected Munsell

%}

%{
% 3D of Munsell samples
figure
F = TriScatteredInterp(x1,y1,Y1);
ti = 0.2: 0.6: 0.8;
tf = 0.2: 0.6: 0.8;
[qx,qy] = meshgrid(ti,tf);
qz = F(qx,qy);
mesh(qx,qy,qz);
hold on;
plot3(x1,y1,Y1,'r.');

% 3D of Gamut
hold on
F2 = TriScatteredInterp(x,y,Ym);
ti = 0:1:1;
[qx,qy] = meshgrid(ti,ti);
qz = F2(qx,qy);
mesh(qx,qy,qz);
hold on;
plot3(x,y,Ym,'b.');

F3 =
TriScatteredInterp(xmunsellselected',ymunsellselected',Ymunsellsele
cted');
ti = 0:1:1;
[qx,qy] = meshgrid(ti,ti);
qz = F3(qx,qy);
mesh(qx,qy,qz);
hold on;
plot3(xmunsellselected',ymunsellselected',Ymunsellselected','g.');

%}

%{
%%%%%%%%%%%%%%%%%%%%  LAB SPACE PLOT
figure
hold on
plot(lab1(:,2),lab1(:,3),'r.');
plot(gamutlab(:,2),gamutlab(:,3),'b.');
plot(lab1(selectedmunsell,2),lab1(selectedmunsell,3),'gs');


% 3D munsell samples, input gamut and selected munsell %%
figure
F = TriScatteredInterp(lab1(:,2),lab1(:,3),lab1(:,1));
ti = 0:1:1;
[qx,qy] = meshgrid(ti,ti);
qz = F(qx,qy);
mesh(qx,qy,qz);
hold on;
plot3(lab1(:,2),lab1(:,3),lab1(:,1),'r.');

%para mostrar 3D
hold on
F3 = TriScatteredInterp(gamutlab(:,2),gamutlab(:,3),gamutlab(:,1));
ti = 0:1:1;
[qx,qy] = meshgrid(ti,ti);
qz = F3(qx,qy);
mesh(qx,qy,qz);
hold on;
plot3(gamutlab(:,2),gamutlab(:,3),gamutlab(:,1),'b.');



F2 =
TriScatteredInterp(lab1(selectedmunsell,2),lab1(selectedmunsell,3),la
b1(selectedmunsell,1));
ti = 0:1:1;
[qx,qy] = meshgrid(ti,ti);
qz = F2(qx,qy);
mesh(qx,qy,qz);
hold on;
plot3(lab1(selectedmunsell,2),lab1(selectedmunsell,3),lab1(selectedm
unsell,1),'gs');
%}

%          Approach based on CIECAM02 space color
%%%%%%%%%%%%%%%%%%%%%%%%%%%%%%%%%%%%
%%%   CIECAM02 of Munsell samples    %%%%%%%%%

JCh1 = XYZ2CIECAM02(XYZ1,Lw); % Lw = measured luminance
white patch.[cd/m2]

Chr1 = JCh1(:,2);
J1 = JCh1(:,1);
ac1 = Chr1 .* cos( pi/180 * JCh1(:,3));
bc1 = Chr1 .* sin( pi/180 * JCh1(:,3));

%%%  CIECAM02 of input Gamut %%%%%%%%%%%%

R02 = 0;
h1 = waitbar(0, 'Calculating input gamut in CIECAM02....please
wait.');
for i=1:length(Ym)

   X=Ym(i)/y(i)*x(i);
   Z=Ym(i)/y(i)*(1-x(i)-y(i));

   XYZin = [X Ym(i) Z];
   JCh = XYZ2CIECAM02(XYZin,Lw); % measured Luminance white
patch.

   gamut02(i,:) = JCh;

%%%%%%%%%%   Differences in CIECAM02 (cilindrical
coordinates)

   deltaJ = JCh1(:,1) - JCh(1);
   Chr = JCh(2);
   deltah = JCh1(:,3) - JCh(3);
   distance = sqrt( (deltaJ).^2 + Chr1.^2 + Chr.^2 - 2.* Chr1 .* Chr .*
cos(deltah*pi/180));
   [mindistance02(i) index] = min(distance);
   R02 = R02 + handles.data.munsell.Rm(index);
   selectedmunsell02(i) = index;
  waitbar(i/length(Ym));
end
close(h1);

R02 = R02 / length(Ym);
```

```
J = gamut02(:,1);
ac = gamut02(:,2) .* cos( pi/180 * gamut02(:,3));
bc = gamut02(:,2) .* sin( pi/180 * gamut02(:,3));

Rmun02 = 0;
j=1;
for i=1:1269
   index=find( selectedmunsell02 == i);
   if ~isempty(index)
      string02(j,:)=[handles.data.munsell.names(i,:) '       '...
                sprintf('%5d',length(index)) '       '...
                sprintf('%7.3f',handles.data.munsell.Rm(i))];
      camselindex(j,:) = [i length(index)] ; %index of CIECAM02
selected munsell and repetitions.
      RGBcamsel(j,:) = RGB1(i,:); % RGB color of CIECAM02 selected
Munsell
      xmunsellselected02(j)=handles.data.munsell.xyY(i,1);
      ymunsellselected02(j)=handles.data.munsell.xyY(i,2);
      %Ymunsellselected02(j)=handles.data.munsell.xyY(i,3);
      j=j+1;
      Rmun02 = Rmun02 + handles.data.munsell.Rm(i);
      end
end

Rmun02 = Rmun02 / j;

handles.data.camselindex=camselindex;
% save 'pixelsinfo.txt' string02 -ASCII; % Information of the Selected
Munsell



string   % CIELAB selected munsell table.
string02  % CIECAM02 selected munsell table.

maxdist02  = max(mindistance02);  % max.of the min.dist.found from
input gamut to munsell
mindist02  = min(mindistance02);  % min.of the min.dist.found from
input gamut to munsell
meandist02 = mean(mindistance02);

Rinfo02 = [sprintf('%s','CIECAM') '    ' sprintf('%5d',length(Ym))...
'    ' sprintf('%5d',size(camselindex,1)) '    ' sprintf('%7.3f', R02) ...
'    ' sprintf('%7.3f',Rmun02) '    ' sprintf('%7.3f',maxdist02) ...
'    ' sprintf('%7.3f',mindist02) '    ' sprintf('%7.3f',meandist02)];

Rinfo = [Rinfo; Rinfo02]

% ------------------------------------------------------------------
% Gray scale of selected Munsell (CIELAB and CIECAM02)

%Rgraylab = handles.data.munsell.Rm(labselindex(:,1))' ./ 100;
%Rgraycam = handles.data.munsell.Rm(camselindex(:,1))' ./ 100;
%random generation of R
%
Rgraylab =
min(1,max(0,(random('norm',0.6,0.3,1,size(labselindex,1)))))';
Rgraycam =
min(1,max(0,(random('norm',0.4,0.1,1,size(camselindex,1)))))';
%
graylab = [Rgraylab Rgraylab Rgraylab];
graycam = [Rgraycam Rgraycam Rgraycam];
%-----------------------------------------------------



handles.data.gamuts.RGBmunsell = RGB1;
handles.data.gamuts.RGBvol = RGBvol;
handles.data.gamuts.RGBsellab = RGBlabsel;
handles.data.gamuts.RGBselcam = RGBcamsel;
handles.data.gamuts.xyYvol =[xvol yvol Yvol];
handles.data.gamuts.labvol =labvol;
handles.data.gamuts.camvol =[acvol bcvol Jvol];
handles.data.gamuts.xyYsel
=[xmunsellselected',ymunsellselected',Ymunsellselected'];
handles.data.gamuts.labsel =labsel;
handles.data.gamuts.camsel =[ac1(camselindex(:,1))
bc1(camselindex(:,1)) J1(camselindex(:,1))];
%=====================================%
%%%%  CIECAM02  %%%%
%%%%  plot of the gamut of the munsell samples at the Horseshoe
(tongue)%%%

figure;
set(gca,'XColor','y','YColor','y');
try
   load('munsellxytongue.mat');
   var=load('xyz.mat');
   minx=xytongue{1}(1); maxx=xytongue{1}(2);
   miny=xytongue{2}(1); maxy=xytongue{2}(2);
   C=xytongue{3};
   image([minx maxx],[miny maxy],C);
   set(gca,'YDir','normal');
   hold on
   plotxyboundary(var.wavelength,var.XYZ,'ciecolor',1);
   axis([minx-.05 maxx+.05 miny-.05 maxy+.05])
   set(gca,'Color',handles.background);
   text(0.5,0.7,'CIE Diagram over','Color','w')
   text(0.5,0.65,'Munsell Region','Color','w')
catch
   [minx, maxx, miny, maxy, C]=plotxytongue(handles);
   axis([minx-.05 maxx+.05 miny-.05 maxy+.05])
   xytongue{1}=[minx maxx];
   xytongue{2}=[miny maxy];
   xytongue{3}=C;
   save munsellxytongue.mat xytongue;
   text(0.45,0.7,'CIE Diagram over','Color','w')
   text(0.45,0.65,'Munsell Region','Color','w')
end

hold on
plot(x1,y1,'k.');                    % munsell samples
plot(x,y,'w.');                      % input gamut
plot(xmunsellselected02,ymunsellselected02,'.'); % selected Munsell
%{
%_____________________________________________
%          First try to plot 3D gamuts          %
%%%%              CIECAM02                %%%%
%  3D of munsell samples, input gamut and selected munsell %
Munsell samples %
figure
F = TriScatteredInterp(ac1, bc1, J1);
ti = 0:1:1;
[qx,qy] = meshgrid(ti,ti);
qz = F(qx,qy);
mesh(qx,qy,qz);
hold on;
plot3(ac1, bc1, J1, 'r.');

% input gamut

F3 = TriScatteredInterp(ac, bc, J);
ti = 0:1:1;
[qx,qy] = meshgrid(ti,ti);
qz = F3(qx,qy);
mesh(qx,qy,qz);
```

Appendix C Matlab code

```
hold on;
plot3(ac, bc, J,'b.');

% Selected Munsell samples

F2 =
TriScatteredInterp(ac1(selectedmunsell02),bc1(selectedmunsell02),J1(
selectedmunsell02));
ti = 0:1:1;
[qx,qy] = meshgrid(ti,ti);
qz = F2(qx,qy);
mesh(qx,qy,qz);
hold on;
plot3(ac1(selectedmunsell02),bc1(selectedmunsell02),J1(selectedmun
sell02),'gs');
%_____________________________________________
%}

%-------------------------------------------------------------
% Figure No. 0
% plot 1269 Munsell samples
% xyY Color space
%-------------------------------------------------------------
figure
scatter3(x1,y1,Y1, 200, RGB1, 'filled');
set(gca,'Color',[0.7 0.7 0.7]);
set(gca,'FontSize',20);
set(gcf,'PaperUnits','centimeters','PaperSize',[8.5 8.5]);
xlabel('x'); ylabel('y'); zlabel('Y'); title('xyY Color space');
%-------------------------------------------------------------------

%-------------------------------------------------------------------
% Figure No. 0A
% plot 1269 Munsell samples
% CIELAB Color space
%-------------------------------------------------------------------
figure
scatter3(lab1(:,2),lab1(:,3),lab1(:,1), 200, RGB1, 'filled');
set(gca,'Color',[0.7 0.7 0.7]);
set(gca,'FontSize',20);
set(gcf,'PaperUnits','centimeters','PaperSize',[8.5 8.5]);
xlabel('a'); ylabel('b'); zlabel('L'); title('CIELAB Color space');
%-------------------------------------------------------------------

%-------------------------------------------------------------------
% Figure No. 0B
% plot 1269 Munsell samples
% CIECAM02 Color space
%-------------------------------------------------------------------
figure
scatter3(ac1, bc1, J1, 200, RGB1, 'filled');
set(gca,'Color',[0.7 0.7 0.7]);
set(gca,'FontSize',20);
set(gcf,'PaperUnits','centimeters','PaperSize',[8.5 8.5]);
xlabel('a'); ylabel('b'); zlabel('J'); title('CIECAM02 Color space');
%-------------------------------------------------------------------

%-------------------------------------------------------------------
% Figure No. 1
% plot Munsell and volume gamut using RGB true colors
% xyY Color space
%-------------------------------------------------------------------
figure
scatter3(x1,y1,Y1, 200, RGB1, 'filled');
set(gca,'Color',[0.7 0.7 0.7]);
set(gca,'FontSize',20);
set(gcf,'PaperUnits','centimeters','PaperSize',[8.5 8.5]);
xlabel('x'); ylabel('y'); zlabel('Y'); title('Color space xyY');
hold on
scatter3(xvol, yvol, Yvol, 80, RGBvol, 'filled');

%-------------------------------------------------------------------
% Figure No. 2A
% plot CRM
% xyY Color space
%-------------------------------------------------------------------
figure
scatter3(x1,y1,Y1, 10, RGB1, 'filled');
set(gca,'Color',[0 0 0]);
set(gca,'FontSize',20);
set(gcf,'PaperUnits','centimeters','PaperSize',[8.5 8.5]);
xlabel('x'); ylabel('y'); zlabel('Y'); title('Color space xyY');
hold on
scatter3(xmunsellselected',ymunsellselected',Ymunsellselected',150,
graylab,'filled');
view(0,90)
%-------------------------------------------------------------------

%-------------------------------------------------------------------
% Figure No. 2B
% plot CRM
% xyY Color space
%-------------------------------------------------------------------
figure
scatter3(x1,y1,Y1, 20, RGB1, 'filled');
set(gca,'Color',[0 0 0]);
set(gca,'FontSize',20);
set(gcf,'PaperUnits','centimeters','PaperSize',[8.5 8.5]);
xlabel('x'); ylabel('y'); zlabel('Y'); title('Color space xyY');
hold on
scatter3(xmunsellselected',ymunsellselected',Ymunsellselected',150,
RGBlabsel,'filled');
view(0,90)


%-------------------------------------------------------------------
% Figure No. 3
% plot Munsell and volume gamut true colors
% CIELAB Color space
%-------------------------------------------------------------------
figure
scatter3(lab1(:,2),lab1(:,3),lab1(:,1), 200, RGB1, 'filled');
set(gca,'Color',[0.7 0.7 0.7]);
set(gca,'FontSize',20);
set(gcf,'PaperUnits','centimeters','PaperSize',[8.5 8.5]);
xlabel('a'); ylabel('b'); zlabel('L'); title('Color Space CIELAB');
hold on
scatter3(labvol(:,2),labvol(:,3),labvol(:,1), 80, RGBvol, 'filled');
%-------------------------------------------------------------------

%-------------------------------------------------------------------
% Figure No. 4
% plot selected munsell in CIELAB
% CIELAB Color space
%-------------------------------------------------------------------
figure
scatter3(lab1(:,2),lab1(:,3),lab1(:,1),'w.');
set(gca,'Color',[0.7 0.7 0.7]);
set(gca,'FontSize',20);
set(gcf,'PaperUnits','centimeters','PaperSize',[8.5 8.5]);
xlabel('a'); ylabel('b'); zlabel('L'); title('Color space CIELAB');
hold on
scatter3(labsel(:,2),labsel(:,3),labsel(:,1), 80, RGBlabsel,'filled');
%-------------------------------------------------------------------

%-------------------------------------------------------------------
```

```
% Figure No. 5
% plot Munsell and volume gamut true colors
% CIECAM02 Color space
%-----------------------------------------------------------------
figure
scatter3(ac1, bc1, J1, 150, RGB1, 'filled');
set(gca,'Color',[0.7 0.7 0.7]);
set(gca,'FontSize',20);
set(gcf,'PaperUnits','centimeters','PaperSize',[8.5 8.5]);
xlabel('a'); ylabel('b'); zlabel('J'); title('Color Space CIECAM02');
hold on
scatter3(acvol, bcvol, Jvol, 50, RGBvol, 'filled');
%-----------------------------------------------------------------

%-----------------------------------------------------------------
% Figure No. 6
% plot selected munsell in CIECAM02
% CIECAM02 Color space
%-----------------------------------------------------------------
figure
scatter3(ac1, bc1, J1,'w.');
set(gca,'Color',[0.7 0.7 0.7]);
set(gca,'FontSize',20);
set(gcf,'PaperUnits','centimeters','PaperSize',[8.5 8.5]);
xlabel('a'); ylabel('b'); zlabel('J'); title('Color space CIECAM02');
hold on
scatter3(ac1(camselindex(:,1)),bc1(camselindex(:,1)),J1(camselindex(:,
1)),...
      80, RGBcamsel,'filled');
%-----------------------------------------------------------------
%
%
%-----------------------------------------------------------------
% Figure No. 7
% plot 18 Color Patches from X-rite Color Checker Card
%-----------------------------------------------------------------
% colorpatches
%-----------------------------------------------------------------
%
% Find the most repetitive selected Munsell (the Mode) CIELAB:
maxrepet = max(labselindex(:,2));
modalabindex = labselindex(:,2) == maxrepet;

% Find the most repetitive selected Munsell (the Mode) CIECAM02:
maxrepet = max(camselindex(:,2));
modalcamindex = camselindex(:,2) == maxrepet;
colordata = [RGBlabsel(modalabindex,:);
RGBcamsel(modalcamindex,:)];

%-----------------------------------------------------------------
% Figure No. 8
% plot the most repetitive color selected by CIELAB and CIECAM02
aproaches
%-----------------------------------------------------------------
%-----------------------------------------------------------------
% twopatches(colordata)
%-----------------------------------------------------------------
%}
%-----------------------------------------------------------------%
%&&&&&&&&&& Begining of colorpatches
%-----------------------------------------------------------------%
% The function directly plots the 18 patches of the  ColorChecker (X-
rite)
% example
%{
 colorpatches;
%}
%-----------------------------------------------------------------

set(handles.analyzedatabase,'enable','on');

guidata(hObject,handles);

   function colorpatches
    No = 18;
    rows = 2; % fixed!! ( no change this value!!)
    xorig = 3;
    yorig = 2;
    height = 8;
    lenght = 7;
    withspace = 10;

% generate adittional 4 vertices at the begining...(because definition
of array)
    vert = [xorig yorig; xorig yorig + height; xorig + lenght yorig +
height;...
            xorig + lenght yorig];
   for j = 1 : rows

      k = 1;
    for i = 5: 4 : ((No * 4)/rows) + 1;
      ylow = yorig + withspace * (j - 1);
      yhigh = ylow + height;
      xlow = xorig + withspace * (k - 1);
      xhigh = xlow + lenght;
      vert1 = [xlow ylow; xlow yhigh; xhigh yhigh; xhigh ylow];
      vert = [vert; vert1];
      k = k + 1;
    end
   end

% Clamp the four fisrt vertices
index = 5: size(vert,1);
verts = vert(index,:);

 xrange = max(verts(:,1));
 yrange = max(verts(:,2));

      j = 1;
    for i = 1 : 4 : size(verts,1)
      faces(j,:) = [i  i+1  i+2  i+3];
      j = j + 1;
    end

% 18 color Patches from the ColorChecker (X-Rite)
% Values for illuminant D65.

sRGBvalues18patches = [ 115  82  68;...
       194 150 130;...
        98 122 157;...
        87 108  67;...
       133 128 177;...
       103 189 170;...
       214 126  44;...
        80  91 166;...
       193  90  99;...
        94  60 108;...
       157 188  64;...
       224 163  46;...
        56  61 150;...
        70 184  73;...
       175  54  60;...
       231 199  31;...
       187  86 149;...
         8 133 161];
 cdata = sRGBvalues18patches/255;
```

Appendix C Matlab code

```
figure
patch('Faces',faces,'Vertices',verts,...
      'FaceColor','flat', 'FaceVertexCData',cdata)
set(gcf,'Color',[0.7 0.7 0.7])
whitebg([0.8 0.8 0.8])
axis ([0 xrange + xorig 0 yrange + yorig])
axis off
%&&&&&&&&&&&&&&&&&&&&&&&&& End of colorpatches


%-------------------------------------------------------------------

%&&&&&&&&&&&&&&&&&&&&&&&&& Begining of twopatches
%-------------------------------------------------------------------
% plot two color patches from the given True Color (sRGB)
%
% The function directly plots the patch using cdata value given in
range [0 1]
% example
%{
 twopatches([0.5729 0.0622 0.1406;...
         0.2196 0.2392 0.5882]
%}
function twopatches (cdata)

    xorig = 2;
    yorig = 2;
    height = 8;
    lenght = 7;
    withspace = 10;

    verts1 = [xorig+withspace yorig; xorig+withspace yorig +
height;...
              xorig+lenght+withspace yorig + height;...
              xorig+lenght+withspace yorig];
    verts2 = [xorig yorig; xorig yorig + height;...
              xorig + lenght yorig + height;...
              xorig + lenght yorig];
    verts = [verts2;  verts1];
    faces = [1 2 3 4; 5 6 7 8];

 figure
 patch('Faces',faces,'Vertices',verts,...
       'FaceColor','flat', 'FaceVertexCData',cdata)
 set(gcf,'Color',[0.7 0.7 0.7])
 whitebg([0.8 0.8 0.8])
 axis ([0 2*withspace + xorig 0 height + 2*yorig])
 axis off
 %&&&&&&&&&&&&&&&&&&&&&&&&& End of twopatch

%&&&&&& Begining of XYZ2sRGB  &&&&&&&&&&&&&&
%-------------------------------------------------------%
% For sRGB, the input XYZ values should be scaled between 0 and 1.
Beware that
%  transformations generally do not constrain colors to be "in
gamut."
%  Particularly, transforming from another space to sRGB may obtain
%  R'G'B' values outside of the [0,1] range.  So the result should be
%  clamped to [0,1] before displaying:
%    image(min(max(B,0),1));  % Clamp B to [0,1] and display
%
%  sRGB (Red Green Blue) is the (ITU-R BT.709 gamma-corrected)
standard
%  red-green-blue representation of colors used in digital imaging.
The
%  components should be scaled between 0 and 1.  The space can
be
%  visualized geometrically as a cube.
%{
  XnYnZn = [95.048 99.998 108.9]       % D65 Illuminant. Values
must given in the
                                              % order of 100!!!
                                      %  This values (D65) are adjusted to
sRGB transformation matrix.
  sRGB = XYZ2sRGB(XYZ, XnYnZn)
%}
function sRGB = XYZ2sRGB(XYZ,XnYnZn)
Td65 = [3.2406 -1.5372 -0.4986; -0.9689 1.8758 0.0415;
0.0557 -0.2040 1.0570];
d65 = [.95048; 0.99998; 1.089];
XnYnZn = XnYnZn / 100;
Tinv = inv(Td65);
Tinv1(1,:) = Tinv(1,:)* XnYnZn(1) / d65(1);
Tinv1(2,:) = Tinv(2,:)* XnYnZn(2) / d65(2);
Tinv1(3,:) = Tinv(3,:)* XnYnZn(3) / d65(3);
T = inv(Tinv1);
%-------------------------Gamma Adjudsments --------------------
a = 0.055; gamma = 2.4; % a = 0.055; gamma = 2.4;
%-------------------------------------------------------------------
XYZ = XYZ';
for i = 1 : size(XYZ,2)
 RGBp(:,i) = T * XYZ (:,i);
end

for i = 1 : size(XYZ,2)
   if RGBp(1,i) > 1; RGBp(1,i) = 1;
     elseif RGBp(1,i) > 0.0031308; RGBp(1,i) = (1 + a) *  (RGBp(1,i)^(1 /
gamma)) - a;
     elseif RGBp(1,i) <= 0.0031308; RGBp(1,i) = 12.92 *  RGBp(1,i);
end
  %sRGB(1,i) = min(max(RGBp(1,i), 0), 1); %clamp sRGB gamut to [0,
1]
   if RGBp(2,i) > 1; RGBp(2,i) = 1;
     elseif RGBp(2,i) > 0.0031308; RGBp(2,i) = (1 + a) *
(RGBp(2,i)^(1 / gamma)) - a;
     elseif RGBp(2,i) <= 0.0031308; RGBp(2,i) = 12.92 *  RGBp(2,i);
  end
  % sRGB(2,i) = min(max(RGBp(2,i), 0), 1); %clamp sRGB gamut to [0,
1]
   if RGBp(3,i) > 1; RGBp(3,i) = 1;
     elseif RGBp(3,i) > 0.0031308; RGBp(3,i) = (1 + a) *
(RGBp(3,i)^(1 / gamma)) - a;
     elseif RGBp(3,i) <= 0.0031308; RGBp(3,i) = 12.92 *  RGBp(3,i);
   end
 end
sRGB = 255 * (min(max(RGBp, 0), 1)); %clamp sRGB gamut to [0, 1]
sRGB = sRGB';
%&&&&&&&&&&&&&& The End of XYZ2sRGB


%&&&&&&&&&&&&&& Begining of XYZ2Lab  &&&&&&&&&&
%-------------------------------------------------------------%
 function [Lab] = XYZ2Lab(XYZ,XnYnZn)
        %Color space convertion from XYZ to L*a*b*.
        %XYZ and XnYnZn are horizontal arrays
        %where XnYnZn are tristimulus coordinates of
        %the reference illuminant.(D65= [95.05 100 108.88])

           f=zeros(size(XYZ));

           u(:,1)=XYZ(:,1)./XnYnZn(1);

           index1=find(u(:,1)> (24/116)^3);
           index2=find(u(:,1) <= (24/116)^3);
           f(index1,1) = u(index1,1).^(1/3);
```

```
        f(index2,1) = (841/108).*u(index2,1)+(16/116);

        u(:,2)=XYZ(:,2)./XnYnZn(2);

        index1=find(u(:,2)> (24/116)^3);
        index2=find(u(:,2) <= (24/116)^3);
        f(index1,2) = u(index1,2).^(1/3);
        f(index2,2) = (841/108).*u(index2,2)+(16/116);

        u(:,3)=XYZ(:,3)./XnYnZn(3);

        index1=find(u(:,3)> (24/116)^3);
        index2=find(u(:,3) <= (24/116)^3);
        f(index1,3) = u(index1,3).^(1/3);
        f(index2,3) = (841/108).*u(index2,3)+(16/116);

        Lab(:,1)=116*f(:,2)-16;
        Lab(:,2)=500*(f(:,1)-f(:,2));
        Lab(:,3)=200*(f(:,2)-f(:,3));
%--------------------------------------------------------------------%
%&&&&&&&&&& Begining of XYZ2CIECAM02 &&&&&&&&&
%--------------------------------------------------------------------%
 function JCh  = XYZ2CIECAM02(XYZ, Lw)
 % function [JCh QMs] = XYZ2CIECAM02(XYZ) %To obtain
Brightness, Colorfulness and Saturation.
XYZ = XYZ';
M_CAT02 = [0.7328  0.4296  -0.1624; -0.7036 1.6975   0.0061;
0.0030  0.0136   0.9834];
Minv_CAT02 = inv(M_CAT02);
M_HPE = [0.38971 0.68898 -0.07868; -0.22981 1.18340
0.04641; 0.0 0.0 1.0];
Minv_HPE = inv(M_HPE);
M_HPEinvCAT02 = M_HPE * inv(M_CAT02);
%                    Viewing Conditions
%            Average surround   Dim surround    Dark surround
F = 1.0;  % F =       1.0           0.9           0.8   Max.Deg.Adap
Nc = 1.0; %  Nc =      1.0           0.9           0.8   ChromaticIndu
c = 0.69; %  c =       0.69          0.59          0.525 Exp.nonlinear
Yb = 20.0;
XYZw = [95.05; 100; 108.88]; % illuminant Daylight 6500K (D65)
% XYZw = [109.85; 100; 35.58]; % illuminant A (incandescent
2848K)
% L_A = 318.31; % Adaptation Luminance in [cd/m^2],
% aprox. 20% (Yb) of the white color luminance.

L_A = Lw * Yb / XYZw(2);
RGB = XYZ_to_CAT02 (XYZ, M_CAT02);
RGBw = XYZ_to_CAT02 (XYZw, M_CAT02);
n = Yb / XYZw(2);                % (16.9)
D = D_factor(F, L_A);            % (16.3)
FL = FL_from_LA_ciecam02(L_A);     % (16.8)
Nbb = 0.725 * (1.0 / n)^ 0.2;      % (16.10)
Ncb = Nbb;
z = 1.48 + sqrt( n );            % (16.11)
Aw = achromatic_response_to_white( XYZw, M_CAT02,
M_HPEinvCAT02, D, FL, Nbb );
RGBc(1,:) = RGB(1,:) .* (((XYZw(2) * D) / RGBw(1)) + (1.0 - D));
RGBc(2,:) = RGB(2,:) .* (((XYZw(2) * D) / RGBw(2)) + (1.0 - D));
RGBc(3,:) = RGB(3,:) .* (((XYZw(2) * D) / RGBw(3)) + (1.0 - D));
RGBprim = CAT02_to_HPE(RGBc,M_HPEinvCAT02);
RGBa_prim = nonlinear_adaptation(RGBprim, FL);
for i = 1 : size(RGBa_prim,2)
   % Opponent color dimensions

   a = RGBa_prim(1,i) - ((12.0 * RGBa_prim(2,i)) / 11.0) +
(RGBa_prim(3,i) / 11.0);
   b = (1.0 / 9.0) * (RGBa_prim(1,i) + RGBa_prim(2,i) - (2.0 *
RGBa_prim(3,i)));
   % Hue
   h = (180.0 / pi) * atan2( b , a );
   if( h < 0.0 )
      h = h + 360.0;
   end

   % Lightness
   A = ((2.0 * RGBa_prim(1,i)) + RGBa_prim(2,i) + ((1.0 / 20.0) *
RGBa_prim(3,i)) - 0.305) * Nbb;
   J = 100.0 * ( A / Aw ) ^ ( c * z );
   % Chroma
   e = ((12500.0 / 13.0) * Nc * Ncb) * (cos( ((h * pi) / 180.0) + 2.0 )
+ 3.8);
   t = (e * sqrt((a * a) + (b * b) )) / (RGBa_prim(1,i) + RGBa_prim(2,i) +
((21.0 / 20.0) * RGBa_prim(3,i)));
   C = ( t ^ 0.9 ) * sqrt( J / 100.0 )*( 1.64 - ( 0.29 ^ n )) ^ 0.73 ;
   JCh(1,i) = J;
   JCh(2,i) = C;
   JCh(3,i) = h;
%{
   % Remove These comment marks to calculate Q, M, and s
     function [JCh QMs] = XYZ2CIECAM02(XYZ)
   % Brightness
   Q = (4/c)* sqrt(J / 100)* (Aw + 4)* (FL ^ 0.25);
   % Colorfulness
   M = C * (FL ^ 0.25);
   % Saturation
   s = 100 * sqrt( M / Q);
   QMs(1,i) = Q;
   QMs(2,i) = M;
   QMs(3,i) = s;
%}
end
 JCh = JCh';
% QMs = Qms' % m x 3 array.
%--------------------------------------------------------------
function FL = FL_from_LA_ciecam02( L_A )
   k = 1/(5 * L_A + 1);
   FL = 0.2 * (k^4) * 5 * L_A + 0.1 * (1.0 - k^4)^2 * (5 * L_A)^(1/3);

function RGB = XYZ_to_CAT02(XYZ, M_CAT02)
   for i = 1 : size(XYZ,2)
      RGB(:,i) = M_CAT02 * XYZ(:,i);
   end

function XYZ = CAT02_to_XYZ(RGB, Minv_CAT02)
   for i = 1 : size(RGB,2)
      XYZ(:,i) = Minv_CAT02 * RGB(:,i);
  end


function XYZ = HPE_to_XYZ(RGB, Minv_HPE)
   for i = 1 : size(RGB,2)
      XYZ(:,i) = Minv_HPE * RGB(:,i);
   end

function RGBh = CAT02_to_HPE(RGB,M_HPEinvCAT02)
   for i = 1 : size(RGB,2)
      RGBh(:,i) = M_HPEinvCAT02 * RGB(:,i);
  end

function D = D_factor(F, L_A)
   D = F * (1.0 - ((1.0 / 3.6) * exp((-L_A - 42.0) / 92.0)));

function RGBa_prim = nonlinear_adaptation(RGBprim, FL)
%input: RGB',FL; output (post-adaptation) RGB'a. (arrrays of size: 3
x m)
```

Appendix C Matlab code

```
P = (FL*RGBprim/100).^0.42;
RGBa_prim = ((400.0 * P)./(27.13 + P)) + 0.1;   % (16.15), (16.16),
(16.17)

function RGBprim = inverse_nonlinear_adaptation(RGBa_prim, FL)
% input: RGB'a, FL ; output: RGB'.   (arrrays of size: 3 x m)
RGBprim = (100.0 / FL) * ((27.13 .* abs(RGBa_prim - 0.1) ./ (400.0 -
abs(RGBa_prim - 0.1)))).^(1/0.42);

function Aw = achromatic_response_to_white(XYZw, M_CAT02,
M_HPEinvCAT02, D, FL, Nbb)

RGBw = XYZ_to_CAT02(XYZw, M_CAT02);
D1 = (XYZw(2)*D)./RGBw;
RGBcw =  (D1 + 1 -D) .* RGBw;

RGBhw = CAT02_to_HPE(RGBcw,M_HPEinvCAT02);
RGBa_pw = nonlinear_adaptation(RGBhw, FL);

Aw = ((2.0 * RGBa_pw(1)) + RGBa_pw(2) + ((1.0 / 20.0) *
RGBa_pw(3)) - 0.305) * Nbb;
%-----------------------------------------------------------------%
%&&&&&&&&& The End of XYZ2CIECAM02  &&&&&&&&&&
%-----------------------------------------------------------------%


%-----------------------------------------------------------------%
%&&&&&&& Begining of volumegamut &&&&&&&&&&&&&&&&&
%-----------------------------------------------------------------%
% Extract volume of a scattered data in n by 3 array.
% input: xyY : gamut data in [x y Y] format,
%       RY  : Desired number or steps in Y-axes, (Recommended: RY =
100 )
%       Rx  : Desired number of steps in 'x-axes'.(Recommended: Rx =
50 )
%
% output: xyYvol : RY by 3 array containing the volume of input
gamut data
%
%    ----------------------------------------------------------------
%
function xyYvol = volumegamut(xyY, RY, Rx)

minis = min(xyY);
maxis = max(xyY);

xmin = minis(1); Ymin = minis(3);
xmax = maxis(1); Ymax = maxis(3);

deltaY = (Ymax - Ymin) / RY;
deltax = (xmax - xmin) / Rx;

in = xyY(:,3) == Ymin;
xyYvol = xyY(in,:);

for k = 0 : RY
   Yk = Ymin + k * deltaY;
   inde1 = find(xyY(:,3) > Yk);
   inde2 = find(xyY(:,3) < Yk + deltaY);
   inde = intersect(inde1, inde2);

   if ~isempty(inde);
   Yf = xyY(inde,3);
   xYf = xyY(inde,1);
   yYf = xyY(inde,2);

   Rxp = round((max(xYf) - min(xYf))/deltax);
      for i = 0 : Rxp
      xi = min(xYf) + i * deltax;
      index1 = find(xYf > xi);
      index2 = find(xYf < xi + deltax);
      index = intersect(index1, index2);
         if ~isempty(index);

            Yfmed = prctile(Yf,50);
            xfyYf = xYf(index);
            xfmed = prctile(xfyYf,50);
            yfmin = prctile(yYf(index),5);
            yfmax = prctile(yYf(index),95);

            if yfmin ~= yfmax
            xyYvol = [xyYvol; xfmed yfmin Yfmed; xfmed yfmax
Yfmed];
            else
            xyYvol = [xyYvol; xfmed yfmin Yfmed];
            end
         end
      end
   end
end

%-----------------------------------------------------------------%
%&&&&&&&&&&&&& The End of volumegamut &&&&&&

function closefigures_Callback(hObject, eventdata, handles)
close all


function importilluminant_Callback(hObject, eventdata, handles)
[option,h]=sourceselection;
close(h);

if isempty(option)
   return;
end

switch option
   case 'fromdatafile'
      [file,path]=uigetfile('*.*','ASCII TEST: 1 (PSD) or 2 (WV,PSD)
COLUMNS');
      if  isfloat(file)
         msgbox('Could not load file. Maybe not an ASCII 2-columns
file?');
         return;
      end
      test=[];

      test=load([path file]);
      if ~isempty(test)
         if size(test,2)==2
            test=interp1(test(:,1),test(:,2),handles.data.wavelength);
            [garbage minindex]=min(test);
            test(isnan(test))=test(minindex);

         elseif size(test,2)==1
            if length(test)~=length(handles.data.wavelength)
               msgbox('Please, provide a txt file with columns:
[wavelength PSD]');
               return;
            end
         else
            msgbox('Please, provide a txt file with columns:
[wavelength PSD]');
            return;
         end
```

```
      else
         msgbox('Please, provide a txt file with columns: [wavelength
PSD]');
         return;
      end
      handles.data.illuminant.psd=test/max(test);
      guidata(hObject,handles);


   case 'fromuser'
      spectradesign;

   case 'fromdatabase'
      [data,h]=spectradb;
      close(h);
      if isempty(data)
         return;
      end

illuminant=interp1(data.spectrum(:,1),data.spectrum(:,2),handles.dat
a.wavelength);
      [garbage minindex]=min(illuminant);
      illuminant(isnan(test))=illuminant(minindex);
      handles.data.illuminant.psd=illuminant/max(illuminant);
      guidata(hObject,handles);

end


function plotilluminant_Callback(hObject, eventdata, handles)
figure
plot(handles.data.wavelength,
handles.data.illuminant.psd,'color','y','Linewidth',2.5);
set(gca,'Color',[.5 .3 .3]);

%============================================
%                    Second Part:
%              Calculating Color Rendering
%============================================

function analyzedatabase_Callback(hObject, eventdata, handles)
%{
[file,path]=uigetfile('*.*','ASCII TEXT: 1st Column = Wavelength,
Others = Spectra');

if  isfloat(file)
   msgbox('Could not load file. Maybe not an ASCII file?');
   return;
end

test=[];
test=load([path file]);
if ~isempty(test)
%}
%-----------------------------------------------
% Variables of Color gamuts
%-----------------------------------------------
%%%%%%%%%%%%%%%%%%%%%%%%%%
x1=handles.data.munsell.xyY(:,1);
y1=handles.data.munsell.xyY(:,2);
Y1=handles.data.munsell.xyY(:,3);
RGB1=handles.data.gamuts.RGBmunsell;
RGBVol=handles.data.gamuts.RGBvol;
RGBlabsel=handles.data.gamuts.RGBsellab;
RGBcamsel=handles.data.gamuts.RGBselcam;
xvol=handles.data.gamuts.xyYvol(:,1);
yvol=handles.data.gamuts.xyYvol(:,2);
Yvol=handles.data.gamuts.xyYvol(:,3);
labvol=handles.data.gamuts.labvol;
acvol=handles.data.gamuts.camvol(:,1);
bcvol=handles.data.gamuts.camvol(:,2);
Jvol=handles.data.gamuts.camvol(:,3);
xmunsellselected=handles.data.gamuts.xyYsel(:,1)';
ymunsellselected=handles.data.gamuts.xyYsel(:,2)';
Ymunsellselected=handles.data.gamuts.xyYsel(:,3)';
% para graficación estas variables no requieren la apóstrofe!
acmunsellselected=handles.data.gamuts.camsel(:,1);
bcmunsellselected=handles.data.gamuts.camsel(:,2);
Jmunsellselected=handles.data.gamuts.camsel(:,3);
%%%%%%%%%%%%%%%%%%%%%%%%%%%%%%%%%%%%%%%%
%%%%%%%%%%%%%
%-----------------------------------------------

%%%lines for lightsources database.
XYZ=handles.data.XYZ;
wv=handles.data.wavelength;
% loading spectra from .mat file
load sp15.mat; % loading 14 spectra database
namek = sp15.name;
test = sp15.spd;

%{
XYZ=handles.data.XYZ;
wv=handles.data.wavelength;
load spdshift1LED20nm.txt;
test = spdshift1LED20nm;
j=1;
steps=size(test,2)-2;
for i = 380:5:380+5*steps
namek(j+1) = i;
j=j+1;
end
%}


if ~isempty(test)
   N=size(test,2)-1;
   h=waitbar(1,'Calculating... Please Wait.');


%-------------------------------------------------------------
beta =  0.;  % weighted factor for Duv, ranged in [0 1]
alpha = 0;   % selecting weighted factor between Ra and Efficacy,
ranged: [0 1]
          % alpha = 1, gives complete weight to Ra
          % alpha = 0, gives complete weight to Efficacy
%-------------------------------------------------------------
%Another aproach of CE
Kcq = 0.5;  % Kcq = 0 means preference by efficacy
       % Kcq = 1 means preference by Color Quality (Rsm)
%-------------------------------------------------------------



%------------ File: spddatabase.txt + LED4KK.txt ------------
  % i = 0; %Wavelength
  % i = 1; %LPS
  % i = 2; %WhiteF
  % i = 3; %MH
  % i = 4; %Neodim
  % i = 5; %TL840
  % i = 6; %TL830
  % i = 7; %LEDph
  % i = 8; % Bkbdy
  % i = 9; % 3xLED
  % i = 10; % 4xLED
```

Appendix C Matlab code

```
  % i = 11; % HgHP
  % i = 12; % 5xLED
  % i = 13; % 4xPeak
  % i = 14; % TL865
  % i = 15; % LED4KK
  %------------- ----- ------------  ---------------------
  %spddatabasenames.txt
 % Wavelength   LPS      WhiteF   MH      Neodim  TL840
          TL830   LEDph   Bkbdy   3xLED   4xLED   HgHP
          5xLED   4xPeak  TL865

%{
%=========================================
%    Ploting spectra database

for i = 2:16
   name=char(sp15.name(i));
   figure
   plot(sp15.spd(:,1),sp15.spd(:,i),'k-','linewidth',3)
   set(gca, 'Fontsize', 20)
   xlabel('Wavelength','FontSize', 20)
   ylabel('a.u.','FontSize', 20)
   title(name)
   grid on
end
%=====================================
%}
      indexes=handles.data.labselindex(:,1);
      indexmultiplicity=handles.data.labselindex(:,2);
      %load colormapCRM.mat
      load colormapCRMbluered.mat
    %for i = 1 : N
    for i = 4
      %wv=handles.data.wavelength;
      spectrum=interp1(test(:,1),test(:,i + 1),wv);
      %[garbage minindex]=min(spectrum);
      [Rm, R,
Efficacy,x,y,ubb,vbb,Deltauv,CorrCT]=CRM(wv,spectrum,wv,XYZ,in
dexes);
      % Weighted Average of CRM indexes owing at their multiplicity

      Rs=0;
      for j=1:length(Rm)
         Rs=Rs+Rm(j)*indexmultiplicity(j);
      end
      Duvk(i) = Deltauv;

      CCTk(i) = CorrCT;

% Selected munsell with multiplicity (number of ocurrences within the
gamut)
      Rsmi = Rs/sum(indexmultiplicity);
      Rsmk(i) = Rsmi;
      Rssi = mean(Rm); %Selected munsell (just once per Munsell
Sample or Reflectance)
      Rssk(i) = Rssi;

      CRI = mean(R(1:8));% General CRI (8 Standard CIE Munsell
samples)
      Rak(i) = CRI;
      R9k(i) = R(9);
      R14k(i) = mean(R(10:14));
      Effk(i) = Efficacy;

     %{
      A = (1 -(2.4 * normpdf(Deltauv / 0.006)))^beta;
      B = (2.5 * normpdf(max(0,Rsmi)/45))^ alpha;
      C = (2.5 * normpdf(Efficacy / 222))^(1-alpha);
      Fobj(i) = ( A + B + C ) / 3; % objetive function for minimization.
      Fo(i) = (1 - (A +  B + C)/3) * 125; %Efficacy & Color Quality Index
     %}

      A1= 1-(exp(-((Deltauv)/0.01).^2));
      B1= 1-(Kcq*exp(-(((Rsmi-100)/20).^2)));
      C1= 1-((1-Kcq)*exp(-(((Efficacy-600)/300).^2)));
      Td=3000;
      sigma=1000;
      D1=1-exp(-((CorrCT-Td)/sigma).^2);
      Fo(i)= (1-(1/sqrt(3))*sqrt((A1^2)+(B1^2)+(C1^2)))*169;
      Fobj(i)= (1-(1/2)*sqrt((A1^2)+(B1^2)+(C1^2)+(D1^2)))*155;
      % init Graphics   ---------------------------------------
      % Assign colormap to RGBlab proportional to Rm Values
      data=colormapCRMbluered(:,1);
      for l=1:length(Rm)
         [minvalue index]= min(abs(data-Rm(l)/100));
         RGBlabCRMi(l,:) = [colormapCRMbluered(index,:)];
      end
      RGBlabCRM = [RGBlabCRMi(:,2) RGBlabCRMi(:,3)
RGBlabCRMi(:,4)];


      % CRM gray scale aproach based on Luminance level
      llabsel =
0.2989*RGBlabsel(:,1)+0.5870*RGBlabsel(:,2)+0.1140*RGBlabsel(:
,3);
      Rmtrns = max(0,Rm'/100);
      RGBl = Rmtrns .* llabsel;
      RGBllabsel = [RGBl RGBl RGBl];


 % CRM color aproach based on own-colormap
%{
%-------------------------------------------------------------
% Figure No. 10
% plot CRM
% xyY Color space
%-------------------------------------------------------------
figure
scatter3(x1,y1,Y1, 20, RGB1, 'filled');
set(gca,'Color',[0.7 0.7 0.7]);
set(gca,'FontSize',20);
set(gcf,'PaperUnits','centimeters','PaperSize',[8.5 8.5]);
xlabel('x'); ylabel('y'); zlabel('Y'); title('Color space xyY');
hold on
scatter3(xmunsellselected,ymunsellselected,Ymunsellselected,150,
RGBlabsel,'filled');
view(0,90)
%-------------------------------------------------------------

%-------------------------------------------------------------
% Figure No. 11
% plot CRM
% xyY Color space
%-------------------------------------------------------------
figure
scatter3(x1,y1,Y1, 20, RGB1, 'filled');
set(gca,'Color',[0.7 0.7 0.7]);
set(gca,'FontSize',20);
set(gcf,'PaperUnits','centimeters','PaperSize',[8.5 8.5]);
xlabel('x'); ylabel('y'); zlabel('Y'); title('Color space xyY');
hold on
scatter3(xmunsellselected,ymunsellselected,Ymunsellselected,150,
RGBllabsel,'filled');
view(0,90)

%-------------------------------------------------------------
```

```
 %}

%-------------------------------------------------------------------
% Figure No. 12
% plot CRM
% xyY Color space
%-------------------------------------------------------------------
%{
figure
scatter3(x1,y1,Y1, 30, RGB1, 'filled');
colorbar('location','north')
caxis([0 100])
set(gca,'Color',[0.7 0.7 0.7]);
set(gca,'FontSize',20);
set(gcf,'PaperUnits','centimeters','PaperSize',[8.5 8.5]);
xlabel('x'); ylabel('y'); zlabel('Y'); title('Color space xyY');
hold on
scatter3(xmunsellselected',ymunsellselected',Ymunsellselected',300
, RGBlabCRM,'filled');
view(0,90)
%}
%Image 1-----------------------------------------------------------
%Reference Set(1269 Munsell Samples)
scrsz = get(0,'ScreenSize');
%scrsz = [1 1 1024 768];

fig=figure
set(fig,'OuterPosition',scrsz)

subplot(1,2,2);
set(gca,'Visible','Off');
text(0.06,0.8,' These are the 1269 Munsell Reflectance
Samples','FontSize',13);
text(0.06,0.65,' Represented in the 1931 CIE xyY
Diagram','FontSize',13);
text(0.06,0.5,' This is the REFERENCE SET','FontSize',13);
text(0.06,0.35,' Now, let''s look into a particular
application…','FontSize',13);
text(0.06,0.2,' and plot the full Observed Gamut from all
pixels.','FontSize',13);


subplot(1,2,1);
scatter3(x1,y1,Y1, 50, RGB1, 'filled');
set(gca,'Color',[0.7 0.7 0.7]);
set(gca,'FontSize',20);
set(gcf,'PaperUnits','centimeters','PaperSize',[5.5 5.5]);
xlabel('x'); ylabel('y'); zlabel('Y'); title('1269 Munsell samples in xyY
Color Space');
hold on

rng=80;
stp=4;
az=0:stp:rng;
za=rng-az;
azn=0:-stp:-rng;
zan=-rng-azn;
el=34;
el1=34:stp:90;
el1n=90:-stp:34;

% Prepare the new file.
vidObj = VideoWriter('crm.avi');
open(vidObj);
%Turn Zero-right
for k=1:length(az)
   view(az(k),el);
   xlim([.1 .6]); ylim([0.1 .6]); %zlim([0 100]);
   currFrame = getframe(fig);
   writeVideo(vidObj,currFrame);
end
%Turn Right-Zero
for k=1:length(za)
   view(za(k),el);
   xlim([.1 .6]); ylim([0.1 .6]); %zlim([0 100]);
   currFrame = getframe(fig);
   writeVideo(vidObj,currFrame);
end
%{
%Turn Zero-left
for k=1:length(azn)
   view(azn(k),el);
   xlim([.1 .6]); ylim([0.1 .6]); %zlim([0 100]);
   currFrame = getframe(fig);
   writeVideo(vidObj,currFrame);
end
%Turn Left-Zero
for k=1:length(zan)
   view(zan(k),el);
   xlim([.1 .6]); ylim([0.1 .6]); %zlim([0 100]);
   currFrame = getframe(fig);
   writeVideo(vidObj,currFrame);
end
%}
%Turn to Top view
for k=1:length(el1)
   view(0,el1(k));
   xlim([.1 .6]); ylim([0.1 .6]); %zlim([0 100]);
   currFrame = getframe(fig);
   writeVideo(vidObj,currFrame);
end
%Stay on Top
for k=1:length(el1/2)
   view(0,90);
   xlim([.1 .6]); ylim([0.1 .6]); %zlim([0 100]);
   currFrame = getframe(fig);
   writeVideo(vidObj,currFrame);
end
%Image2

_____________________________________________________
% Observed Gamut (volume) + Reference Set

subplot(2,2,2)
cla
set(gca,'Visible','Off');
axis([0 1 0 1]);
text(0.06,0.95,' The OBSERVED GAMUT is obtained through the
','FontSize',13);
text(0.06,0.8, ' luminance and color photograph taken to objects
','FontSize',13);
text(0.06,0.65,' and color checker card under standard illuminant
emulator','FontSize',13);
text(0.06,0.5, ' light source. ','FontSize',13);
text(0.06,0.35,' After editting and processing color data
from','FontSize',13);
text(0.06,0.2, ' photograph, a volume representing the Observed
Gamut','FontSize',13);
text(0.06,0.05,' is created','FontSize',13);


subplot(2,2,4)
cla
im=imread('artwork.jpg');
image(im);xlim([0 530]); ylim([0 480]);
set(gca,'Visible','Off');
```

Appendix C Matlab code

```
subplot(2,2,[1 3])
scatter3(x1,y1,Y1, 50, RGB1, 'filled');
set(gca,'Color',[0.7 0.7 0.7]);
set(gca,'FontSize',20);
set(gcf,'PaperUnits','centimeters','PaperSize',[5.5 5.5]);
scatter3(xvol,yvol,Yvol,50, handles.data.gamuts.RGBvol,'filled');
title('OBSERVED GAMUT in xyY Color Space');

%Stay on Top
for k=1:length(el1/2)
   view(0,90);
   xlim([.1 .6]); ylim([0.1 .6]); zlim([0 100]);
   currFrame = getframe(fig);
   writeVideo(vidObj,currFrame);
end

%Turn from top to lat Zero
for k=1:length(el1n)
   view(0,el1n(k));
   xlim([.1 .6]); ylim([0.1 .6]); zlim([0 100]);
   currFrame = getframe(fig);
   writeVideo(vidObj,currFrame);
end

%Turn Zero-right
for k=1:length(az)
   view(az(k),el);
   xlim([.1 .6]); ylim([0.1 .6]); zlim([0 100]);
   currFrame = getframe(fig);
   writeVideo(vidObj,currFrame);
end
%Turn Right-Zero
for k=1:length(za)
   view(za(k),el);
   xlim([.1 .6]); ylim([0.1 .6]); zlim([0 100]);
   currFrame = getframe(fig);
   writeVideo(vidObj,currFrame);
end
%{
%Turn Zero-left
for k=1:length(azn)
   view(azn(k),el);
   xlim([.1 .6]); ylim([0.1 .6]); zlim([0 100]);
   currFrame = getframe(fig);
   writeVideo(vidObj,currFrame);
end
%Turn Left-Zero
for k=1:length(zan)
   view(zan(k),el);
   xlim([.1 .6]); ylim([0.1 .6]); zlim([0 100]);
   currFrame = getframe(fig);
   writeVideo(vidObj,currFrame);
end
%}
%Turn to Top view
for k=1:length(el1)
   view(0,el1(k));
   xlim([.1 .6]); ylim([0.1 .6]); zlim([0 100]);
   currFrame = getframe(fig);
   writeVideo(vidObj,currFrame);
end
%Stay on Top
for k=1:length(el1/2)
   view(0,90);
   xlim([.1 .6]); ylim([0.1 .6]); zlim([0 100]);
   currFrame = getframe(fig);
   writeVideo(vidObj,currFrame);
end

%Image 3----------------------------------------------------
%Test Set
%set(fig,'OuterPosition',scrsz)
subplot(1,2,2);
cla
set(gca,'Visible','Off');
axis([0 1 0 1]);
text(0.06,0.65,' The TEST SET (in big dots) is obtained from the
','FontSize',13);
text(0.06,0.5,' Observed Gamut by calculating the nearest points
','FontSize',13);
text(0.06,0.35,' to the Reference Set, for which the reflectances
','FontSize',13);
text(0.06,0.2,' are available and the Ri''s scores can be
calculated.','FontSize',13);
set(gca,'Visible','Off');

subplot(1,2,1);
cla
set(gca,'Color',[0.7 0.7 0.7]);
set(gca,'FontSize',20);
set(gcf,'PaperUnits','centimeters','PaperSize',[5.5 5.5]);
scatter3(x1,y1,Y1, 8, RGB1, 'filled');
xlim([.1 .6]); ylim([0.1 .6]); zlim([0 100]);
scatter3(xmunsellselected',ymunsellselected',Ymunsellselected',60,
handles.data.gamuts.RGBsellab,'filled');
title('Test Set in xyY Color Space');

%Stay on Top
for k=1:length(el1/2)
   view(0,90);
   xlim([.1 .6]); ylim([0.1 .6]); %zlim([0 100]);
   currFrame = getframe(fig);
   writeVideo(vidObj,currFrame);
end

%Turn from top to lat Zero
for k=1:length(el1n)
   view(0,el1n(k));
   xlim([.1 .6]); ylim([0.1 .6]); %zlim([0 100]);
   currFrame = getframe(fig);
   writeVideo(vidObj,currFrame);
end

%Turn Zero-right
for k=1:length(az)
   view(az(k),el);
   xlim([.1 .6]); ylim([0.1 .6]); %zlim([0 100]);
   currFrame = getframe(fig);
   writeVideo(vidObj,currFrame);
end
%Turn Right-Zero
for k=1:length(za)
   view(za(k),el);
   xlim([.1 .6]); ylim([0.1 .6]); %zlim([0 100]);
   currFrame = getframe(fig);
   writeVideo(vidObj,currFrame);
end
%{
%Turn Zero-left
for k=1:length(azn)
   view(azn(k),el);
   xlim([.1 .6]); ylim([0.1 .6]); zlim([0 100]);
   currFrame = getframe(fig);
   writeVideo(vidObj,currFrame);
end

%Turn Left-Zero
```

```
for k=1:length(zan)
   view(zan(k),el);
   xlim([.1 .6]); ylim([0.1 .6]); zlim([0 100]);
   currFrame = getframe(fig);
   writeVideo(vidObj,currFrame);
end
%}
%Turn to Top view
for k=1:length(el1)
   view(0,el1(k));
   xlim([.1 .6]); ylim([0.1 .6]); %zlim([0 100]);
   currFrame = getframe(fig);
   writeVideo(vidObj,currFrame);
end
%Stay on Top
for k=1:length(el1/2)
   view(0,90);
   xlim([.1 .6]); ylim([0.1 .6]); %zlim([0 100]);
   currFrame = getframe(fig);
   writeVideo(vidObj,currFrame);
end
% Image 4_____________________________________
% CRM
subplot(2,2,2)
cla
set(gca,'Visible','Off');
axis([0 1 0 1]);
text(0.06,0.95,' Finally, the Color Rendering Map (CRM) is created
','FontSize',13);
text(0.06,0.8, ' over the Test Set, illustrating how a particular
','FontSize',13);
text(0.06,0.65,' light source (see spectrum below) performs in color
rendering','FontSize',13);
text(0.06,0.5, ' a concrete application given by the Test
Set.','FontSize',13);
text(0.06,0.35,' A 0-100 score (as in the CRI) is calculated for each
point ','FontSize',13);
text(0.06,0.2, ' of the Projected Gamut, represented by a colormap
from ','FontSize',13);
text(0.06,0.05,' deep blue (no rendering) to deep red (perfect
rendering).','FontSize',13);

subplot(2,2,4)
cla
im2=imread('Neodim_figVIDEO.jpg');
image(im2);xlim([0 2386]); ylim([0 1665]);
set(gca,'Visible','Off');
title('Spectrum of the light source under test')

subplot(2,2,[1 3])
scatter3(x1,y1,Y1, 8, RGB1, 'filled');
set(gca,'Color',[0.7 0.7 0.7]);
set(gca,'FontSize',20);
set(gcf,'PaperUnits','centimeters','PaperSize',[5.5 5.5]);
colorbar('location','north')
caxis([0 100])
scatter3(xmunsellselected',ymunsellselected',Ymunsellselected',60,
RGBlabCRM,'filled');
title('CRM over the Test Set');
%Stay on Top
for k=1:length(el1/2)
   view(0,90);
   xlim([.1 .6]); ylim([0.1 .6]); %zlim([0 100]);
   currFrame = getframe(fig);
   writeVideo(vidObj,currFrame);
end

%Turn from top to lat Zero
for k=1:length(el1n)
   view(0,el1n(k));
   xlim([.1 .6]); ylim([0.1 .6]); %zlim([0 100]);
   currFrame = getframe(fig);
   writeVideo(vidObj,currFrame);
end

for i=1:length(az)
   view(az(i),el(1));
   xlim([0.1 .6]); ylim([0.1 .6]); %zlim([0 100]);
   currFrame = getframe(fig);
   writeVideo(vidObj,currFrame);
end
for i=1:length(az)
   view(za(i),el(1));
   xlim([0.1 .6]); ylim([0.1 .6]); %zlim([0 100]);
   currFrame = getframe(fig);
   writeVideo(vidObj,currFrame);
end
%Turn to Top view
for k=1:length(el1)
   view(0,el1(k));
   xlim([.1 .6]); ylim([0.1 .6]); %zlim([0 100]);
   currFrame = getframe(fig);
   writeVideo(vidObj,currFrame);
end
%Stay on Top
for k=1:length(el1)
   view(0,90);
   xlim([.1 .6]); ylim([0.1 .6]); %zlim([0 100]);
   currFrame = getframe(fig);
   writeVideo(vidObj,currFrame);
end

%5-------------------------------------------------
%{
subplot(1,2,2)
cla
image(im);
set(gca,'Visible','Off');

subplot(1,2,1)
title('CRM with assistance of Reference Set (Munsell)');

scatter3(x1,y1,Y1, 30, RGB1, 'filled');
for i=1:length(az)
   view(az(i),el(1));
   xlim([0.1 .6]); ylim([0.1 .6]); zlim([0 100]);
   currFrame = getframe(fig);
   writeVideo(vidObj,currFrame);
end
for i=1:length(az)
   view(za(i),el(1));
   xlim([0.1 .6]); ylim([0.1 .6]); zlim([0 100]);
   currFrame = getframe(fig);
   writeVideo(vidObj,currFrame);
end
%}
% Close the file.
close(vidObj);
 %}

 % end Graphics ----------
     waitbar(i/N);
   end
   close(h);

  % sort things out by F Ranking
```

Appendix C Matlab code

```
      [F,sortindex] = sort(Fo,'descend');
       name = namek(sortindex + 1);
       Eff = Effk(sortindex);
       CCT = CCTk(sortindex);
       Duv = Duvk(sortindex);
       Ra = Rak(sortindex);
       R9 = R9k(sortindex);
       R14 = R14k(sortindex);
       Rss = Rssk(sortindex);
       Rsm = Rsmk(sortindex);
       Fob = Fobj(sortindex);
%Info1 = [sprintf('%s','(CRI_and_Eff_fac.)  Alpha= ')
sprintf('%7.2f',alpha) sprintf('\n')...
 Info1 = [sprintf('%s',' Quality Color coef.  Kcq= ') sprintf('%7.2f',Kcq)
sprintf('\n')...
      sprintf('%s',' Desired color tempe.  Td= ') sprintf('%7.2f',Td)
sprintf('\n')...
      sprintf('%s','Sel.Muns.Refl.       No.= ')
sprintf('%7.2f',length(Rm)) sprintf('\n')...
      sprintf('%s','(Calculus  Efficacy and Color Quality Index (ECQ)')
sprintf('\n')...
      sprintf('%s','A = (1 -(2.4 * normpdf(Deltauv / 0.006))) ^ beta')
sprintf('\n')...
      sprintf('%s','B = (2.5 * normpdf(max(0,Rsm)/45))^ alpha')
sprintf('\n')...
      sprintf('%s','C = (2.5 * normpdf(Efficacy / 222))^(1 - alpha)')
sprintf('\n')...
      sprintf('%s','ECQ = (1 - (A +  B + C)/3) * 125')];

Info2(1,:) = [sprintf('%s','Lamp_Type    ') '    ' sprintf('%s','Efficacy  ')...
    '    ' sprintf('%s','CCT ') '  ' sprintf('%s', '  Duv   ')...
    '  ' sprintf('%s', 'CRI ' ) ' ' sprintf('%s', '  Rss ' )...
    '    ' sprintf('%s', '  Rsm ' ) '  ' sprintf('%s',' ECQ')...
    '    ' sprintf('%s','ECQr')];
Info2(2,:) = [sprintf('%s','(Description)') '    ' sprintf('%s',' lm/W    ')...
    '    ' sprintf('%s',' K  ') '  ' sprintf('%s', '  ---   ')...
    '  ' sprintf('%s', '--- ' ) ' ' sprintf('%s', '  --- ' )...
    '   ' sprintf('%s', '  --- ' ) '  ' sprintf('%s',' ---')...
    '   ' sprintf('%s',' --- ')];
%for i = 1 : size(test,2)-1
i=1;
Info2(i+2,:) = [sprintf('%13s',char(name(i))) '    ' sprintf('%7.1f',Eff(i)) '
'...
     '    ' sprintf('%5.0f',CCT(i)) '  ' sprintf('%7.4f',Duv(i))...
    ' ' sprintf('%7.1f',Ra(i)) '' sprintf('%7.1f',Rss(i))...
    ' ' sprintf('%7.1f',Rsm(i)) sprintf('%7.1f',F(i))...
    ' ' sprintf('%7.3f',Fob(i))];
%end
Info2
Info1
R9_14 = [R9' R14']
%=========================================
end
%{

%=========================================%
Finding the  optimal SPD using genetic algoritm
% Optimal SPD based on 5 1nmFWHM-LED

 init = [  0.0983  422.0129    5.2054    0.8294  481.1741
4.9227...
       0.4361  554.0351   19.3818    0.7905  623.6760   18.5667...
        0.0640  737.9905    4.2570];

peak_ub=1;
peak_lb=0;
avglambda_lb1=350;
avglambda_ub1=350+400/5;
avglambda_lb2=avglambda_ub1;
avglambda_ub2=350+2*400/5;
avglambda_lb3=avglambda_ub2;
avglambda_ub3=350+3*400/5;
avglambda_lb4=avglambda_ub3;
avglambda_ub4=350+4*400/5;
avglambda_lb5=avglambda_ub4;
avglambda_ub5=350+5*400/5;
fwhm_lb=1;
fwhm_ub=20;

lb=[peak_lb avglambda_lb1 fwhm_lb...
   peak_lb avglambda_lb2 fwhm_lb...
   peak_lb avglambda_lb3 fwhm_lb...
   peak_lb avglambda_lb4 fwhm_lb...
   peak_lb avglambda_lb5 fwhm_lb];

ub=[peak_ub avglambda_ub1 fwhm_ub...
   peak_ub avglambda_ub2 fwhm_ub...
   peak_ub avglambda_ub3 fwhm_ub...
   peak_ub avglambda_ub4 fwhm_ub...
   peak_ub avglambda_ub5 fwhm_ub];

% minimizacion fmincon
%err=fmincon(@(a)
jordi(a,wavelength,XYZ,labselindex),init,[],[],[],[],lb,ub)
%jordi(init,wavelength,XYZ,labselindex)
% minimizacion Algoritmos Genéticos
%options = gaoptimset('PlotFcns', (@gaplotbestf))
%err = ga(@(a)
jordi(a,wv,XYZ,indexes,indexmultiplicity,alpha,beta),15,[],[],[],[],lb,u
b)
%options=gaoptimset('PlotFcns', (@gaplotbestf))
jordi(init,wv,XYZ,indexes,indexmultiplicity,alpha,beta);

%[x,fval,exitflag,output] = gamultiobj(@(a)...
%                              jordi(a,wavelength,XYZ,labselindex),...
%                              15,[],[],[],[],lb,ub)
%jordi(x,wavelength,XYZ,labselindex)

end

% function [Eff_max Rs_max]=jordi(a,wavelength,XYZ,labselindex)
% function [Rss_max] =jordi(a,wavelength,XYZ,labselindex)
function [Fobj] =jordi(a,wv,XYZ,indexes,indexmultiplicity,alpha,beta)
peak1=a(1);
avglambda1=a(2);
fwhm1=a(3);
peak2=a(4);
avglambda2=a(5);
fwhm2=a(6);
peak3=a(7);
avglambda3=a(8);
fwhm3=a(9);
peak4=a(10);
avglambda4=a(11);
fwhm4=a(12);
peak5=a(13);
avglambda5=a(14);
fwhm5=a(15);
%wv=wavelength;
lambda = wv;
z1=peak1*(exp(-((lambda-avglambda1)/fwhm1).^2)+2*exp(-
((lambda-avglambda1)/fwhm1).^2).^5)/3;
z2=peak2*(exp(-((lambda-avglambda2)/fwhm2).^2)+2*exp(-
((lambda-avglambda2)/fwhm2).^2).^5)/3;
z3=peak3*(exp(-((lambda-avglambda3)/fwhm3).^2)+2*exp(-
((lambda-avglambda3)/fwhm3).^2).^5)/3;
```

```
z4=peak4*(exp(-((lambda-avglambda4)/fwhm4).^2)+2*exp(-
((lambda-avglambda4)/fwhm4).^2).^5)/3;
z5=peak5*(exp(-((lambda-avglambda5)/fwhm5).^2)+2*exp(-
((lambda-avglambda5)/fwhm5).^2).^5)/3;
espectro = (z1 + z2 +z3 + z4 + z5);
spectrum = interp1(lambda,espectro,wv);
[garbage minindex]=min(spectrum);

[Rm, R, Efficacy,up_t,vp_t,ubb,vbb,Duv,CCT] =
CRM(wv,spectrum,wv,XYZ,indexes);
      % Weighted Average of CRM indexes owing at their multiplicity
 Rs=0;
 for j=1:length(Rm)
    Rs=Rs+Rm(j)*indexmultiplicity(j);
 end
 Rsm = Rs/sum(indexmultiplicity); % Selected munsell with multiplicity
(number of ocurrences within the gamut)
 Rss = mean(Rm); %Selected munsell (just once per Munsell Sample
or Reflectance)
 Ra = mean(R);
%-------------------------------------------------------------

     A =  (1 -(2.4 * normpdf(Duv / 0.006)))^beta;
     B = (2.5 * normpdf(max(0,Rsm)/45))^ alpha;
     C = (2.5 * normpdf(Efficacy / 222))^(1-alpha);
     Fobj = ( A + B + C ) / 3    % objetive function for minimization.
     ECQ = (1 - (A +  B + C)/3) * 125;    %Efficacy & Color Quality
Index

Info3= [sprintf('%13s', 'iteration_pro') '    ' sprintf('%7.1f',Efficacy) '
'...
     '    ' sprintf('%5.0f',CCT) '  ' sprintf('%7.4f',Duv)...
     ' ' sprintf('%7.1f',Ra) '' sprintf('%7.1f',Rss)...
     ' ' sprintf('%7.1f',Rsm) sprintf('%7.1f',ECQ)]

  figure
     subplot(311)
     plot(lambda,espectro)
     subplot(312)
     plot(1,Rsm,'ro')
     subplot(313)
     plot(1,Efficacy,'ro')

%}
```